Optimal Vehicle Stability Control with Driver Input and Bounded Uncertainties

Seyed Hossein Tamaddoni

Dissertation submitted to the faculty of the Virginia Polytechnic Institute and State University in partial fulfillment of the requirements for the degree of

Doctor of Philosophy
In
Mechanical Engineering

Saied Taheri
Mehdi Ahmadian
Ali H. Nayfeh
Daniel J. Inman
Steve C. Southward

February 4, 2011
Blacksburg, VA

Keywords: Vehicle Dynamics; Vehicle Stability; Vehicle Control; Game Theory; Optimal Control; Robust Control; Driver Model; Integral Sliding Model

Optimal Vehicle Stability Control with Driver Input and Bounded Uncertainties

Seyed Hossein Tamaddoni

ABSTRACT

For decades vehicle control has been extensively studied to investigate and improve vehicle stability and performance. Such controllers are designed to improve driving safety while the driver is still in control of the vehicle. It is known that human drivers are capable to learn and adapt to their built-in vehicle controller in order to improve their control actions based on their past driving experiences with the same vehicle controller. Although the learning curve varies for different human drivers, it results in a more constructive cooperation between the human driver and the computer-based vehicle controller, leading to globally optimal vehicle stability.

The main intent of this research is to develop a novel cooperative interaction model between the human driver and vehicle controller in order to obtain globally optimal vehicle steering and lateral control. Considering the vehicle driver-controller interactions as a common two-player game problem where both players attempt to improve their payoffs, i.e., minimize their objective functions, the Game Theory approach is applied to obtain the optimal driver's steering inputs and controller's corrective yaw moment. Extending this interaction model to include more realistic scenarios, the model is discretized and a road preview model is added to account for the driver's preview-time characteristic. Also, a robust interaction model is developed to stabilize the vehicle performance while taking bounded uncertainty effects in driver's steering behavior into consideration using the Integral Sliding Mode control methodology.

For evaluation purposes, a nonlinear vehicle dynamics model is developed that captures nonlinear tire characteristics and includes driver steering controllability and vehicle speed control systems such as cruise control, differential braking, and anti-lock braking systems. A graphical user interface (GUI) is developed in MATLAB to ease the use of the vehicle model and hopefully encourage its widespread application in the future.

Simulation results indicate that the proposed cooperative interaction model, which is the end-product of human driver's and vehicle controller's mutual understanding of each other's objective and performance quality, results in more optimal and stable vehicle performance in lateral and yaw motions compared to the existing LQR controllers that tend to independently optimize the driver and vehicle controller inputs.

To my lovely wife, Hedieh
and my parents

ACKNOWLEDGEMENTS

I am deeply indebted to my advisors, Professors Saied Taheri and Mehdi Ahmadian for the incomparable opportunity that provided me. I am grateful for their encouraging guidance, for their close attention to our research, and for their mentorship.

I would like to thank the members of my committee, Professors Ali Nayfeh, Daniel Inman, Steve Southward, and Muhammad Hajj for reviewing my dissertation and providing me with their comments, which greatly helped me to improve the quality of this dissertation.

Seyed Hossein Tamaddoni

February 2011

Blacksburg, Virginia

CONTENTS

1 Introduction 1

1.1 Research Objectives……... 2

1.2 Thesis Contribution…….……... 2

1.3 Document Organization…….……...……. 3

2 Background 5

2.1 Historical Background on Driver-Vehicle Modeling and Control.....…... 5

2.1.1 Vehicle Dynamics Modeling……... 6

2.1.2 Driver Steering Control Modeling…...…….……. 10

2.1.3 Vehicle Stability and Control…….…….…… 13

2.2 Historical Background of Game Theory Study……..…… 15

2.3 Introduction to Handling Stability....…….…… 16

3 Vehicle and Driver Modeling 20

3.1 Coordinate System..……... 21

3.2 Vehicle Dynamics…….……. 23

3.2.1 Body Dynamics……..…..…….. 24

3.2.2 Wheel Dynamics……...…….……...…… 27

3.2.3 Tire Dynamics…….…… 28

3.2.4 Simplified Linear Model of 4-Wheel Road Vehicles …….. 37

3.3 Control Systems…….…… 40

3.3.1 Cruise Control…..…….…….…….. 40

3.3.2 Differential Braking…..…….…….. 42

3.4 Driver Models…… 46

3.4.1 Continuous-Time Model…….……. 46

3.4.2 Discrete-Time Model……..……. 47

3.5 Simulation and Results…....…….…….. 49

3.5.1 Nonlinear Model…….……..…….. 51
3.5.2 Linear Models……..…..…….. 55
3.5.3 Non-dimensional Analysis…….…….. 57

4 Vehicle Control Design Based On Game Theory 59
4.1 Continuous-Time Interaction Model…..…… 62
4.1.1 Control Design……...…..…… 63
4.1.2 Simulation and Results……...…….…… 65
4.2 Discrete-Time Interaction Model……...…… 71
4.2.1 Control Design……...…..…… 72
4.2.2 Simulation and Results……...…..…… 75
4.3 Sensitivity Analysis…….……... 79
4.3.1 μ-Sensitivity…… 80
4.3.2 Simulation and Results……...…..…… 81
4.4 Robust Interaction Model….....…...…… 88
4.4.1 Robust Control Design...…….…… 89
4.4.2 Simulation and Results……...…..…… 92

5 Discussion and Future Work 98
5.1 Discussion…....…….. 98
5.2 Future Work……... 99

References 100

Appendix
A Nomenclature……..... 110
B Detailed Vehicle Body Dynamics…...…. 114
C Evaluation Parse File……. 116

LIST OF FIGURES

Figure 2.1. General classification of vehicles…… 6

Figure 2.2. History of vehicle study.…….. 7

Figure 2.3. History of game theory study……...……... 15

Figure 2.4. Yaw velocity gain as a function of velocity……..…..... 18

Figure 2.5. Vehicle handling characteristics…….. 19

Figure 3.1. Vehicle body coordinate system…..…… 22

Figure 3.2. Tire and wheel coordinate system……..……. 23

Figure 3.3. Vehicle schematics…….……. 24

Figure 3.4. Vehicle's lower-body schematics…… 26

Figure 3.5. Rotational degree of freedom of wheels…...……..... 28

Figure 3.6. Vertical force schematics……..……..... 29

Figure 3.7. Tire slip angle……...……... 30

Figure 3.8. Tire force in pure conditions based on Magic Formula tire model……. 32

Figure 3.9. LuGre model of tire longitudinal force…..…….. 33

Figure 3.10. Circle of friction…… 34

Figure 3.11. Combined-slip tire forces……...……... 36

Figure 3.12. Actual circle of friction based on combined-slip theory.……..... 36

Figure 3.13. Linear tire forces……..…….. 37

Figure 3.14. Vehicle 2-DOF bicycle model……..……..... 38

Figure 3.15. Linear 3-DOF vehicle model……..……..... 39

Figure 3.16. Cruise control system……..……..... 41

Figure 3.17. Differential Braking System…….……..……..... 42

Figure 3.18.ASC static map……..…….……..……..... 43

Figure 3.19.ABS operation limit cycle using bang-bang control strategy……..... 45

Figure 3.20. Schematics of maneuver task geometry…..…… 47

Figure 3.21. Schematics of discrete maneuver task geometry…..……..…… 48

Figure 3.22. MATLAB GUI of Vehicle System Simulator…..……..…… 50

Figure 3.23. Evaluation results; vehicle states……..……..…… 52
Figure 3.24. Evaluation results; tire forces……..…..……..……... 54
Figure 3.25. Evaluation results; vehicle states……..……..…… 56
Figure 3.26. Effect of wheel steering angle on vehicle states…..……..…… 58

Figure 4.1. Continuous-time interaction model; vehicle states…….……. 69
Figure 4.2. Continuous-time interaction model; control inputs…….…… 70
Figure 4.3. Down-sampling of frequency in simulation model……. 76
Figure 4.4. Discrete-time interaction model; vehicle states…….…..……. 78
Figure 4.5. Discrete-time interaction model; control inputs…….……..…… 79
Figure 4.6. Standard feedback configuration…….…… 80
Figure 4.7. Effect of uncertainty in driver feedback gain of lateral position…..... 82
Figure 4.8. Effect of uncertainty in driver feedback gain of lateral velocity…..... 83
Figure 4.9. Effect of uncertainty in driver feedback gain of yaw angle…..... 84
Figure 4.10. Effect of uncertainty in driver feedback gain of yaw rate……..... 85
Figure 4.11. µ-plot of the continuous-time driver-controller interaction model..... 87
Figure 4.12. Uncertainty tube of driver input around estimate value..……..…… 88
Figure 4.13. Robust interaction model; vehicle states…….…..…… 95
Figure 4.14. Robust interaction model; sliding surface…….…… 96
Figure 4.15. Robust interaction model; control inputs…….…….……. 97

LIST OF TABLES

Table 3.1. ABS parameters……..... 45
Table 4.1. Feedback gains on significant vehicle states and control actions…..... 61

Chapter 1
Introduction

For decades vehicle control has been extensively studied to investigate and improve vehicle stability and performance. Vehicle stability control systems help drivers to improve ride and handling, maintain vehicle stability and avoid spinning out and rolling over during emergency braking and steering maneuvers. In June 2006 the United States Insurance Institute for Highway Safety reported that more than 10,000 fatal crashes could be prevented by vehicle stability control systems annually in the US. A comprehensive literature review by Ferguson [2007] reveals that vehicle stability control systems can effectively reduce single-vehicle crashes in cars and sport utility vehicles by 30-50%. Additionally, equipping vehicles with stability controllers fatal rollover crashes are estimated to decrease about 70-90%. Hence, the automotive industry's demand for multifaceted controllers that can deal with common safety and performance issues such as rollover, skidding, and handling has been rapidly increasing in the recent years. Such systems must be able to work in nearly all cases, including those with unknown vehicle parameters, unmeasured states, unknown road disturbance, and unpredictable driver steering and speed control.

Vehicle stability control systems are mostly designed to improve driving safety while the driver is still in control of the vehicle. It is known that human driver have the ability to learn and adapt to the built-in vehicle controller in order to improve his/her action based on their past driving experiences with the same vehicle controller. Although the learning curve varies for different human drivers, it would result in a move towards constructive cooperation between the vehicle's human operator and computer-based controller, leading to globally optimal vehicle performance.

The advancement of smart systems in vehicles that can augment the driver input, in order to improve the vehicle handling and dynamics, necessitates a better understanding of how the vehicle driver and controller inputs can co-exist in a manner that are complementary, not contradictory. Hence, this research is devoted to developing a driver-controller interaction framework in which the vehicle driver and controller cooperate optimally with each other in order to guarantee system stability and improve vehicle handling.

1.1. Research Objectives

The primary objectives of this research are to

1. develop a novel vehicle driver-controller interaction model that will take advantage of combining driver steering behavior with vehicle stability control in order to improve vehicle handling and lateral stability;
2. evaluate the effectiveness of the suggested driver and vehicle controller models using a validated nonlinear vehicle model that allows for controlling the steering, braking, and traction; and
3. explore the effects of uncertainty in driver steering control on the robustness of the proposed control framework, and develop a robust optimal vehicle driver-controller interaction model.

1.2. Document Organization

In chapter 2, the state of the art is described through a comprehensive literature search. The survey includes a historical background of vehicle study including modeling vehicle dynamics and driver steering control, and design and implementation of vehicle stability control systems.

Chapter 3 is devoted to evaluation and control models. Throughout this chapter vehicle dynamics, traction/braking control systems and driver directional control is explained. First, a nonlinear vehicle model is developed base on Multibody dynamics approach, and nonlinear tire models, both physical and semi-empirical, are described. The assumption of constant forward speed that consequently reduces the number of differential equations

leads to linear vehicle models. These simple models will be applied to better understand yaw and roll motions of the vehicle, and mainly to serve as the control platform for handling and stability purposes. Cruise Control and Differential Braking systems are also introduced to control the vehicle speed. The cruise control is mainly based on PID control concept while the differential braking system includes Active Slip Control (ASC), Differential Brake Distributor, and Anti-lock Braking System (ABS) to distribute the braking torques on the wheels. Also, two driver steering control models are reviewed; the first one is a continuous-time first-order preview driver steering model with time lag, and the second one is a discrete-time preview driver directional model based on optimal linear control theory. The vehicle model is finally validated by the commercially available vehicle dynamics simulation software CarSim, and the results are illustrated for a test scenario.

Chapter 4 introduces the main contribution of this research, i.e. a novel interaction model for optimal linear vehicle steering and yaw control based on the Game Theory concept. In this chapter, an optimal vehicle stability controller is developed while the driver is controlling the steering angle within a bounded uncertainty range. The first section reviews the continuous-time interaction model of steering and yaw control design based on the linear quadratic (LQ) differential game approach, followed by the application of the LQ difference game theory to obtain optimal steering angle and corrective yaw moment for a driver with road preview information. This chapter also studies the effect of uncertainty in driver steering behavior and derives robust control strategies to deal with bounded uncertain driver control structure based on Integral Sliding Mode control.

Finally, Chapter 5 concludes the study and proposes significant future works to improve the study presented in this research.

1.3. Thesis Contribution

The primary contributions of this study are:

1. novel interaction framework for optimal driver steering and vehicle stability control based on Game Theory;

2. optimal robust vehicle control design based on the Integral Sliding Mode (ISM) control to deal with uncertainty in driver's steering angle in a linear quadratic game system;
3. MATLAB graphical user interface (GUI) toolbox called "Vehicle System Simulator" that simulates vehicle/tire nonlinear dynamics in the MATLAB/Simulink environment with any user-defined arbitrary inputs and outputs.

Chapter 2
Background

In this chapter, the prior state-of-the-art related to this research is studied. The historical backgrounds of vehicle dynamics, driver steering models, and vehicle stability control systems are discussed in Section 2.1 and that of game theory is briefly reviewed in Section 2.2.

2.1. Historical Background of Driver-Vehicle Modeling and Control

Vehicles, derived from the Latin word “vehiculum” are nonliving means of transport. Transportation can be considered as a means of conveyance from one point or place to another. Generally, vehicles can be classified by their support which balances the gravity acting on the vehicles, and propulsion principles which is planned to generate the forward speed. Figure 2.1 shows a simple classification of vehicles based on support and propulsion principles.

Most vehicles represent interesting and complex dynamics systems that require careful analysis and design to make sure they perform properly and hold stability. The stability aspect of vehicle motion has to do with assuring that the vehicle does not deviate spontaneously from a desired path and is still under control. The control aspect of vehicle stability has to do with the ability of a human operator or an automated system to guide the vehicle along the desired path. In either case, the dynamic parameters of such vehicles should be properly tailored to allow controllability with reasonable ease and precision.

The inherent complexity of actual vehicle systems makes an exact analysis of the system impossible; however, simplifying assumptions may reduce the system complexity level in such a way that the behavior or performance approximates that of the real system. This process is called “modeling”, and the simplified version of the real system is called the mathematical model of the system.

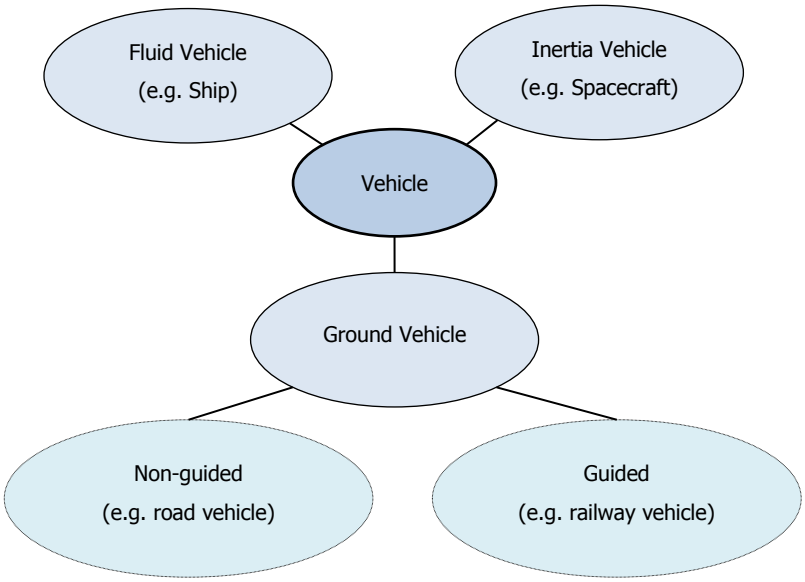

Figure 2.1 General classification of vehicles

The study of automobile stability and control is a relatively new field. Figure 2.2 shows some significant steps in the history of vehicle study.

2.1.1. Vehicle Dynamics Modeling

While the first self-propelled steam road vehicle was successfully tested in 1767 by Cugnot, the pioneer work in vehicle engineering occurred in 1903 when the Wright brothers successfully built their first airplane. A few years later, G. H. Bryan started his pioneering work on a mathematical theory of airplane stability [Bryan, 1911]. Development of scale models and wind tunnels evolved the understanding of aerodynamics and how it affects the stability of an aircraft. Yet lack of understanding of the role of the tire mechanics in the stability of an automobile had slowed down the development of an automotive stability theory.

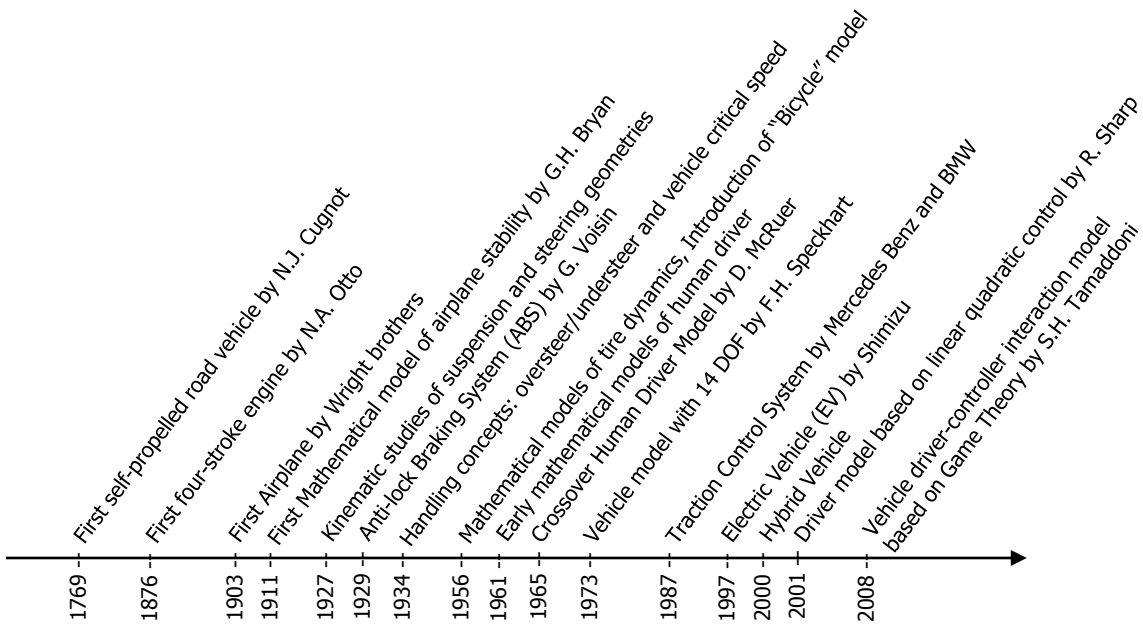

Figure 2.2 History of vehicle study

During 1900 and 1930, the emphasis on improving the ability of the driver to control the vehicle led to kinematic studies of suspension and steering geometries resulting in improved designs including Ackermann steering geometry [Gears, 1927]. In that period, vehicles were plagued with the phenomenon of steering shimmy. To explain this phenomenon, Broulheit introduced the basic concepts of sideslip and slip angle for the first time [Broulheit, 1925]. Following Broulheit's work, Becker, Fromm, and Maruhn published a text on the role of the tire in steering system vibrations and further developed the field of tire mechanics [Becker, 1931].

In 1930's, the Cadillac Suspension Group of General Motors (GM) developed the first independent front suspension system. Olley and his co-researchers in GM found that certain steering geometries led to a condition called roll oversteer which was later recognized unsafe at high speeds [Olley, 1937]. In 1934 an unpublished report by Olley stated the proposition of oversteer/understeer and the idea of critical speed [Olley, 1934]. In 1935 Goodyear Tire and Rubber Company began rolling drum tests to determine tire

characteristics. The results of lateral tire characteristics including data on cornering force and self-aligning torque were published in [Evans, 1935].

During 1940's very little progress was made due to World War II. In 1950 Lind Walker introduced the concept of the neutral steer line and the stability margin [Walker, 1950]. Although these concepts had already been established in aeronautical circles, Walker for the first time suggested them as criteria for steady state directional stability in automobiles.

By the middle of the 1950s a basic understanding of the tire enabled the creation of reasonably accurate mathematical tire models. In 1956 William F. Milliken, David W. Whitcomb, and Leonard Segel of the Cornell Aeronautical Laboratory, published the first major quantitative and theoretical analysis of vehicle handling in a series of papers [Milliken, 1956; Segel, 1956's; Whitcomb, 1956].

Milliken [1956] stated that the major effort in handling research to date has been in the recognition of individual effects, their isolation, and examination as separate entities. There were no universally accepted set of reference axes and measured tire data of the period were typically confined to two or three of the possible six force/moments. This made translation of the data from one set of axes to another difficult if not impossible. Milliken also emphasized the need to concentrate on the objective analysis of car stability and control; therefore, he made the following distinctions between stability and control, performance and ride. In general, an automobile has six-degrees-of-motion freedom, and stability and control may be thought of as those lateral motions out of the plane of symmetry involving rolling, yawing and side slipping. ("Performance", by way of distinction, is concerned with fore-and-aft motions in the plane of symmetry, such as acceleration, speed, and braking, while "ride" is composed of the vertical and pitching motions in the plane of symmetry.)

Leonard Segel's work [1956b] was devoted to derivation of a set of nondimensionalized linearized three degree of freedom equations for lateral and directional motion. Segel ignored the bounce and pitch degrees of freedom of the chassis and used a fixed longitudinal roll axis parallel to the ground. The other simplifying assumptions included constant forward velocity, fixed driving thrust divided equally between the rear wheels,

decoupled tire lateral properties from longitudinal properties, and a single non-rolling lumped mass as the unsprung mass. An experimental validation of the model was performed by a 1953 Buick Super four door sedan at 32 mph in a series of frequency response curves with the results showing good correlation.

D. W. Whitcomb's paper [1956] introduced the concept of the "static margin" and discussed automobile stability and control using a two degree of freedom model including yaw and side-slip which is today referred as bicycle model.

In 1961 Martin Goland and Frederick Jindra added the roll degree of freedom as a quasi-coordinate to the two degree of freedom (yaw and sideslip) vehicle model of Segel in order to calculate the vertical load on the tires. The effects of load transfer and the variation of the cornering performance of the tires with vertical loading were thus presented in [Goland, 1961].

In 1965 Walter Bergman published his findings of the nature of vehicle understeer and oversteer. He noted that understeer and oversteer could be recognized by considering the change in the yaw velocity induced by a change in lateral acceleration. This definition is in accordance with the standardized definitions of oversteer and understeer put forth by the Society of Automotive Engineers (SAE).

In 1967 R. Thomas Bundorf of General Motors published the relation of vehicle design parameters to the characteristic speed and to understeer [Bundorf, 1967]. Bundorf argued that under most normal driving conditions, which he characterized as having lateral accelerations below 1/3 g, a vehicle can be accurately modeled by a linear model.

In 1973 Frank H. Speckhart presented a vehicle model containing fourteen degrees of freedom [Speckhart, 1973]. Six degrees of freedom were assigned to the sprung mass, four degrees of freedom were associated with the suspension movement at the four corners of the vehicle, and four rotational degrees of freedom were assigned to the wheels. He used a Lagrangian approach in deriving his equations.

During 1970's several time-saving methods were published such as Bernard's digital simulation code for Highway Safety Department [Bernard, 1973], Hybrid Computer Vehicle Handling Program [Jindra, 1976], and Ford Motor Company's model containing detailed three degree of freedom model of the front suspension [Morman, 1977].

In 1987 twenty-five different suspension types were tested to understand the effects of suspension design on the stability of vehicles [Nalecz, 1987]. A typical three degree of freedom lateral dynamics model was used with the addition of a quasi-static pitch degree of freedom. The roll axis of sprung mass was a function of body roll. This set of tests helped Nalecz to understand that the assumption of a fixed roll axis could not be justified for certain types of suspensions such as double wishbone and MacPherson strut.

In 1992 another model with eight degrees of freedom, consisted of a three degree of freedom lateral dynamics model coupled to a five degree of freedom planar rollover model, was developed [Nalecz, 1992]. The lateral dynamics model was derived in the same manner as Segel's original model. The rollover model consisted of sprung and unsprung masses connected through the various elements of the suspension system. The effects of aerodynamic forces and moments and lateral and longitudinal weight transfer were also included in this model.

In 1996 Michael R. Petersen and John M. Starkey described a relatively detailed straight-line acceleration vehicle model for predicting vehicle performance [Petersen, 1996]. The model included longitudinal weight transfer effects, tire slip, aerodynamic drag, aerodynamic lift, transmission and driveline losses and rotational inertias of the wheels, engine and driveline components. The model used a manual transmission with fully clutch engagement in such a way that shifts were simulated by disengaging the clutch completely, assuming that the engine torque is zero during the shift, changing the gear ratio, and then reapplying the full torque of the motor. This model enabled the authors to conduct sensitivity analyses in order to determine which design parameters most strongly affected vehicle performance.

2.1.2. Driver Steering Control Modeling

The principal roots of driver modeling extend back to the early years of human-machine and aircraft pilot studies which helped to reveal various properties unique to, or characteristic of, the human as a controller of dynamical plants and certain vehicles. In 1963, Ornstein proposed a transfer function as a model of the human operator for pursuit-type manual tracking tasks and included coefficients associated with the effective

transport time delay and the anticipatory behavior of the human operator which was adaptive to changing plant dynamics and methods of visual presentation [Ornstein, 1963]. In effect, this was an early observation of the adaptive nature of a human when interacting with different or changing plant dynamics and the use of prediction by the human operator.

In the late 1950s and early 1960s, Rashevsky addressed the mathematical biology of automobile driving wherein the basic model of the driver as a steering controller was treated in a purely geometric/kinematic manner [Rashevsky, 1959]. The proposed algorithm for steering an automobile of designated width and length along a straight road of specified width amounted to issuing instantaneous steering corrections to the vehicle whenever it approached to within a specified margin of either lane edge. Although no vehicle dynamics were considered within this mathematical treatment, driver anticipation and driver delay properties were included as key parameters.

During 1970's Weir and McRuer introduced useful and simple forms of the driver control models are based on the crossover model of the human operator [Weir, 1970]. This model applies to a wide variety of manual control tasks including driving a car or piloting an aircraft. In 1977 McRuer proposed a three-level servo-control model of driver steering behavior [McRuer, 1977]. The model describes driving as consisting of a hierarchy of navigation, guidance and control phases conducted simultaneously with visual search, recognition and monitoring operations. It also distinguishes between closed-loop (compensatory) control and open-loop (anticipatory) control. Compensatory steering is described as two feedback loops. Firstly, the lateral position is fed back and compared to the desired path, and if there is a deviation it will result in an error-correcting action, which is compared to current heading angle and, if needed, a steering wheel correction will be made. The perceived road curvature derived from visual input guides the pursuit control. Secondly, pursuit control is an open-loop feed-forward control element that permits the driver to follow the anticipated road curvature. An interesting third control is the precognitive control that in practice is a first phase of dual-mode control, that is, both open-loop and closed-loop controls. Precognitive control consists of previously learned

control actions, which are triggered by situation and vehicle motion but works as pure open-loop control.

The following year in 1978, Donges developed a two-level driver steering control model (anticipatory and compensatory) and evaluated the performance of the driver-vehicle system [Donges, 1978].

In 1988 Charles MacAdam developed a driver-vehicle steering interaction models for dynamic analysis [MacAdam, 1988]. MacAdam's model replicated the driver steering behavior during path-following and obstacle-avoidance maneuvers by tuning only two design parameters.

In 1996 Cho Young studied the handling characteristics of the vehicle moving along a curved path using the two degree of freedom bicycle model [Young, 1996]. As a result, Young proposed the concept of look-ahead distance as a mean to calculate the previewed lateral error of the vehicle with respect to the center of the road.

Later in 2000, Robin Sharp designed a mathematical driver model using a proportional correction of the yaw angle and the lateral displacement [Sharp, 2000]. The following year, Sharp [2001] developed a driver model using linear quadratic discrete optimization.

In 2000 Liang-Kuang Chen used a Ford Driving Simulator (FDS) to acquire data from twelve human drivers with the aim of identifying the parameters of the driver model using the ARMAX algorithm [Chen, 2000].

In 2006 Cole introduced a new representation of optimal linear car steering control where the standard lateral/yaw linear car model was transformed into discrete-time formation that constructed a quadratic cost function consisting of terms describing path and attitude errors with respect to the road path. Based on this cost function, steer angle control was minimized by the Linear Quadratic Regulator (LQR) control [Cole, 2006].

In 2007 Plöchl developed an analytical method to determine the parameters of the driver model using a nonlinear two wheel vehicle model which was tested on a simulation model of the whole vehicle [Plöchl, 2007].

A year later in 2008, Vito Cerone developed a driver model that combined two tasks, namely automatic lane-keeping and driver steering, for either obstacle avoidance or lane-change maneuvers [Cerone, 2008].

2.1.3. Vehicle Stability and Control

In order to cope with the complicated operation conditions and to improve vehicle safety and comfort when the vehicle is at the physical limit of its performance, various active control systems such as Anti-lock Braking System (ABS), Four Wheel Steering (4WS), Electronic Stability Control (ESC) and semi-active/active suspensions were equipped in vehicles one after another since the late 1970s.

In 1929 Anti-lock Braking System (ABS) was first developed for aircraft application by Gabriel Voisin, a French automobile and aircraft pioneer.

In the 1950s, Dunlop's Maxaret system introduced an early ABS system with 30% improvement in braking performance in some aircraft models [Ellam, 1958]. The experiments on the Maxaret anti-lock brake in 1958 demonstrated that anti-lock brakes can be of great value to motorcycles, for which skidding is involved in a high proportion of accidents and stopping distances were reduced in most of the tests compared with locked wheel braking, particularly on slippery surfaces.

In 1971 a computerized three-channel four-sensor all-wheel anti-skid system called "Sure Brake" was introduced for passenger cars by Chrysler and the Bendix Corporation [Douglas, 1971]. In the same year, General Motors (GM) introduced the “Trackmaster” rear-wheel-only ABS as an option on their rear-wheel drive Cadillac models [Oakley, 1973]. In the same year, Nissan offered an EAL (Electro Anti-lock System) as an option on the Nissan President, which became Japan's first electronic antilock braking system [Nissan, 1971].

In 1986 Yuhara proposed a design methodology for an Adaptive Rear Wheel Steering Control System (ARWSCS) that maintains desirable vehicle response through computer control regardless of changes in vehicle dynamics [Matsushita, 1986]. The system controls the rear wheels based on a Self Tuning Controller (STC) in such a manner that the vehicle follows the prescribed reference model which presents the desired response to driver's input. In the same year, another passive four wheel steering (4WS) control scheme was introduced by Takiguchi based on gain-schedule control system in which the rear-to-front steer angle ratio varies as a function of vehicle speed [Takiguchi, 1986]. During very low speed driving, this control system steers the rear wheels in the opposite

direction to the front ones at the maximum steer angle ratio; whereas at high speed, it steers the rear wheels in the same direction as the front ones.

In 1987 the earliest innovators of Electronic Stability Controllers (ESC), Mercedes-Benz and BMW, introduced their first traction control systems. Traction control (TCL) works by applying individual wheel braking and throttle to keep traction while accelerating. The system has since evolved into Mitsubishi's modern Active Skid and Traction Control (ASTC) system which was developed to help the driver maintain the intended path through a corner using an onboard computer to monitor several vehicle operating parameters through various sensors. When too much throttle has been used while taking a curve, engine output and braking are automatically regulated to ensure the proper path through a curve and to provide the proper amount of traction under various road surface conditions. While conventional traction control systems at the time featured only a slip control function, Mitsubishi developed a traction control system which had a preventive (active) safety feature. This improved the course tracing performance by automatically adjusting the traction force, thereby restraining the development of excessive lateral acceleration, while turning. The TCL system's standard wheel slip control function improves traction on slippery surfaces or during cornering. In addition to the TCL's traction control feature, it also works together with Diamante's electronic controlled suspension and four-wheel steering that Mitsubishi had equipped to improve total handling and performance [Tanaka, 1991].

In 1989 Kanai applied the design theory of model reference adaptive control to the four wheel steering system and proposed a design method for a system that would adaptively control yaw rate and lateral acceleration [Kanai, 1989].

During 1987 and 1992, Mercedes-Benz and Robert Bosch GmbH co-developed a lateral slippage control system called Electronic Stability Control (ESC) [Klinkner, 1995].

In 1992 BMW, working with Robert Bosch GmbH and Continental Automotive Systems, developed a system to reduce engine torque to prevent loss of control and applied it to the entire 1992 BMW model line [Leffler, 1994].

In 1995 automobile manufacturers commercially introduced ESC systems. Mercedes-Benz supplied by Bosch was the first to implement this with their W140 S-Class model.

That same year BMW and Volvo Cars began to offer ESC on some of their models while Toyota's own Vehicle Stability Control system appeared on the Crown Majesta. General Motors (GM) worked with Delphi Corporation and introduced its version of ESC called “StabiliTrak” in 1997 for select Cadillac models [Ghoneim, 2000]. StabiliTrak was made standard equipment on all GM SUVs and vans sold in the U.S. and Canada by 2007 except for certain commercial and fleet vehicles.

2.2. Historical Background of Game Theory Study

Game theory deals with the development of suitable concepts to describe and understand conflict situations. Figure 2.3 shows the significant progress in the study of game theory.

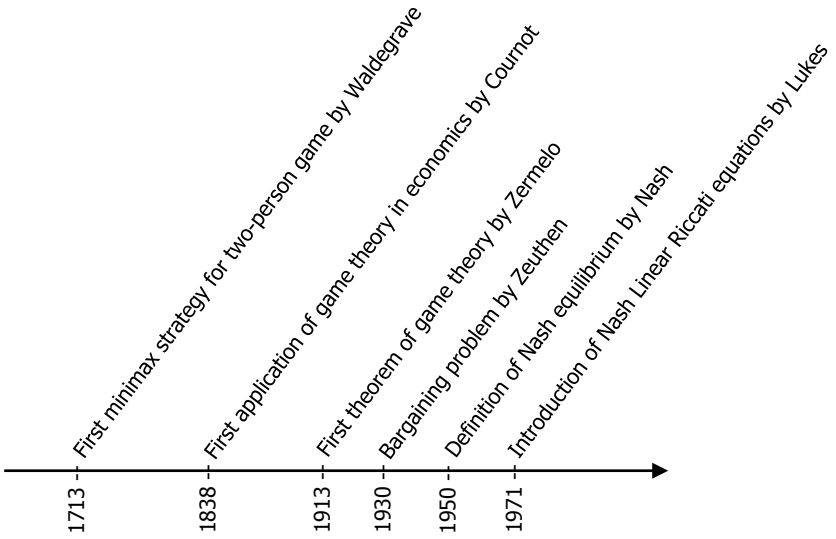

Figure 2.3 History of game theory study

It was first in 1713 that Waldegrave, inspired by a card game, provided the first known minimax mixed strategy solution to a two-person game. The economic aspect of game system (duopoly) was first discussed by Cournot in 1838 that questioned the equilibrium price in case of two producers who sell an identical product [Cournot, 1838]. Cournot’s works resulted in a restricted version of the non-cooperative Nash equilibrium. Later in 1881, Edgeworth proposed the contract curve as a solution to cooperative trading between individuals [Edgeworth, 1881], followed by Pareto in 1896 that used the

formalism of ordinary utility theory to introduce the notion of efficient allocation [Pareto, 1896].

In 1913 Zermelo proposed the first theorem of game theory asserting that assuming that only an a-priori fixed number of moves is allowed the chess is a strictly determined game and the black, i.e. second starting player, has no strategy to always win the game [Zermelo, 1913].

In 1930 The bargaining problem in which the players decide to cooperate with each other to maximize their profits was considered by Zeuthen [1930].

In early 1950s, Nash [1950, 1951, 1953] proved the existence of a strategic equilibrium - the Nash equilibrium - for non-cooperative games, and approached the cooperative games via their reduction to non-cooperative games. Nash equilibrium for a game system is defined as a self-enforcing strategy in which no player can gain by one-sidedly deviating from it. Later in 1956, Harsanyi showed that the Zeuthen's solution is equivalent to Nash's bargaining solution [Harsanyi, 1956].

In 1971 Lukes stated that for a game with a sufficiently small planning horizon, there is a unique linear feedback Nash equilibrium that can be computed by solving a set of so-called Nash Riccati differential equations [Lukes, 1971]. Later in 1979, Papavassilopoulos and Cruz [1979] proved that the Nash equilibrium is unique, if it exists, provided that the set of strategy spaces is restricted to analytical functions of the current state and time, and discussed parametric conditions under which the coupled set of algebraic feedback Nash Riccati equations has a solution.

Since the 1980's the analytical solutions of the Riccati equations have been studied for different aspects of differential game theory including, but not limited to, open-loop equilibrium, finite and infinite time horizon and stochastic system [Başar, 1974, 1995; Abou-Kandil, 1993; Engwerda, 1998].

2.3. Introduction to Handling Stability

Vehicle handling performance is becoming increasingly significant for today's discerning customers. The handling behavior is referred to direction control and disturbance

stabilization issues. Handling is a measure of the directional response of a vehicle, thus playing an important role in vehicle dynamics.

Cornering is defined as the ability of the vehicle to travel on a curved path. Cornering ability of a vehicle may be affected by different factors such as tire construction, tire tread, road surface, tire loading, suspension design, and alignment. As a vehicle turns, centrifugal force is generated pushing outward on the vehicle's center of gravity. The interaction of centrifugal force and the tire traction force distributes the weight on both sides of the vehicle causing the vehicle roll about its roll axis.

A vehicle may be considered as a control system upon which various inputs are imposed. During a turning maneuver, the steer angle induced by the driver can be considered as an input to the system, and the motion variables of the vehicle such as yaw velocity, lateral acceleration, and curvature, may be regarded as outputs. Yaw velocity gain which is defined by the proportion of vehicle yaw rate $\dot{\theta}_z$ to the front wheel steering angle δ_F measures the steering response of road vehicles. A car with infinite value of yaw velocity gain will turn violently in response to the slightest steering input or external disturbance. Consider a vehicle of mass m and length $(l_F + l_B)$ where l_F is the horizontal distance between vehicle CG and front axle, and l_B is the horizontal distance between vehicle CG and rear axle, . Yaw velocity gain is given by

$$\frac{\dot{\theta}_z}{\delta_F} = \frac{v_x}{(l_F + l_B)\left(1 + k_{us} v_x^2\right)} \tag{2.1}$$

where this ratio represents a gain that is proportional to velocity on the case of neutral steer vehicle [Wong, 2001]. k_{us} is called the understeer gradient and is calculated as

$$k_{us} = \frac{m\left(l_B c_{\alpha B} - l_F c_{\alpha F}\right)}{\left(l_F + l_B\right)^2 c_{\alpha F} c_{\alpha B}} \tag{2.2}$$

where c_α represents the cornering stiffness defined as the change in lateral force per unit slip angle change at a specified normal load in the linear range of the tire.

Based on this definition, the steady-state response of the vehicle can be classified in three categories: neutral steer, understeer, and oversteer, as shown in Figure 2.4.

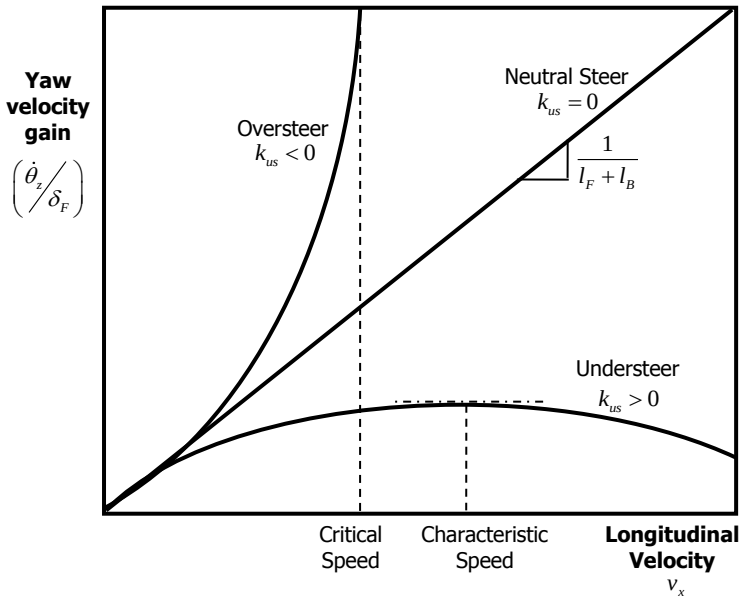

Figure 2.4 Yaw velocity gain as a function of velocity

Neutral steering happens when $k_{us} = 0$, or in the other words,

$$\frac{\dot{\theta}_z}{\delta_F} = \frac{v_x}{l_F + l_B}$$

which means that the yaw velocity gain is proportional to the velocity of the vehicle with a slope of $1/(l_F + l_B)$. On a constant-radius turn, no change in the steer angle will be required as the speed is varied. As shown in Figure 2.5, the center line of a neutral steering vehicle is tangent to the instantaneous radius of curvature of vehicle trajectory.

When $k_{us} < 0$, the denominator of (2.2) is smaller than 1, and $\dot{\theta}_z / \delta_F$ is not linearly proportional to the vehicle velocity, the vehicle is called to oversteer. An oversteering vehicle large slip angles are the rear tires. Therefore, the rear of the vehicle appears to slide out from under the driver.

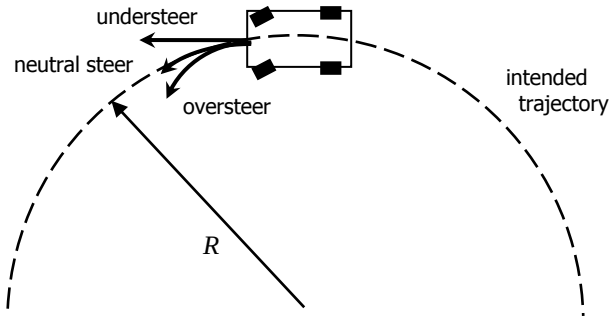

Figure 2.5 Vehicle handling characteristics

An understeering vehicle needs relatively large slip angles at the front tires, requiring excessive steering input to track a given trajectory. Understeering occurs when $k_{us} > 0$, the denominator of (2.2) is larger than one. Just as an oversteering vehicle is perceived as twitchy, an understeering vehicle is sluggish.

Although neutral steering characteristics are desired, passenger vehicles generally exhibit varying degrees of understeer. This intrinsic degree of understeer is placed to minimize the occurrence of transient situations such as heavy acceleration or obstacle avoidance when the vehicle can tend toward oversteer. All other factors equal, a vehicle with a forward weight bias will exhibit understeer. Steering characteristics also can be influenced by factors other than weight bias. As an example, if the side force generated by a tire for a given slip angle is reduced, a larger slip angle will be necessary to develop the required moment balance which results in yaw to track the desired trajectory.

Chapter 3
Vehicle and Driver Modeling

With the advent of modern computational technologies, the use of vehicle modeling and simulation has become far more practical for more users. The low cost of computer simulation as compared with actual testing is a significant benefit to vehicle designers. Computer modeling allows the user to test out various dynamic maneuvers and driving scenarios without spending the time, money, and equipment to conduct testing on a track. These mathematical models can be used for evaluating various functional performance characteristics of the vehicle such as ride and handling. Furthermore, vehicle control strategies are often derived based on simple but comprehensive mathematical models that contain the key characteristics under investigation. Therefore, an appropriately derived vehicle model is an important factor in the development of vehicle control algorithms.

Over the past century, there has been extensive growth in the use of dimensionless framework to study the governing dynamics of complex systems in various fields of research. The non-dimensional analysis simplifies the comparison of systems with different dimensions, as well as it reduces simulation time and cost. The basis for this analysis approach is the well-known Buckingham's Π-theorem [Buckingham, 1914] which can be found in many standard textbooks on Fluid Mechanics. The Buckingham's Π theorem states that:

"*If there are n variables in a problem and these variables contain m primary dimensions, the equation relating all the variables will have (n-m) dimensionless groups.*"

The seven primary dimensions are recognized as: mass [M], length [L], time [T], amount of a substance, electric current, temperature, and luminous intensity. Only the first three dimensions whose abbreviations are shown in the brackets will be used in this

study. On the other hand, secondary or derived dimensions are made up of primary dimensions, such as velocity which is distance (length) per unit of time [LT^{-1}].

The dimensionless groups, i.e., π groups, must be independent of each other and no one group should be formed by multiplying together powers of other groups. In this framework, there are 2 conditions:

1. each fundamental dimensions must appear in at least one of the m variables;
2. it must not be possible to form a dimensionless group from one of the variables within a recurring set.

A recurring set is a group of variables forming a dimensionless group.

In this chapter, the dimensionless modeling of vehicle handling dynamics with different complexities, assumptions, and limitations and driver steering control with preview time are developed. These models are either used for vehicle dynamics evaluation or to derive control algorithms.

3.1. Coordinate System

Multibody vehicle dynamics models are typically generated using right-handed coordinate systems. For vehicle dynamics modeling based on ISO 8855, the standard coordinate system has forward X-axis, upward Z-axis, and Y-axis pointing to the left-hand side of the vehicle; vertical tire forces are always positive; and wheel spin rates are positive for forward vehicle speeds.

All of the coordinate systems and axes are built from four reference directions: (i) vertical, as defined by the direction of the gravity vector, (ii) the X axis of the vehicle reference frame, (iii) the Y (spin) axis of a wheel of interest, and (iv) the direction normal to the road at the center of tire contact. Figure 3.1 shows the three axis systems associated with the entire vehicle. Figure 3.2 shows the tire and wheel axis systems. The mathematical definitions of five axis systems are described below.

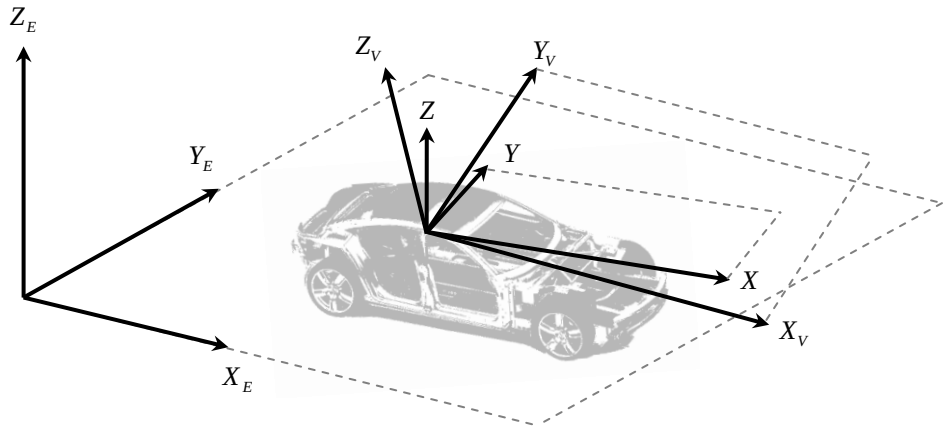

Figure 3.1 Vehicle body coordinate system

- *Earth-fixed axis system* $(O_E;X_E,Y_E,Z_E)$: right-handed orthogonal axis system fixed in the inertial reference. The Z_E axis is parallel to the gravity vector with upward Z_E orientation.
- *Intermediate axis system* $(O;X,Y,Z)$: right-handed orthogonal axis system whose Z axis is parallel to Z_E, and whose Y axis is perpendicular to both Z_E and X_V. This axis system can be obtained by rotating the Earth-fixed axis system about the Z_E axis by the vehicle yaw angle.
- *Vehicle axis system* $(O_V;X_V,Y_V,Z_V)$: right-handed orthogonal axis system fixed in the vehicle reference frame. The X_V axis is primarily horizontal in the vehicle plane of symmetry and points forward. The Z_V axis is vertical and the Y_V axis is lateral. The directions should coincide with the earth-fixed axis system when the vehicle is upright and aligned with the X_V axis parallel to the X_E axis.

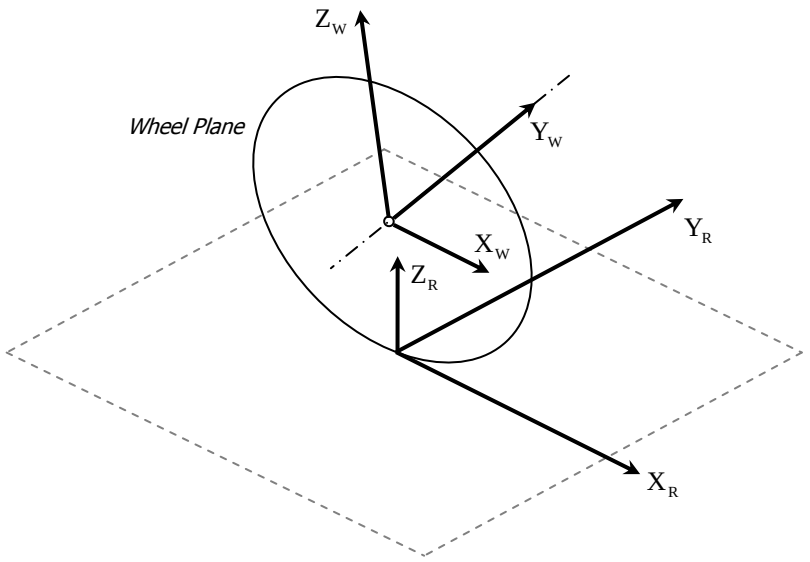

Figure 3.2 Tire and Wheel Coordinate System

- *Road axis system* $(O_R;X_R,Y_R,Z_R)$: right-handed orthogonal axis system whose Z_R axis is normal to the road, at the center of tire contact, and whose X_R axis is perpendicular to the wheel spin axis Y_W.
- *Wheel axis system* $(O_W;X_W,Y_W,Z_W)$: right-handed orthogonal axis system whose Y_W axis is parallel with the spin axis of the wheel and whose X_W axis is perpendicular to Z_R.

The following sections are devoted to mathematical derivation of various models that will be used throughout this research.

3.2. Vehicle Dynamics

In order to study the handling and roll dynamic responses of the vehicle, a nonlinear model of a vehicle is derived which includes longitudinal and lateral translational motions, and roll and yaw motions with rotational dynamics of each of the four wheels.

To analyze vehicle dynamics in a non-dimensional manner, the procedure of the Buckingham's Π Theorem is applied such that the vehicle parameters are collected in

groupings of dimensionless groups, or Π groups, that can be equivalently obtained by normalizing the primary dimensions of mass, length, and time respectively by scaling factors dependent directly on the vehicle's total mass M, front to rear axle length L, and longitudinal speed V_x. In this study, the following convention is followed:

- lower-case, normal, italic (e.g. p): dimensionless (Π) parameter
- upper-case, normal, italic (e.g. P): dimensional (actual) parameter

The resulting Π parameters are included in Appendix A.

3.2.1. Body Dynamics

Figure 3.3 depicts the sprung and unsprung body coordinates of a four-wheel vehicle. The unsprung mass is connected to the sprung mass with four suspension linkage shown by hashed lines. The body coordinates U and S are intermediate axis systems for the unsprung and sprung masses, respectively.

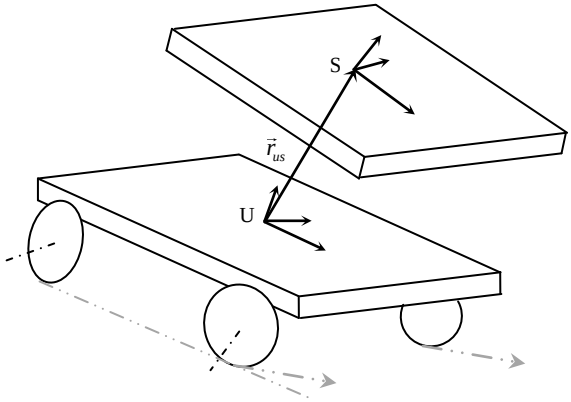

Figure 3.3 Vehicle schematics

The presented vehicle handling model has five degrees of freedom: longitudinal velocity v_x, lateral velocity v_y, roll angle θ_x, pitch angle θ_y, and yaw angle θ_z. The nonlinear vehicle model is derived by writing the translational and rotational equations in the vehicle fixed coordinate frame.

Assuming that the sprung mass can only rotate along the X and Y axes of the unsprung coordinates, the sprung body will perform the pitch and roll motion. It is also assumed

that the unsprung mass performs yaw motion and there is no relative yaw angle between the sprung and unsprung bodies.

The rotation matrices of roll and pitch motions of the sprung coordinate S along the X and Y axes of the unsprung coordinate U are given by

$$ {}^{S}_{U}R_x = \begin{bmatrix} 1 & 0 & 0 \\ 0 & \cos\theta_x & -\sin\theta_x \\ 0 & \sin\theta_x & \cos\theta_x \end{bmatrix} \quad , \quad {}^{S}_{U}R_y = \begin{bmatrix} \cos\theta_y & 0 & \sin\theta_y \\ 0 & 1 & 0 \\ -\sin\theta_y & 0 & \cos\theta_y \end{bmatrix} \tag{3.1} $$

The location of the sprung coordinate relative to the unsprung coordinate is given by

$$ {}^{S}_{U}\vec{r}_{us} = {}^{U}_{S}R_y \cdot {}^{U}_{S}R_x \cdot \begin{bmatrix} 0 \\ 0 \\ -h \end{bmatrix} \tag{3.2} $$

The angular velocities and accelerations are obtained as

$$ {}^{U}\vec{\omega}_u = \begin{bmatrix} 0 \\ 0 \\ \dot{\theta}_z \end{bmatrix} \quad , \quad {}^{S}_{U}\vec{\omega}_s = {}^{U}\vec{\omega}_u + \begin{bmatrix} \dot{\theta}_x \\ \dot{\theta}_y \\ 0 \end{bmatrix} \tag{3.3} $$

$$ {}^{U}\vec{\alpha}_u = \begin{bmatrix} 0 \\ 0 \\ \ddot{\theta}_z \end{bmatrix} \quad , \quad {}^{S}_{U}\vec{\alpha}_s = {}^{U}\vec{\alpha}_u + \begin{bmatrix} \ddot{\theta}_x \\ \ddot{\theta}_y \\ 0 \end{bmatrix} + {}^{U}\vec{\omega}_u \times {}^{S}_{U}\vec{\omega}_s \tag{3.4} $$

The translational velocities and accelerations are

$$ {}^{U}\vec{V}_u = \begin{bmatrix} v_x \\ v_y \\ 0 \end{bmatrix} \quad , \quad {}^{U}\vec{a}_u = \begin{bmatrix} \dot{v}_x \\ \dot{v}_y \\ 0 \end{bmatrix} + {}^{U}\vec{\omega}_u \times {}^{U}\vec{V}_u \tag{3.5} $$

$$ {}^{U}\vec{V}_s = {}^{U}\vec{V}_u + {}^{S}_{U}\vec{\omega}_s \times {}^{S}_{U}\vec{r}_{us} \tag{3.6} $$

$$ {}^{U}\vec{a}_s = {}^{U}\vec{a}_u + {}^{S}_{U}\vec{\omega}_s \times {}^{S}_{U}\vec{\omega}_s \times {}^{S}_{U}\vec{r}_{us} + {}^{S}_{U}\vec{\alpha}_s \times {}^{S}_{U}\vec{r}_{us} \tag{3.7} $$

The sprung-mass moment of inertia matrix is also transformed to the unsprung body coordinate system as

$$ {}^{U}_{S}\vec{I}_s = {}^{S}_{U}R_y \cdot ({}^{S}_{U}R_x \cdot {}^{S}\vec{I}_s \cdot {}^{S}_{U}R_x^T) \cdot {}^{S}_{U}R_y^T \tag{3.8} $$

Using equations (3.1)-(3.3), the equations of motion can be written as

$$\begin{cases} (m-m_s).{}^{U}\vec{a}_u + m_s.{}^{U}\vec{a}_s = \sum_i {}^{U}\vec{f}_i \\ {}^{U}\dot{\vec{H}}_u + {}^{U}_{S}\dot{\vec{H}}_s + {}^{S}_{U}\vec{r}_{us} \times \left(m_s.{}^{U}_{S}\vec{a}_s\right) = \sum_i {}^{U}\vec{\tau}_i \end{cases} \tag{3.9}$$

where

$$\begin{aligned} {}^{U}\dot{\vec{H}}_u &= {}^{U}\vec{I}_u.{}^{U}\vec{\alpha}_u + {}^{U}\vec{\omega}_u \times \left({}^{U}\vec{I}_u.{}^{U}\vec{\omega}_u\right) \\ {}^{U}_{S}\dot{\vec{H}}_s &= {}^{U}_{S}\vec{I}_s.{}^{U}_{S}\vec{\alpha}_s + {}^{U}\vec{\omega}_u \times \left({}^{U}_{S}\vec{I}_s.{}^{U}_{S}\vec{\omega}_s\right) \end{aligned} \tag{3.10}$$

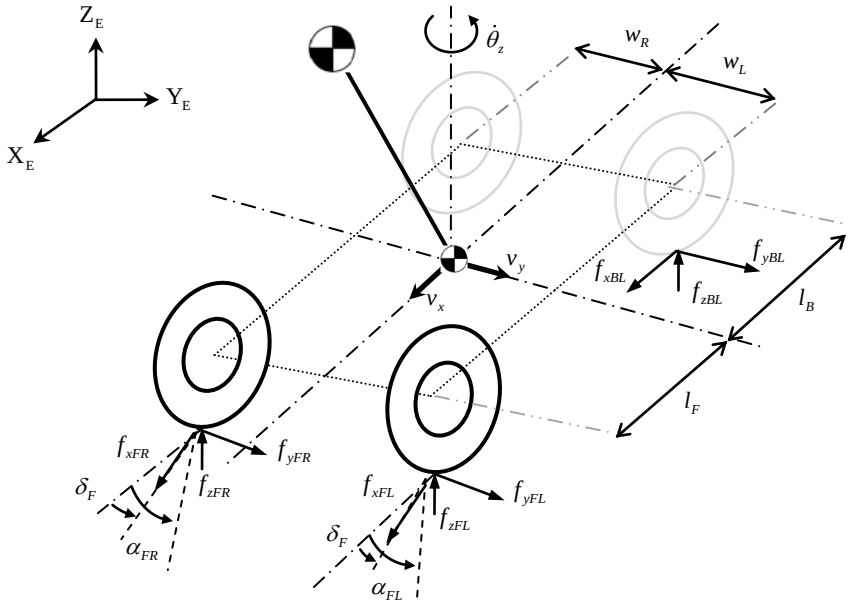

Figure 3.4 Vehicle's lower-body schematics

The final equations are in form of

$$\mathbf{A}(q)\,\ddot{q} + \mathbf{B}(q,\dot{q}) = \eta \tag{3.11}$$

where the generalized forces are given by

$$\eta_x = \frac{MU^2}{L}\left(\sum f_x \cos\delta - \sum f_y \sin\delta\right) \tag{3.12}$$

$$\eta_y = \frac{MU^2}{L}\left(\sum f_x \sin\delta + \sum f_y \cos\delta\right) \tag{3.13}$$

$$\eta_{\theta x} \equiv MU^2\left(-k_x\theta_x - c_x\dot{\theta}_x + gh_s\left(\sin\theta_x\cos\theta_y - \cos\theta_x\sin\theta_y\right)\right) \tag{3.14}$$

$$\eta_{\theta y} = MU^2\left(-k_y\theta_y - c_y\dot{\theta}_y + gh_s\left(\cos\theta_x \sin\theta_y + \sin\theta_x \cos\theta_y\right)\right) \tag{3.15}$$

$$\eta_{\theta z} = MU^2\left(\sum l' f_x \sin\delta - \sum l' f_y \cos\delta + \sum w' f_x \cos\delta - \sum w' f_y \sin\delta\right) \tag{3.16}$$

where

$$l' = \begin{bmatrix} l_F & l_F & -l_B & -l_B \end{bmatrix}^T,\ w' = \begin{bmatrix} w_R & -w_R & w_L & -w_L \end{bmatrix}^T,\ \delta = \begin{bmatrix} \delta_F & \delta_F & 0 & 0 \end{bmatrix}^T \tag{3.17}$$

The vehicle states and parameters are defined in Appendix A. The complete sets of equations are reported in Appendix B.

For a simple case in which there is no pitch motion, i.e., $\forall t:\ \theta_y = 0$, and relatively small roll motion, i.e., $\forall t:\ \theta_x, \dot{\theta}_x \ll 1$, the simplified equations of motion are given by

$$m\left(\dot{v}_x - v_y\dot{\theta}_z\right) - m_s h_s\left(\theta_x\ddot{\theta}_z + 2\dot{\theta}_x\dot{\theta}_z\right) = \sum f_x \cos\delta - \sum f_y \sin\delta \tag{3.18}$$

$$m\left(\dot{v}_y + v_x\dot{\theta}_z\right) - m_s h_s\left(\theta_x\dot{\theta}_z^2 - \ddot{\theta}_x\right) = \sum f_x \sin\delta + \sum f_y \cos\delta \tag{3.19}$$

$$\begin{aligned} &m_s h_s\left(\dot{v}_y + v_x\dot{\theta}_z\right) + \left(i_{sx} + m_s h_s^2\right)\ddot{\theta}_x + \left(i_{sz} - i_{sy} - m_s h_s^2\right)\theta_x\dot{\theta}_z^2 \\ &\qquad = -k_x\theta_x - c_x\dot{\theta}_x + m_s h_s g \sin\theta_x \end{aligned} \tag{3.20}$$

$$\begin{aligned} &-m_s h_s\theta_x\left(\dot{v}_x - v_y\dot{\theta}_z\right) + \left(i_{uz} + i_{sz}\right)\ddot{\theta}_z \\ &\qquad = \sum l' f_x \sin\delta - \sum l' f_y \cos\delta + \sum w' f_x \cos\delta - \sum w' f_y \sin\delta \end{aligned} \tag{3.21}$$

where l' and w' are defined in (3.17).

The equations (3.18)-(3.21) form the vehicle body dynamics that will be used to derive and evaluate control algorithms.

3.2.2. Wheel Dynamics

In addition to the rigid body vehicle degrees of freedom, one rotational degree of freedom was considered for each wheel. Wheel dynamics will be of importance when studying the brake dynamics of the vehicle. Figure 3.5 shows a free body diagram of a wheel.

The equation of motion for each wheel is given by:

$$i_w\ddot{\theta}_w = -f_x r_w + \tau_{wDr} - \tau_{wBr} \tag{3.22}$$

where i_w is the wheel y-axis moment of inertia, f_x is the longitudinal tire force applied on each wheel, $\dot{\theta}_w$ is the wheel rotational velocity, r_w is the effective radius of the wheel,

and τ_{wDr}, τ_{wBr} represent the non-dimensional applied driving and braking moments on each wheel, respectively.

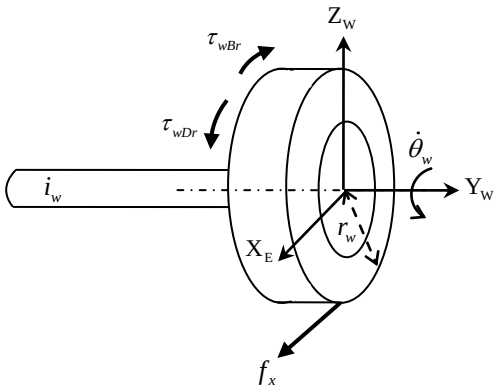

Figure 3.5 Rotational degree of freedom of wheels

3.2.3. Tire Dynamics

For vehicle dynamics modeling, proper representation of tire dynamics is essential since the functional characteristics of the vehicle (e.g. handling, ride) are significantly influenced by the tire forces. As shown in Equations (3.17)-(3.21), tire forces and moments are the dominant factors in calculating the generalized forces and play important roles in wheel dynamics. Therefore, analysis of tire dynamics is the basis for the analysis of vehicle dynamics.

Tire models can be categorized as physical, empirical, or a combination of the two, i.e., semi-empirical. Physical tire models focus on representing the interaction of the tire compound and structure mathematically. Empirical tire models curve-fit test data of existing tires to predict how the tire will respond. Semi-empirical models combine the attributes of a physical and empirical model. Most tire models that are currently available are only sufficient for modeling steady-state conditions. Many of these models lack the capabilities of modeling transient handling maneuvers, especially the response of tire friction forces. The steady-state tire models often have computational benefits, but lack the capability to model evasive or high-speed maneuvers, where the tire transient forces and moments become dominant.

Tire longitudinal force f_x and lateral force f_y depend on the vertical load on the tire such that they increase with increasing vertical tire force in pure slip conditions. The significance of tire force estimation in the modeling vehicle dynamics necessitates an accurate approximation of the vertical load on each tire. Figure 3.6 shows the vertical forces acting on a vehicle.

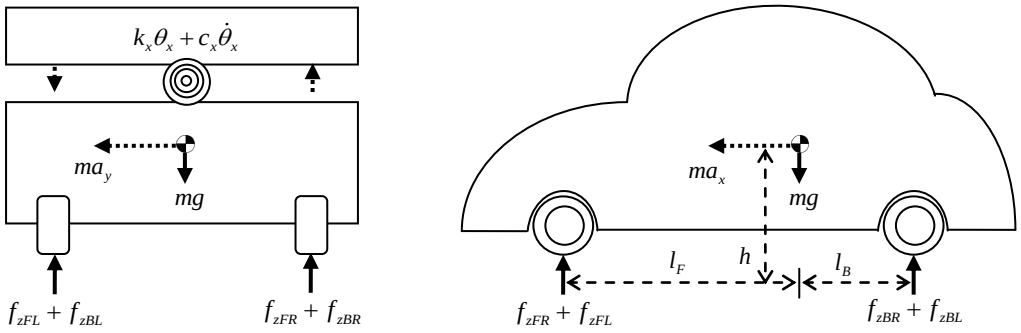

Figure 3.6 Vertical force schematics

Total tire vertical load on each wheel is the summation of static and dynamic weight distributions and are given by:

$$
\begin{aligned}
f_{zFR} &= \frac{m}{2}\left(\left(\frac{l_B}{l_F+l_B}\right)g - \left(\frac{h_s}{l_F+l_B}\right)a_x - \left(\frac{h_s}{w_R+w_L}\right)a_y - \left(\frac{h_s}{w_R+w_L}\right)\left(\frac{k_x\theta_x + c_x\dot{\theta}_x}{m_s}\right)\right)\\
f_{zFL} &= \frac{m}{2}\left(\left(\frac{l_B}{l_F+l_B}\right)g - \left(\frac{h_s}{l_F+l_B}\right)a_x + \left(\frac{h_s}{w_R+w_L}\right)a_y + \left(\frac{h_s}{w_R+w_L}\right)\left(\frac{k_x\theta_x + c_x\dot{\theta}_x}{m_s}\right)\right)\\
f_{zBR} &= \frac{m}{2}\left(\left(\frac{l_F}{l_F+l_B}\right)g + \left(\frac{h_s}{l_F+l_B}\right)a_x - \left(\frac{h_s}{w_R+w_L}\right)a_y - \left(\frac{h_s}{w_R+w_L}\right)\left(\frac{k_x\theta_x + c_x\dot{\theta}_x}{m_s}\right)\right)\\
f_{zBL} &= \frac{m}{2}\left(\left(\frac{l_F}{l_F+l_B}\right)g + \left(\frac{h_s}{l_F+l_B}\right)a_x + \left(\frac{h_s}{w_R+w_L}\right)a_y + \left(\frac{h_s}{w_R+w_L}\right)\left(\frac{k_x\theta_x + c_x\dot{\theta}_x}{m_s}\right)\right)
\end{aligned}
\tag{3.23}
$$

The first term in Equation (3.23) is the component of static weight due to vehicle center of gravity location; the second and third terms are the effects of longitudinal and lateral acceleration, respectively; and the fourth term comes from the suspension dynamics.

Calculation of other significant tire forces, i.e., lateral and longitudinal, depends on adequate knowledge of tire properties and contact patch properties. There are some semi-empirical and/or simplified models that provide tire forces as functions of slip angle,

longitudinal slip, and normal load. Before the tire models are introduced, important variables such as longitudinal slip and sideslip angle are defined.

The longitudinal slip κ is defined as the difference between the tire tangential speed and the speed of the axle relative to the road, and is given by

$$\kappa = \begin{cases} 0 & , v_{w,x} = r_w \dot{\theta}_w = 0 \\ \dfrac{r_w \dot{\theta}_w - v_{w,x}}{\max\left(r_w \dot{\theta}_w, v_{w,x}\right)} . \operatorname{sgn}\left(\left|r_w \dot{\theta}_w\right| - \left|v_{w,x}\right|\right) & , otherwise. \end{cases} \tag{3.24}$$

where the tire velocity for each wheel is approximated as

$$\begin{aligned} v_{wFL} &= \begin{pmatrix} v_x + w_L \dot{\theta}_z \\ v_y + l_F \dot{\theta}_z \end{pmatrix} \quad , \quad v_{wFR} = \begin{pmatrix} v_x - w_R \dot{\theta}_z \\ v_y + l_F \dot{\theta}_z \end{pmatrix} \\ v_{wBL} &= \begin{pmatrix} v_x + w_L \dot{\theta}_z \\ v_y - l_B \dot{\theta}_z \end{pmatrix} \quad , \quad v_{wBR} = \begin{pmatrix} v_x - w_R \dot{\theta}_z \\ v_y - l_B \dot{\theta}_z \end{pmatrix} \end{aligned} \tag{3.25}$$

The lateral tire slip angle α is defined as the angular difference between the treads in the contact patch and the direction the wheel is turned, and for each tire in steady-state condition is given by

$$\alpha_{ss} = \delta - \tan^{-1}\left(\frac{v_{w,y}}{v_{w,x}}\right) \tag{3.26}$$

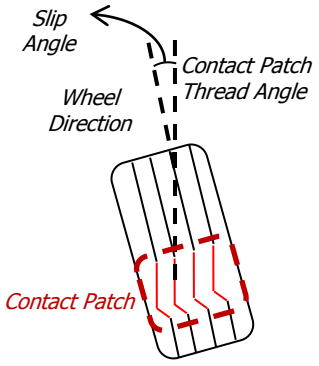

Figure 3.7 Tire slip angle

To include the tire relaxation characteristics, a first order lag model is added to equation (3.26); hence, the new slip angle definition reads

$$\sigma \dot{\alpha} + v_{w,x}\left(\alpha - \alpha_{ss}\right) = 0 \tag{3.27}$$

where σ is the tire relaxation coefficient and controls the transient response of tire sideslip angle.

3.2.3.1 Pacejka Tire Model

The Magic Formula is a semi-empirical tire model used to calculate the steady state tire forces and moment characteristics for use in vehicle dynamics studies [Pacejka, 2006]. By studying the tire force characteristic curves from physical tests, it was observed that the curves could be closely approximated by mathematical functions.

The forces (either in the longitudinal or the lateral direction) are characterized by an important number of coefficients. In pure longitudinal slip condition, the magic formula for the tire force is,

$$f = f_0\left(x, f_z\right) = D.\sin\left[C.\arctan\left(B.x' - E.\left(B.x' - \arctan\left(B.x'\right)\right)\right)\right] + S_V \tag{3.28}$$

where

$x' = x + S_H$: Slip ratio

$C = P_{C1}$: Shape factor

$D = \mu.f_z$: Peak factor

$\mu = \left(P_{D1} + P_{D2}.\delta f_z\right)$: Friction coefficient

$E = \left(P_{E1} + P_{E2}.\delta f_z\right).\mathrm{sgn}\left(x'\right)$: Curvature factor

$K = P_{K1}.f_z$

$B = K / \left(C.D\right)$: Stiffness factor

$S_H = P_{H1} + P_{H2}.\delta f_z$: Horizontal shift

$S_V = f_z\left(P_{V1} + P_{V2}.\delta f_z\right)$: Vertical shift

$\delta f_z = \left(f_z - f_{zn}\right) \big/ f_{zn}$: Normalized change in vertical load

f_{zn} : Normalized vertical load

For a set of Pacejka parameters shown in Appendix C, the normalized longitudinal and lateral tire forces in pure slip condition are plotted in Figure 3.8.

Magic Formula is later extended for combined-slip situations when the pure slip conditions are not satisfied, and the form of equation reads

$$f = G.f_0 + S_V' \tag{3.29}$$

where

f_0 : Force at pure condition as in Equation (3.28)

G : weighing function

S_V' : vertical shift induced by the other parameters

More details on combined-slip theory are provided later in this chapter.

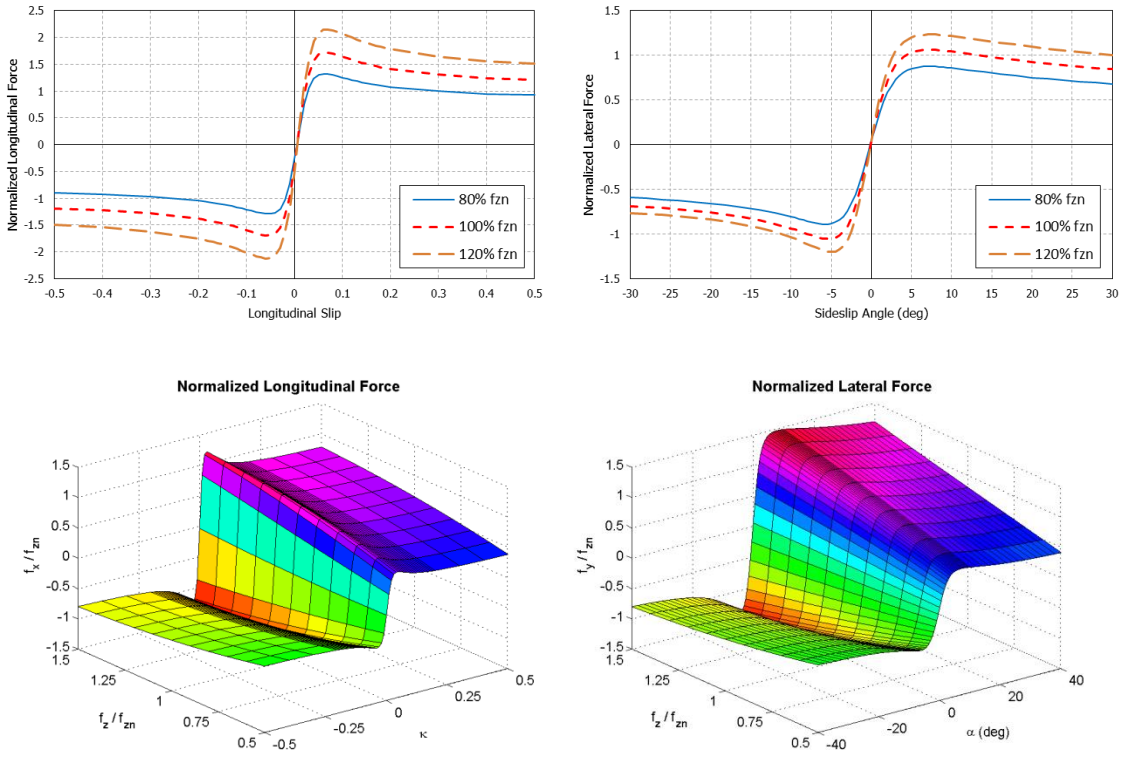

Figure 3.8 Tire forces in pure conditions based on Magic Formula tire model

3.2.3.2 LuGre Tire Model for Longitudinal Force

The LuGre model is a physics-based dynamic friction model which provides an interpretation of the friction forces as the result of elastic deformation of the surfaces in contact.

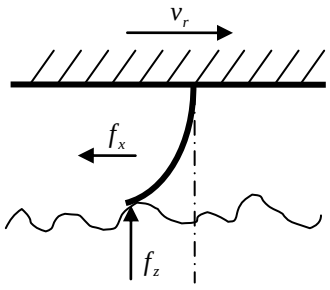

Figure 3.9 LuGre model of tire longitudinal force

The dynamic nature of the model allows the study of the transient behavior of the tire. The LuGre model also includes the Stribeck effect which accounts for the variations from the static friction, when there is no slip, to the sliding friction.

The equations for the LuGre model [Canudas de Wit, 1995] are:

$$f_x = \left(\sigma_0 \mu_n + \sigma_1 \dot{\mu}_n + \sigma_2 v_r\right) f_z \tag{3.30}$$

where

$$\dot{\mu}_n + \left(\frac{\sigma_0 |v_r|}{g(v_r)} + \bar{\kappa} \left| r_w \dot{\theta}_w \right| \right) \mu_n = v_r \tag{3.31}$$

and

$$g(v_r) = \mu_c + (\mu_s - \mu_c) e^{-|v_r / v_s|^{\bar{\alpha}}} \tag{3.32}$$

The above parameters are described as

f_x : Normalized longitudinal friction force

μ_n : Normalized longitudinal friction

f_z : Normal force

σ_0 : Normalized rubber longitudinal lumped stiffness

σ_1 : Normalized rubber longitudinal lumped damping

σ_2 : Normalized viscous relative damping

μ_c : Normalized Coulomb friction

μ_s : Normalized static friction

v_s : Stribeck relative velocity

v_r : Relative velocity between surfaces

$\bar{\alpha}$: Constant used to capture the steady-state slip characteristics

$\bar{\kappa}$: Parameter related to normal force distribution

$\dot{\theta}_w$: Angular velocity of the tire

3.2.3.3 Combined-slip Theory

Tire's tread can only generate as much horizontal force as the maximum tire-road friction force. Hence, the sum of longitudinal and lateral forces acting on each tire is limited to maximum friction force between the tire treads and the road. This effect can be illustrated in Figure 3.10 which is known as “Circle of Friction”.

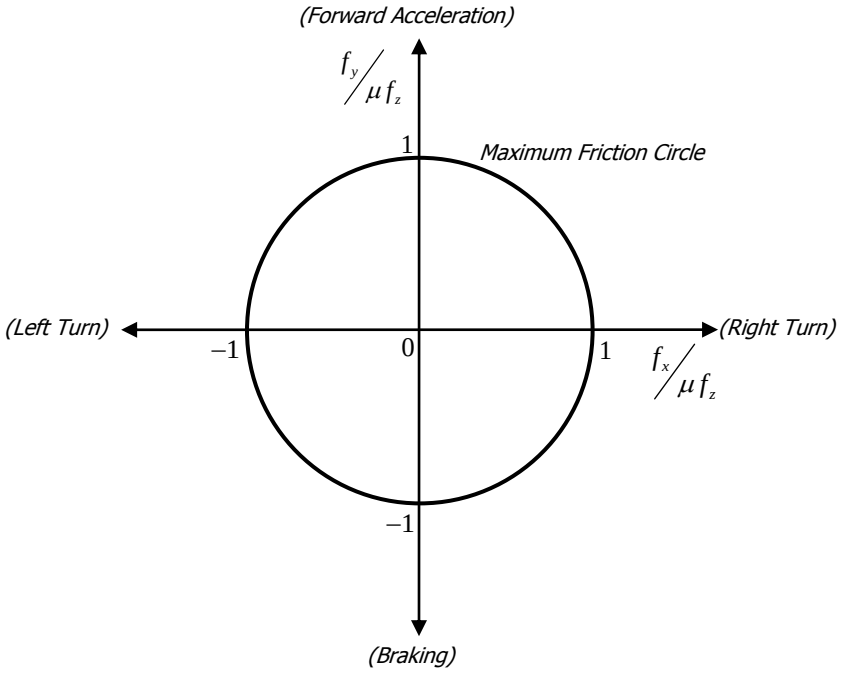

Figure 3.10 Circle of Friction

The longitudinal and lateral slips are combined to get total theoretical (combined) slip as

$$s_t = \sqrt{s_x^2 + s_y^2} \tag{3.33}$$

where the relationship between these theoretical slip quantities and the practical slip quantities are

$$s_x = -\frac{\kappa}{1+\kappa} \quad , \quad s_y = \frac{\tan(\alpha)}{1+\kappa} \tag{3.34}$$

The theoretical slips are then normalized by peak slip values, $s_{x,\max}$ and $s_{y,\max}$. Peak slip values are those that cause peak longitudinal and lateral tire forces, f_x and f_y. The total normalized slip is

$$s_{tn} = \sqrt{s_{xn}^2 + s_{yn}^2} \tag{3.35}$$

where

$$s_{xn} = \frac{s_x}{s_{x,\max}} \quad , \quad s_y = \frac{s_y}{s_{y,\max}} \tag{3.36}$$

The equivalent longitudinal and lateral slips are calculated from the normalized total theoretical slip with the friction ratio μ_0/μ,

$$\begin{aligned} \kappa_n &= \frac{\mu_0}{\mu}\left(\frac{s_{tn}.s_{x,\max}.\mathrm{sgn}(s_x)}{1+s_{tn}.s_{x,\max}.\mathrm{sgn}(s_x)}\right) \\ \alpha_n &= \frac{\mu_0}{\mu}\left(\tan^{-1}\left(s_{tn}.s_{y,\max}.\mathrm{sgn}(s_y)\right)\right) \end{aligned} \tag{3.37}$$

Using the equivalent longitudinal and lateral slips, the so-called 'base-curves' are obtained from the tire model as f_{x0}, f_{y0}. The base-curves are then modified to account for the anisotropic properties of the tire-road friction.

$$\begin{aligned} f_{x0n} &= f_{x0} - \varepsilon\left(f_{x0} - f_{y0}\right).\left(\frac{s_{yn}}{s_{tn}}\right)^2 \\ f_{y0n} &= f_{y0} - \varepsilon\left(f_{y0} - f_{x0}\right).\left(\frac{s_{xn}}{s_{tn}}\right)^2 \end{aligned} \tag{3.38}$$

where

$$\varepsilon = \begin{cases} s_{tn} & , s_{tn} < 1 \\ 1 & , s_{tn} \geq 1 \end{cases} \tag{3.39}$$

The longitudinal and lateral tire forces are then calculated by

$$f_x = f_{x0n} \cdot \frac{\mu}{\mu_0} \cdot \frac{s_x}{s_t}$$
$$f_y = f_{y0n} \cdot \frac{\mu}{\mu_0} \cdot \frac{s_y}{s_t} \tag{3.40}$$

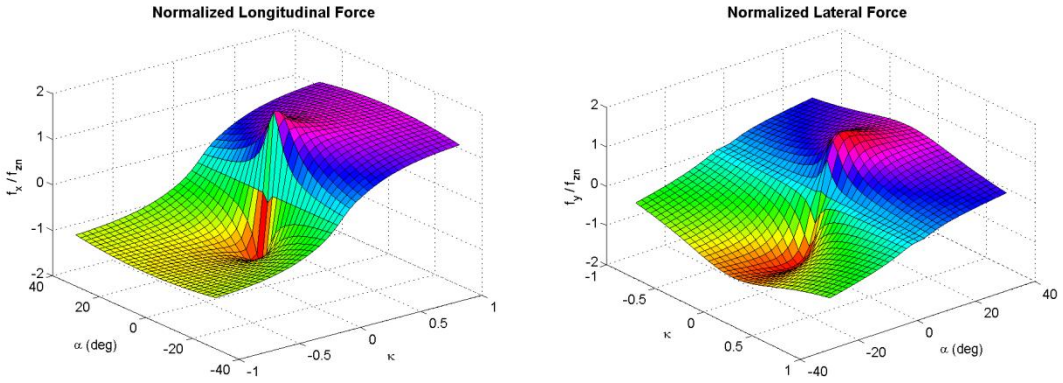

Figure 3.11 Combined-slip tire forces

For the tire parameters listed in Appendix C, the friction circle is plotted in Figure 3.12.

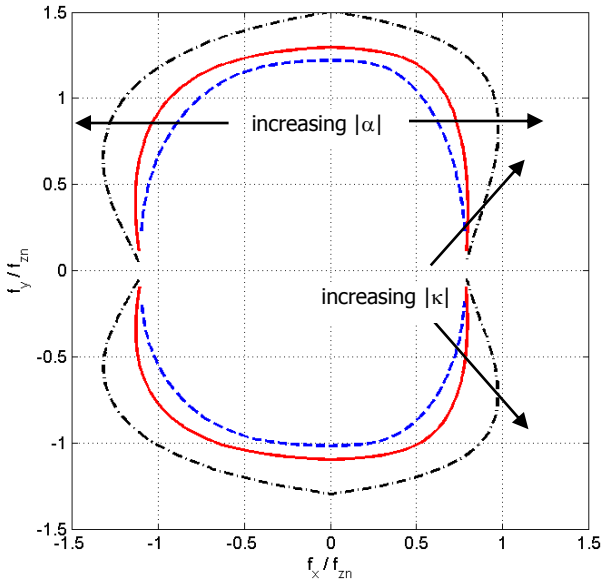

Figure 3.12 Actual circle of friction based on combined-slip theory

3.2.3.4 Linear Tire Models

Vehicle control systems are often based on a simple linear model that captures the essential characteristics that are required for the purpose of simulation and/or control task. As shown in Figure 3.13, tire forces exhibit a linear behavior for a limited range of slip. If the vehicle performs within the linear range of longitudinal slip (or sideslip angle), the tire longitudinal (or lateral) force can be represented by a linear function of longitudinal slip (or sideslip angle) as

$$f_x = c_\kappa \kappa \quad , \quad f_y = c_\alpha \alpha \tag{3.41}$$

where longitudinal slip of the tire κ was defined in (3.24), and slip angle α_{ss} is simplified to its linear form (3.26) as

$$\alpha_{linear} = \delta - \tan^{-1}\left(\frac{v_{w,y}}{v_x}\right) \tag{3.42}$$

where δ is the wheel steering angle, $v_{w,y}$ is the wheel lateral velocity, and v_x is the vehicle longitudinal speed.

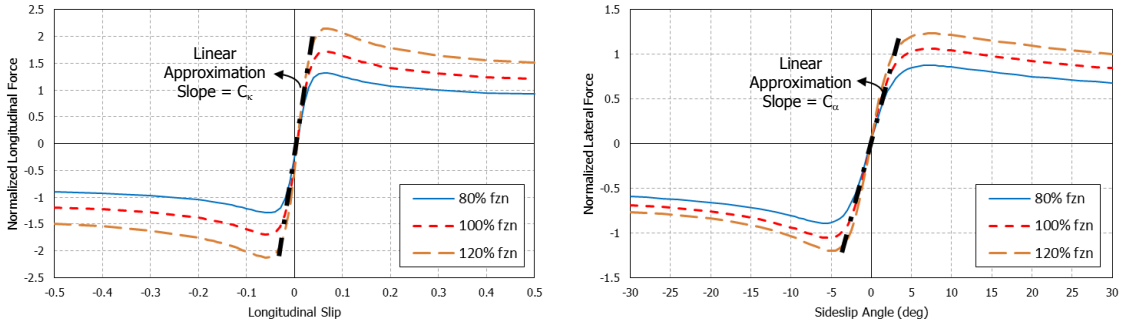

Figure 3.13 Linear tire forces

3.2.4 Simplified Linear Model of 4-Wheel Road Vehicles

Vehicle handling is becoming increasingly important for today's customers. The handling stability can be improved through various chassis control systems most of which use a linear vehicle model to estimate vehicle performance and driver's intention. Two common models include yaw, lateral velocity, and roll motions of vehicle center of gravity. These are explained in the following sections.

3.2.4.1 Linear 2-DOF Bicycle Model

Consider a simplified linear single-track bicycle model shown in Figure 3.14 which captures the essential vehicle steering dynamics including yaw and lateral motions. The tire lateral forces are assumed to be linear functions of tire slip angles.

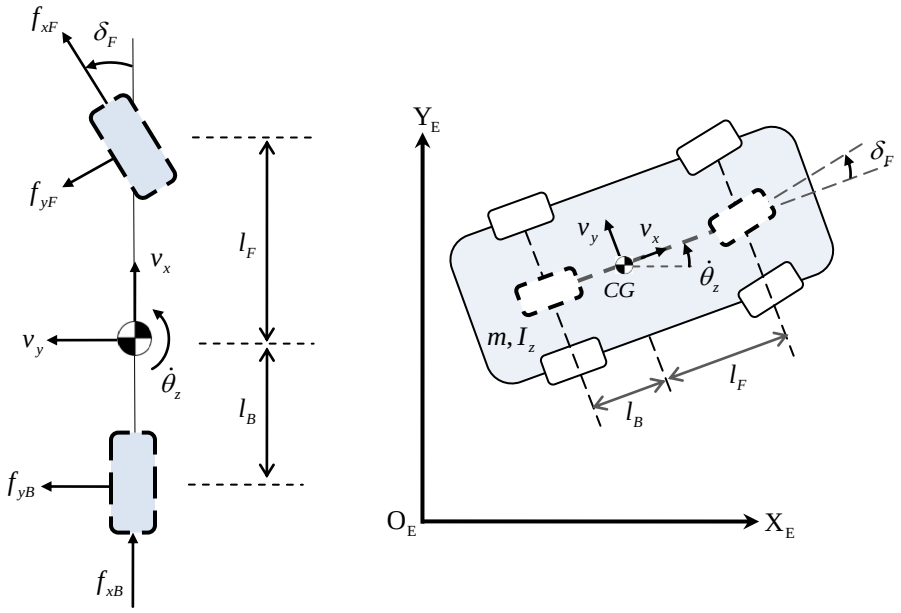

Figure 3.14 Vehicle 2-DOF bicycle model

The vehicle motion is represented by global lateral position and velocity of the vehicle center of mass as well as the yaw angle and yaw rate as shown in Figure 3.14. The state variable vector becomes

$$x = \begin{pmatrix} y & \dot{y} & \theta_z & \dot{\theta}_z \end{pmatrix}^T \tag{3.43}$$

For the sake of simplicity, the mathematical model is linearized around the operating conditions $x^* = 0_{4\times1}, \delta_F^* = 0$. The equations of motion for a constant forward speed v_x are given by

$$\dot{x} = \mathbf{A}x + \mathbf{B}\delta_{sw} \tag{3.44}$$

where

$$\mathbf{A}=\begin{bmatrix} 0 & 1 & v_x & 0 \\ 0 & -\dfrac{c_{\alpha F}+c_{\alpha B}}{mv_x} & 0 & -v_x-\dfrac{l_F c_{\alpha F}-l_B c_{\alpha B}}{mv_x} \\ 0 & 0 & 0 & 1 \\ 0 & \dfrac{l_F c_{\alpha F}-l_B c_{\alpha B}}{i_z v_x} & 0 & -\dfrac{l_F^2 c_{\alpha F}+l_B^2 c_{\alpha B}}{i_z v_x} \end{bmatrix}, \mathbf{B}=\begin{bmatrix} 0 \\ \dfrac{c_{\alpha F}}{r_{st} m} \\ 0 \\ \dfrac{l_F c_{\alpha F}}{r_{st} i_z} \end{bmatrix}$$

The linear model (3.44) considers only two degrees of motion, namely, lateral and yaw. Therefore, this simple model can be only applied to generate later control strategies for lateral and yaw stability while the other parameters of vehicle dynamics are negligible. When the effects of other dynamics parameters are large enough, adequate degrees of freedom should be added to take those parameters into account.

3.2.4.2 Linear 3-DOF Model

In some cases the effect of load transfer due to roll cannot be neglected; therefore, roll motion is added to the linear bicycle model. The schematic front view of a simple vehicle model with three degrees of freedom, i.e., lateral velocity, yaw rate, and roll angle, is shown in Figure 3.15. The state variable vector becomes

$$x=\begin{pmatrix} \dot{y} & \dot{\theta}_z & \theta_x & \dot{\theta}_x \end{pmatrix}^T \tag{3.45}$$

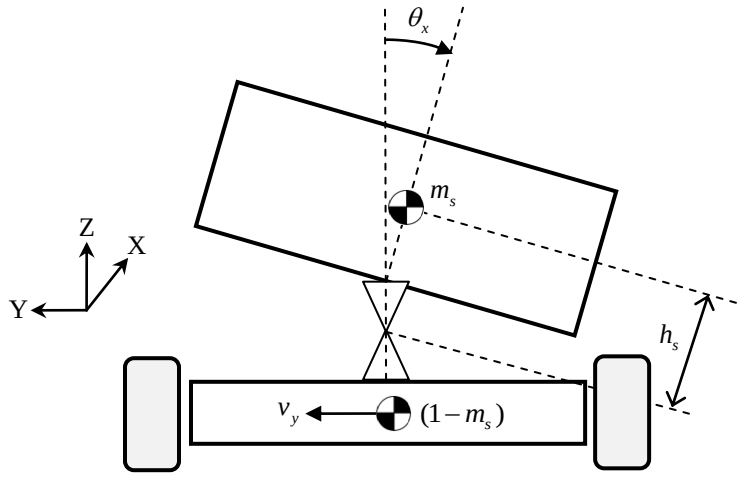

Figure 3.15 Linear 3-DOF Vehicle Model

The equations of motion for a linear 3-DOF vehicle model can be formulated as

$$\dot{x}=\underset{\mathbf{A}}{\mathbf{C}^{-1}\mathbf{D}}\,x+\mathbf{B}\delta_{sw} \tag{3.46}$$

where

$$\mathbf{C}=\begin{bmatrix} m & 0 & 0 & m_s h_s \\ 0 & i_z & 0 & 0 \\ 0 & 0 & 1 & 0 \\ mh & 0 & c_x & i_x + m_s h_s^2 \end{bmatrix},\ \mathbf{D}=\begin{bmatrix} -\dfrac{c_{\alpha f}+c_{\alpha B}}{v_x} & -v_x - \dfrac{l_F c_{\alpha F} - l_B c_{\alpha B}}{v_x} & 0 & 0 \\ -\dfrac{l_F c_{\alpha F} - l_B c_{\alpha B}}{v_x} & -\dfrac{l_F^2 c_{\alpha F} + l_B^2 c_{\alpha B}}{v_x} & 0 & 0 \\ 0 & 0 & 0 & 1 \\ 0 & -mh_s v_x & -k_x + m_s g h_s & 0 \end{bmatrix}$$

$$\mathbf{B}=\begin{bmatrix} \dfrac{c_{\alpha F}}{r_{st} m} & \dfrac{l_F c_{\alpha F}}{r_{st} i_z} & 0 & 0 \end{bmatrix}^T$$

where k_x is total roll stiffness, c_x is total roll damping, and g is the gravity constant.

The presented model includes three degrees of freedom, namely, lateral, yaw, and roll. While the linear bicycle model is good enough for yaw stabilization, linear formulation of this model as given by (3.46) makes it quite simple for designing control strategies that stabilize not only yaw and lateral motions, but also roll motion of the vehicle at the same time.

3.3. Control Systems

Various types of active control systems have been developed in the past to enhance the stability and handling characteristics of the vehicle. Active front steering, active rear steering, four-wheel steering, active suspension, and antilock braking system are some of the options widely explored. In this research, the system of wheel speed control, i.e., cruise/brake, are developed and implemented in the final design.

3.3.1. Cruise Control

The cruise control system offers three major advantages: maintained vehicle speed, improved fuel economy by maintaining a steady accelerator pressure, and increased driver comfort on long distance trips [Givens, 1975]. A modern cruise control system will maintain a near constant vehicle speed $v_{x,des}$ and help those heavy-footed drivers from exceeding the legal speed limit.

Ignoring the engine model and throttle dynamics, a simple PID cruise control can be introduced for a rear-axle drive vehicle as

$$\tau_{wDr} = \begin{cases} \frac{1}{2}\mathfrak{L}_{PID}\left(v_{x,des} - v_x\right).\begin{bmatrix}0 & 0 & 1 & 1\end{bmatrix}^T & , v_{xd} > v_x \\ 0_{1\times 4} & , v_{xd} \le v_x \end{cases} \tag{3.47}$$

where τ_{wDr} is the wheel driving torque as shown in Figure 3.5, and the PID operator $\mathfrak{L}_{PID}$ is defined as

$$\mathfrak{L}_{PID} = k_{pcc} + k_{icc}\int_0^t dt + k_{dcc}\frac{d}{dt} \tag{3.48}$$

Finally, the cruise control system (3.47) is modified as shown in Figure 3.16,

Figure 3.16 Cruise control system

to account for the driving torque threshold of the engine as well as the wheel slip control. In this research, a simple version of Active Slip Control (ASC) is applied in which the wheel driving torques are weighted as

$$ASC = \begin{cases} 0 & , v_x \le 0.7v_{avg} \\ \frac{1}{0.15}\left(\frac{v_x}{v_{avg}} - 0.7\right) & , 0.7v_{avg} < v_x < 0.85v_{avg} \\ 1 & , v_x \ge 0.85v_{avg} \end{cases} \tag{3.49}$$

where v_{avg} for a rear-axle drive vehicles is the average of the rear wheel rotational speeds as

$$v_{avg} = \left(\frac{r_w\dot{\theta}_{wBR} + r_w\dot{\theta}_{wBL}}{2}\right) \tag{3.50}$$

As discussed in Section 3.2.4, a key assumption in developing linear vehicle models is constant vehicle speed. Since the linear vehicle models form the main structure of the

control strategies in this research, later in the next chapter the proposed cruise control (3.47)-(3.49) will be applied to maintain the vehicle speed at a desired level.

3.3.2. Differential Braking

Differential Braking controls the yaw motion of the vehicle by distributing the wheel braking torques. The proposed Differential Braking system is composed of a series of control blocks including Active Slip Control (ASC), Differential Brake Distributor (DBD), and Anti-lock Braking System (ABS). It interprets the desired corrective yaw moment τ_{zc} as the desired wheel braking torques τ^*_{wBr} such that excessive wheel slip are controlled using ASC. The desired wheel braking torques are then fed to ABS which controls the tire slip ratio through a bang-bang control strategy. The schematic view of the proposed Differential Braking system is shown in Figure 3.17.

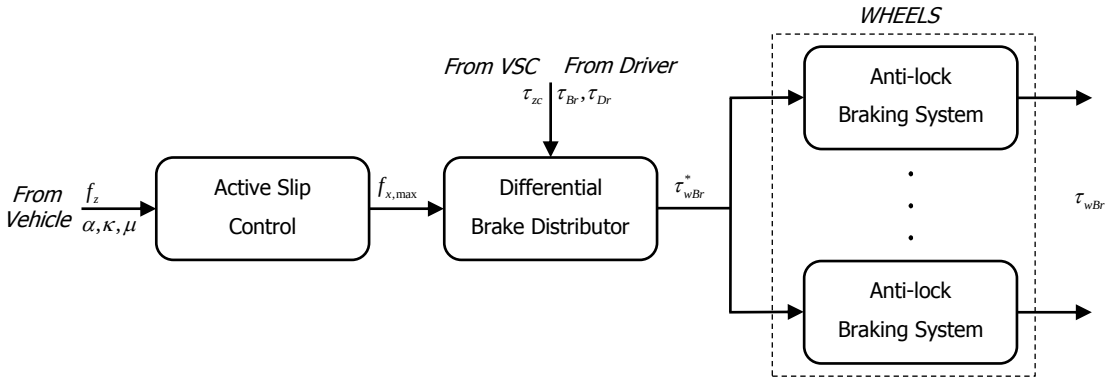

Figure 3.17 Differential Braking System

As a part of differential braking system, an Active Slip Control (ASC) for braking system is developed such that the maximum braking force at each wheel is estimated as

$$f_{x,\max} = \begin{cases} 0 & , \ \kappa \geq 0.8 \\ \mu f_z \left(\dfrac{\kappa}{\sqrt{\kappa^2 + \tan^2(\alpha)}} \right) & , \ \kappa < 0.8 \end{cases} \tag{3.51}$$

based on the current tire-road friction μ and the tires vertical loads f_z, longitudinal slip κ, and side slip angle α. The static map of the Active Slip Control (ASC) strategy

(3.51) for the braking system is shown in Figure 3.18 in which the normalized maximum braking force $f_{x,\max}/\mu f_z$ is plotted against longitudinal slip κ and side slip angle α.

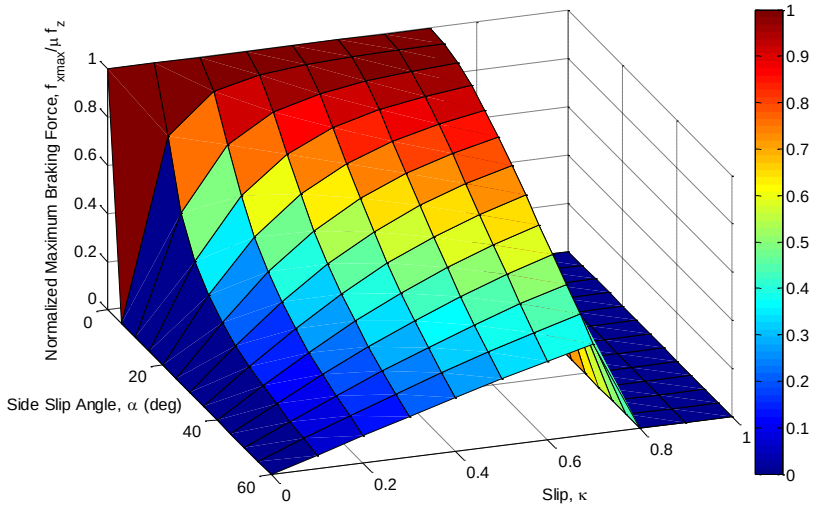

Figure 3.18 ASC static map

Differential Brake Distributor (DBD) consists of a microprocessor that computes the braking/driving torques at each wheel based on the desired total braking/driving torques, i.e., $\tau_{decel}, \tau_{accel}$, from the deceleration/acceleration pedals and the maximum allowed longitudinal force at each wheel $f_{x,\max}$ as well as the required corrective yaw moment τ_{zc} from the Vehicle Stability Control (VSC) system. The system minimizes the squared sum of wheel longitudinal forces f_x constrained to the following set of equalities and inequalities:

$$\begin{cases} f_{xFR} + f_{xFL} + f_{xBR} + f_{xBL} = \dfrac{\tau_{accel} - \tau_{decel}}{r_w} \\ f_{xFR} - f_{xFL} + f_{xBR} - f_{xBL} = \dfrac{\tau_{zc}}{w} \\ |f_{xFR}| \le f_{xFR,\max} \\ |f_{xFL}| \le f_{xFL,\max} \\ |f_{xBR}| \le f_{xBR,\max} \\ |f_{xBL}| \le f_{xBL,\max} \end{cases} \tag{3.52}$$

Solving (3.52) for the wheel longitudinal forces f_x, the wheel braking torques are given by

$$\tau^{*}_{wBr,i} = \max\left(r_w f_{x,i} + \tau_{wDr,i}, \tau_{wBr,\max}\right), \quad i = \{FR, FL, BR, BL\} \tag{3.53}$$

where the wheel driving torques $\tau_{wDr,i}$ are the output of the cruise control system as described in Section 3.3.1, and the maximum allowed braking torque at wheels is given by $\tau_{wBr,\max}$.

After the Differential Brake Distributor system calculates the wheel braking torques $\tau^{*}_{wBr,i}$ the outputs are fed into the Anti-lock Braking Systems. The Anti-lock Braking System (ABS) is a closed-loop control device that prevents wheel lock-up during braking, and as a result vehicle stability and steering is maintained [SAE, 1992]. Wheel lock-up is an unwanted situation due to a high braking force. In ABS-equipped vehicles ECU recognizes the wheel lock-up as a sharp increase in wheel deceleration, ABS functions to limit the braking pressure to prevent wheel lock-up. The Braking force is reapplied until the onset of wheel lock-up is again detected at which point it again reduces the brake force in a closed loop process. The cyclic application and reduction of braking force ensures that the brakes operate near their most efficient point and maintains steering control [Burton, 2004]. When the driver applies the brake, brake slip increases and at the point of maximum friction between tire and road surface the limit between the stable and unstable range is reached. At this point any increase in brake pressure will not increase the stopping force; as further brake pressure is applied the friction reduces and the wheel tends towards skidding.

Adopting from [Tanelli, 2007], the Antilock Braking System (ABS) actuator is considered as a Hydraulic Actuated Brake (HAB) in which the pressure exerted by the driver on the pedal is transmitted to the hydraulic system via a valve such that the increase and decrease pressure actions are physically limited by the actuator rate limit as $\dot{\tau}_{wBr} = k_b$ with a positive rate limit k_b. The switching logic that governs ABS is based on a bang–bang control strategy introduced by Tanelli [2007] and is given by

$$\begin{cases} \tau_{wBr} = \tau_{wBr}^{*} & ,\kappa < \kappa_{\min} & \text{(A)} \\ \dot{\tau}_{wBr} = k_b & ,\kappa_{\min} < \kappa \le \kappa_{\max} \;\&\; \tau_{wBr,\min} \le \tau_{wBr} \le \tau_{Br,\max} & \text{(B)} \\ \dot{\tau}_{wBr} = 0 & ,\kappa_{\min} < \kappa \le \kappa_{\max} \;\&\; \tau_{wBr} \ge \tau_{Br,\max} & \text{(C)} \\ \dot{\tau}_{wBr} = 0 & ,\kappa_{\min} < \kappa \le \kappa_{\max} \;\&\; \tau_{wBr} \le \tau_{Br,\min} & \text{(D)} \\ \dot{\tau}_{wBr} = -k_b & ,\kappa > \kappa_{\max} & \text{(E)} \end{cases} \tag{3.54}$$

Figure 3.19 shows a sample ABS operation limit cycle created by the bang–bang control (also known as the hysteresis control) strategy (3.54).

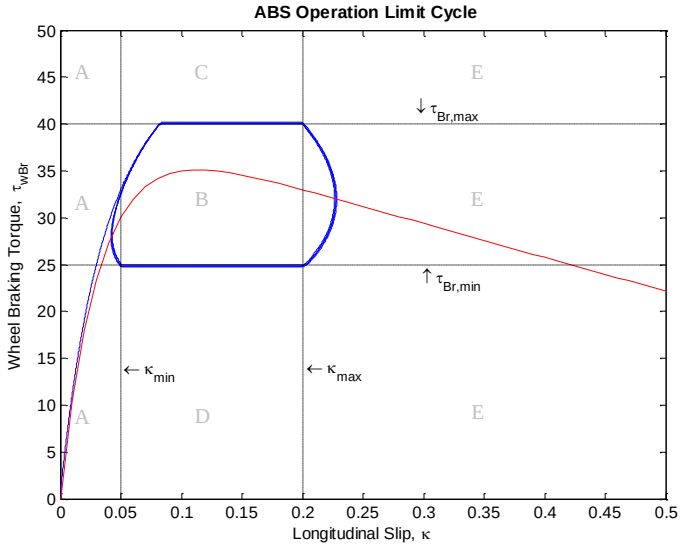

Figure 3.19 ABS operation limit cycle using bang-bang control strategy

Based on CarSim8 [Mechanical Simulation, 2009], the following values are implemented in the final design of the Anti-lock Braking System (ABS):

Table 3.1 ABS parameters

Wheel / Parameters	$\kappa_{\min}$	$\kappa_{\max}$	$\tau_{B,\min}$	$\tau_{B,\max}$	k_b
Front Wheels	0.09	0.15	25	40	10
Rear Wheels	0.09	0.12	25	40	10

The proposed Differential Braking system interprets the desired corrective yaw moment τ_{zc} as the wheel braking torques τ_{wBr} while controlling the wheel slip, and thus, preventing wheel lockup through implementation of an Antilock Braking System (ABS).

The application of the proposed differential braking system to generate a desired yaw moment will be illustrated in the next chapter.

3.4. Driver Models

Driver steering control in regulation tasks have been investigated in numerous driver/vehicle related studies. The directional control models of interest here apply to straight or curving roadways, with approximately constant driver steering actions to stay in the center of the lane in the presence of a random (directional) yaw disturbance.

First, a continuous-time preview driver model is reviewed based on [Weir, 1970]. This preview/predictor model provides a steer input that would minimize the error between a desired path and actual vehicle position using preview time t_p and human lag time t_d.

Adopted from Sharp [2001], the second model is a mathematical driver model using a proportional correction of the yaw angle and the lateral displacement. The final driver model is derived using quadratic discrete optimization of the vehicle lateral and yaw errors.

3.4.1. Continuous-Time Model

Preview/predictor models attempt to provide a steer input that would minimize the error between a desired path and actual vehicle position. The schematics of the maneuver task geometry is shown in Figure 3.20 where the driver compare the vehicle position at some future distance with the target path corresponding to that point. The vehicle position ahead is estimated from the current position of the vehicle. The driver estimates the vehicle's future position at the preview point by assuming the vehicle continues to travel in a straight line at the current heading angle.

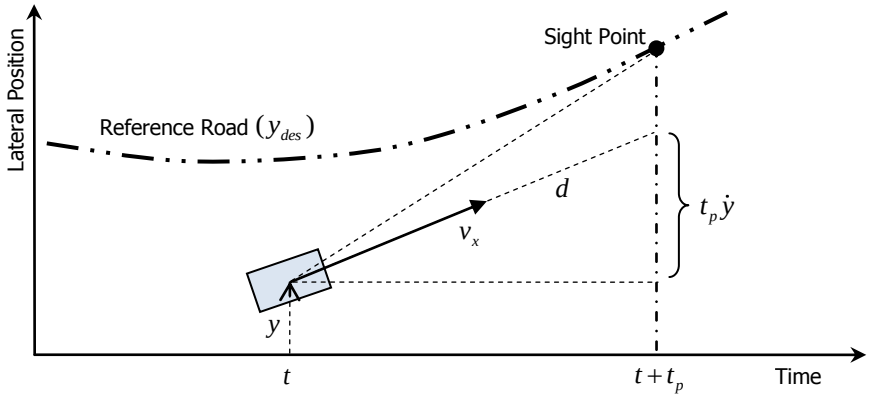

Figure 3.20 Schematic of maneuver task geometry

The desired steering wheel angle δ_{SW}^* that minimizes the error between the target path and the actual vehicle position is given by

$$\delta_{sw}^*(t+t_d) = \frac{2r_{st}d}{\left(v_x t_p\right)^2}.\left(y_{des}(t+t_p) - y(t) - t_p\dot{y}(t)\right) \tag{3.55}$$

The driver reaction time which represents the driver's decision time plus the time required to transmit the actuation signal to his/her limbs is modeled as a first-order time lag t_d.

3.4.2. Discrete-Time Model

This linear vehicle model is translated to discrete-time difference equation as

$$x_d^+ = \mathbf{A}_d x_d + \mathbf{B}_d \delta_{sw} \tag{3.56}$$

where x_d, x_d^+ represent the discrete state (3.43) for current and next time step, respectively, and $\mathbf{A}_d, \mathbf{B}_d$ are obtained from the discrete bilinear transformation [Matsuno, 1984] of the corresponding continuous-time matrices $\mathbf{A}, \mathbf{B}$ in (3.44).

To extend the vehicle model (3.56) by road preview, the concept of multi-point preview model of path-following steering control is adopted from Sharp [2001] which originates from linear discrete-time preview control of active suspension. The inputs to the model are effectively the discrete states of the vehicle x_d and the reference road samples y_{ri};

the output of the model is the steering angle δ_{sw}. Hence, the lateral profile of the road is considered in discrete sample value form with sample values from road observations being stored as states of the full vehicle/road system.

$$z = \left(x_d^T, y_{r0}, y_{r1}, y_{r2}, ..., y_{rN} \right)^T \tag{3.57}$$

where y_{r0} is the road reference position at one step before the current time, y_{r1} is the current reference position, and $y_{r2}, ..., y_{rN}$ are road reference positions at $(N-1)$ time steps ahead.

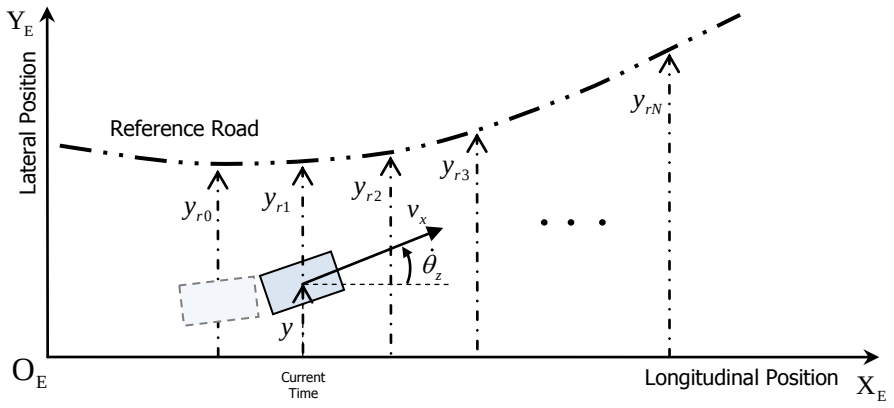

Figure 3.21 Schematic of discrete maneuver task geometry

As the system moves forward in time, a new road sample value is read in and the oldest stored value is discarded. All the other road sample values are shifted through the time step which may be represented mathematically by

$$y_r^+ = \mathbf{A}_r y_r + \mathbf{B}_r y_{r(N+1)} \tag{3.58}$$

where

$$\mathbf{A}_r = \begin{bmatrix} \mathbf{0}_{N\times 1} & \mathbf{I}_{N\times N} \\ 0 & \mathbf{0}_{1\times N} \end{bmatrix} \quad , \quad \mathbf{B}_r = \begin{bmatrix} \mathbf{0}_{N\times 1} \\ 1 \end{bmatrix}$$

Combining vehicle and road equations (3.56) and (3.58) yields the full dynamic system description

$$\underbrace{\begin{bmatrix} x_d^+ \\ y_r^+ \end{bmatrix}}_{z^+} = \underbrace{\begin{bmatrix} \mathbf{A}_d & 0 \\ 0 & \mathbf{A}_r \end{bmatrix}}_{\mathbf{A}} \underbrace{\begin{bmatrix} x_d \\ y_r \end{bmatrix}}_{z} + \underbrace{\begin{bmatrix} \mathbf{B}_d \\ 0 \end{bmatrix}}_{\mathbf{B}} \delta_{sw} + \underbrace{\begin{bmatrix} 0 \\ \mathbf{B}_r \end{bmatrix}}_{\mathbf{E}} y_{r(N+1)} \tag{3.59}$$

If the reference sample y_{ri} is a white-noise sample from a random sequence, the state-preview system (3.59) is controllable if the state system (3.44) is controllable, i.e., if $(\mathbf{A}, \mathbf{B})$ is controllable [Sharp, 2001].

For the discrete preview model (3.59), the driver steering control can be represented as linear feedback system in which the gains are derived using linear quadratic regulation (LQR) method. The driver control objective is to reduce the vehicle state error with respect to their corresponding desired values while keeping the steering angle bounded. Hence, if the driver priorities over the vehicle state errors are known, the objective function can be written as

$$J = \sum_t \left((z - z_d)^T \mathbf{Q} (z - z_d) + \delta_{sw}^2 \right) \tag{3.60}$$

Solving the LQR problem for the system (3.59) constrained to the objective function (3.52), the optimal steering angle is found in the following linear feedback form:

$$\delta_{sw}^* = \mathbf{G} \left(z - z_d \right) \tag{3.61}$$

This preview model will be discussed in more details in the next chapter.

3.5. Simulation and Results

Based on the vehicle dynamics discussed in this chapter, a user-friendly MATLAB toolbox is developed that is called Vehicle System Simulator (or VSS). This toolbox uses the discrete-time ode-3 solver and is mainly based on Level-2 s-function design. The GUI part of the toolbox takes user inputs including vehicle parameters, event specifications, and plot configurations, while the Simulink model contains the mathematical model of the designated vehicle dynamics. The screenshots of Vehicle System Simulator are shown in Figure 3.22.

For the non-dimensional analysis, the vehicle speed U_{car}, total mass M_{car}, and front to rear axle length L_{car} are considered to form the three primary dimensions: time $[T]$, mass $[M]$, and length $[L]$ as

$$[M] = M_{total} \quad , \quad [L] = L_{car} \quad , \quad [T] = L_{car} \Big/ U_{car} \tag{3.62}$$

The evaluation vehicle is the CarSim's D-class sedan with parameters listed in Appendix C. The vehicle is moving at $20(m/s)$, i.e., $72(km/h)$, when it starts to constantly steer at $-30°$ steering wheel angle. The significant non-dimensional vehicle parameters are

$$\begin{aligned} &[M] = 1450 \quad , \quad [L] = 2.78 \quad , \quad [T] = 0.139 \\ &m = 1 \quad , \qquad m_s = 0.9448 \\ &l_F = 0.3993, \qquad l_B = 0.6007, \qquad h_s = 0.1457 \\ &i_x = 0.0541, \qquad i_y = 0.3741, \qquad i_z = 0.3741 \\ &k_x = 0.3448, \qquad c_x = 0.0496, \qquad \mathrm{r}_{st} = 17.25 \end{aligned} \tag{3.63}$$

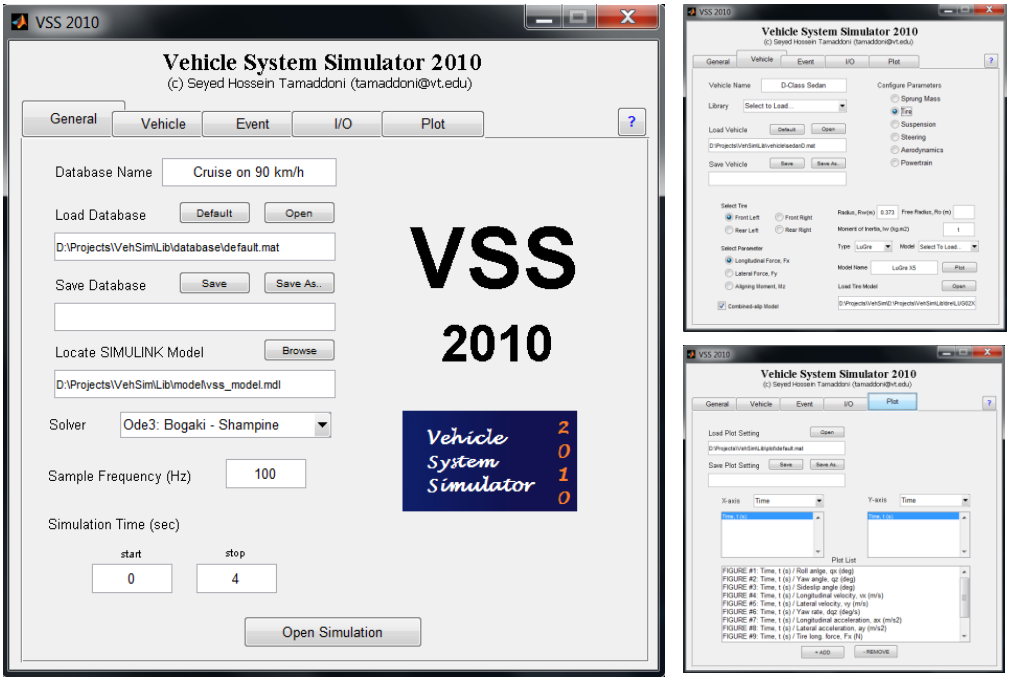

Figure 3.22 MATLAB GUI of Vehicle System Simulator

In order to assess the viability of the control algorithms that are designed, a more realistic simulation environment is required. CarSim is a software package developed by

Mechanical Simulation Corporation that offers an accurate representation of real world road vehicles. To assure the accuracy of the vehicle simulation model the mathematical models are validated against CarSim8.

3.4.1. Nonlinear Model

To evaluate our vehicle dynamics model, the evaluation scenario is done in both CarSim8 and Vehicle System Simulator (VSS). The CarSim8 plot data are then plotted along with the VSS results. The simulation results are shown in Figure 3.23 and 3.24.

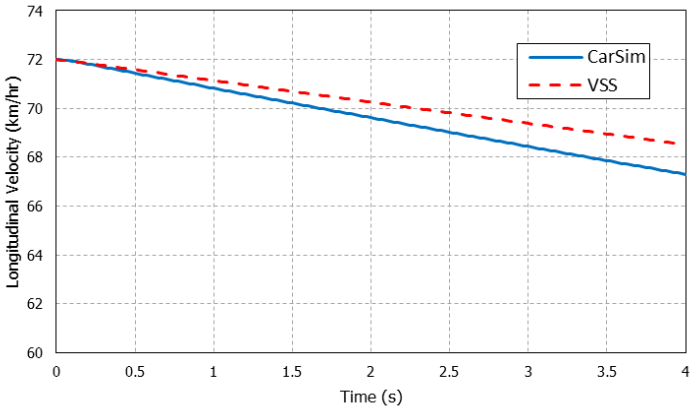

(a)

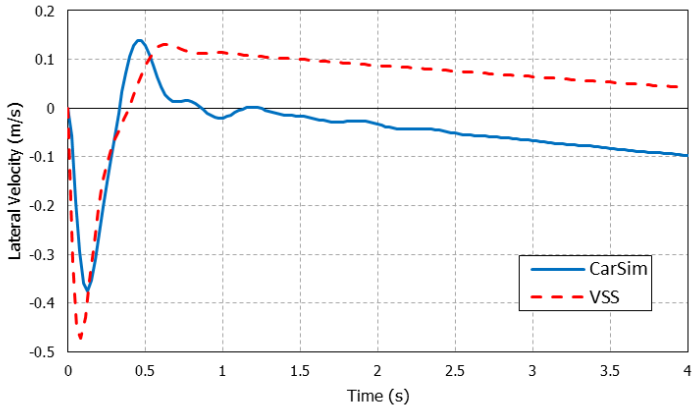

(b)

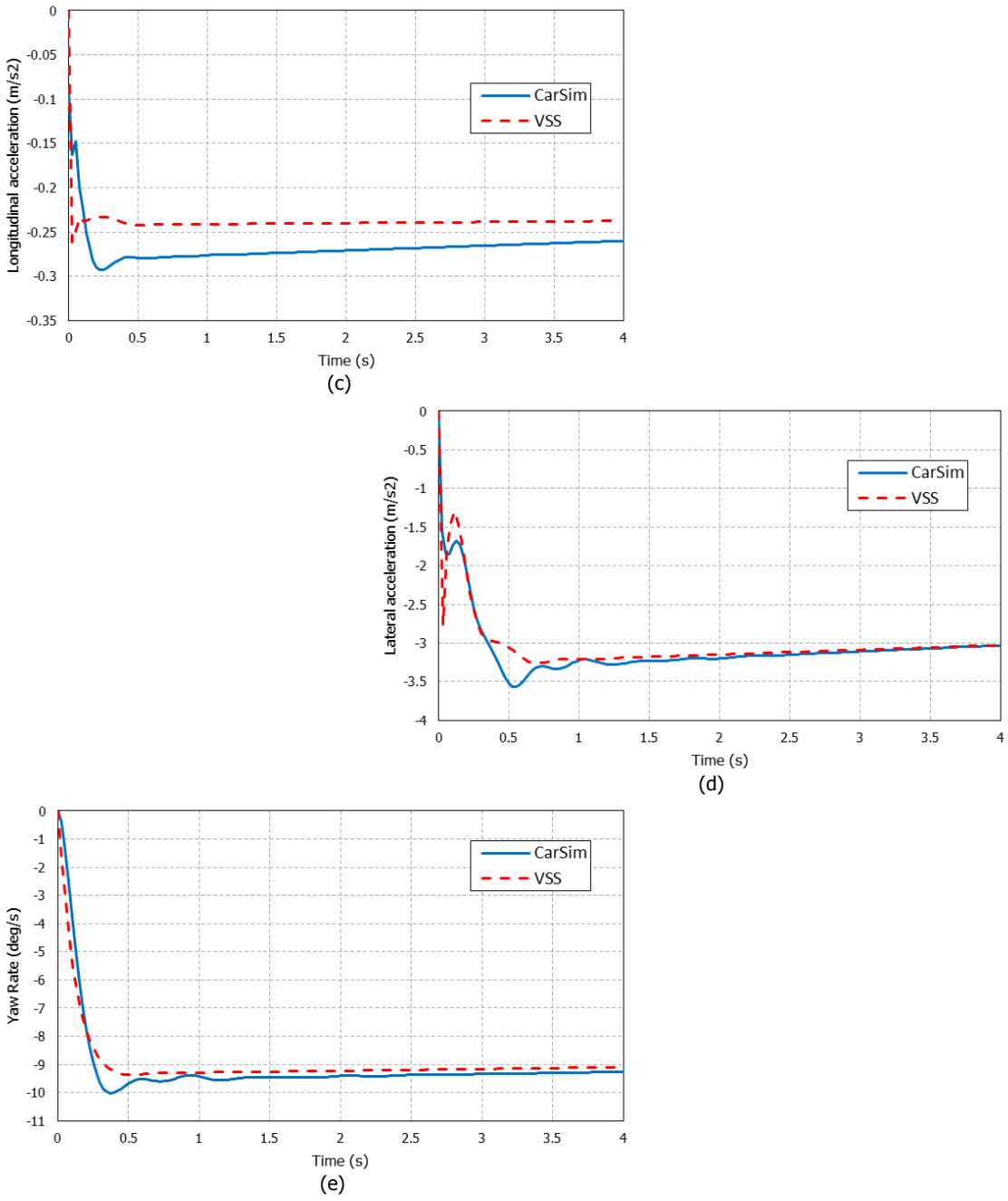

Figure 3.23 Evaluation results; vehicle sates: (a) longitudinal velocity, (b) lateral velocity, (c) longitudinal acceleration, (d) lateral acceleration, (e) yaw rate

Figure 3.23 shows that the vehicle states throughout the simulation. Although the simulation results fairly match the CarSim results, slight deviations are expected due to inadequacy of degrees of freedom in the developed model, particularly in the suspension and powertrain systems.

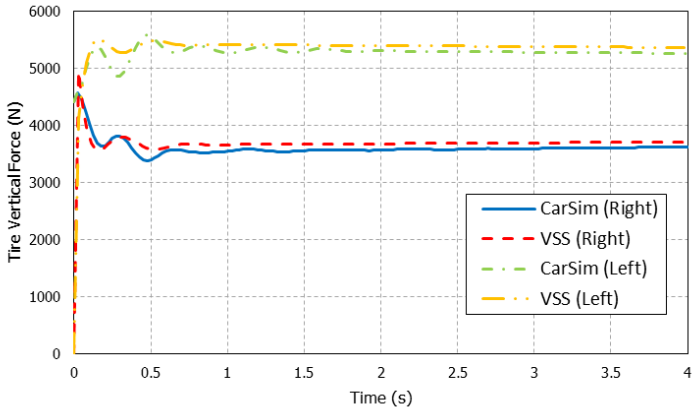
Tire Vertical Force (N)
Time (s)
CarSim (Right)
VSS (Right)
CarSim (Left)
VSS (Left)

(a)

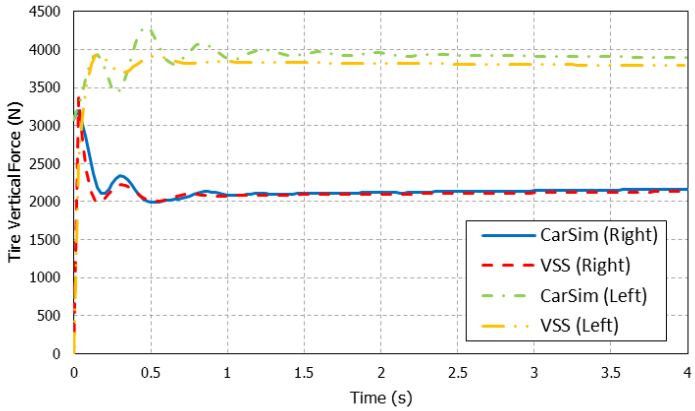
Tire Vertical Force (N)
Time (s)
CarSim (Right)
VSS (Right)
CarSim (Left)
VSS (Left)

(b)

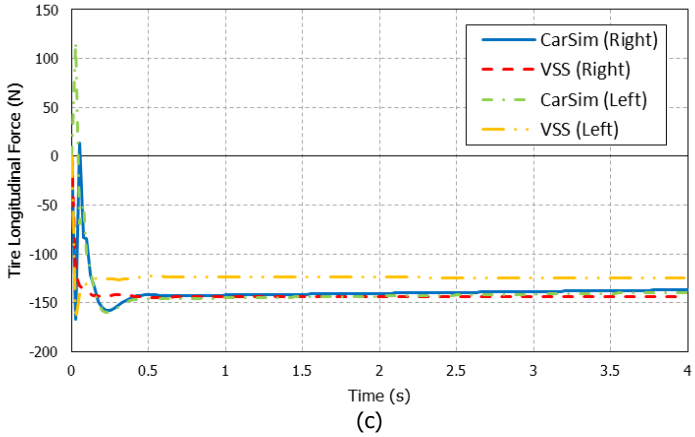
Tire Longitudinal Force (N)
Time (s)
CarSim (Right)
VSS (Right)
CarSim (Left)
VSS (Left)

(c)

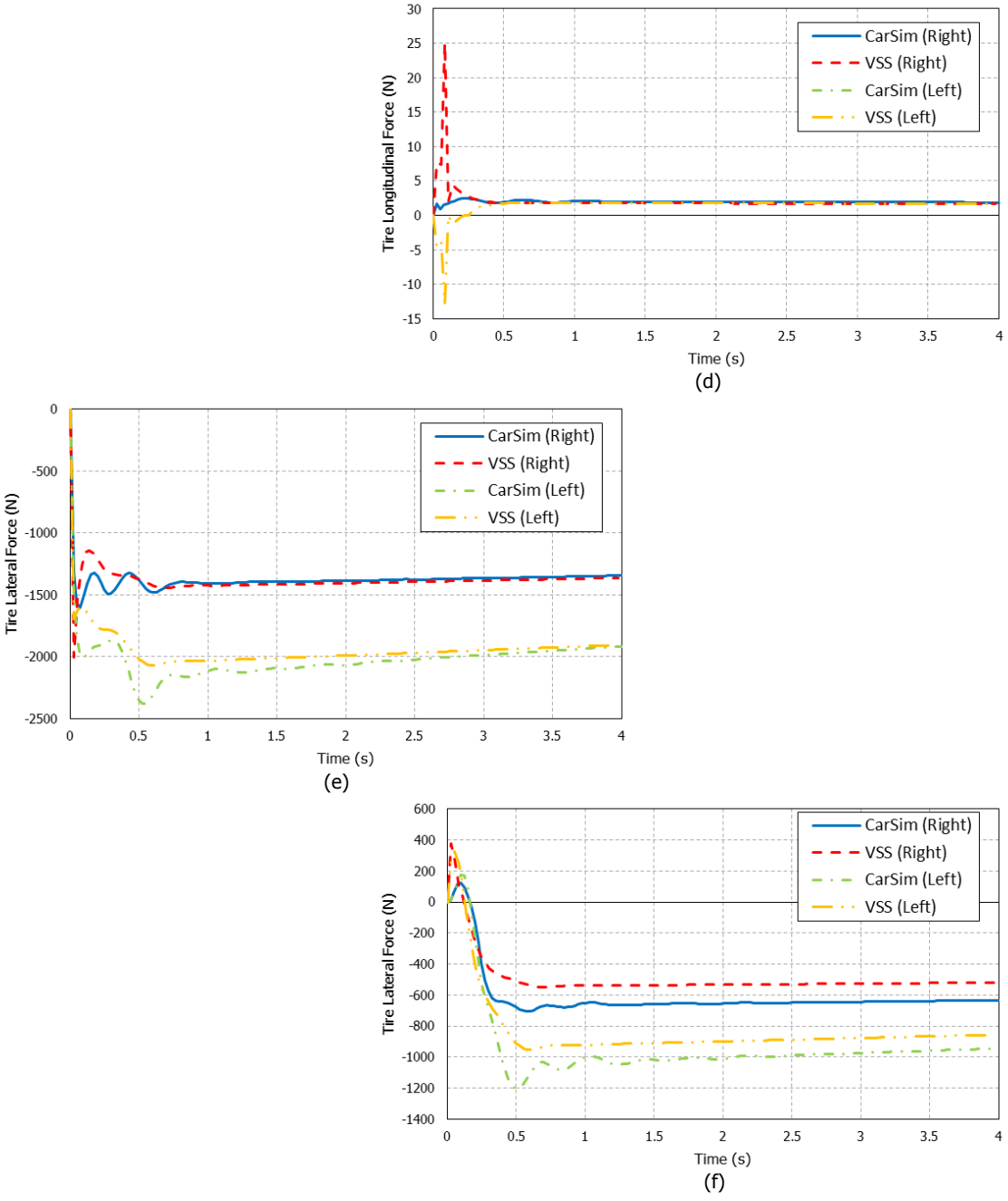

Figure 3.24 Evaluation results; tire forces: (a) vertical force on front axle wheels, (b) vertical force on rear axle wheels, (c) longitudinal force on front axle wheels, (d) longitudinal force on front axle wheels, (e) lateral force on front axle wheels, (f) lateral forces on rear axle wheels

Figure 3.24 shows that the tire forces throughout the simulation. The simulation results fairly match the CarSim results for vertical and longitudinal forces, while the lateral force estimation slightly differs from what the CarSim gives out which is emerged from the simplicity assumption in the developed model, particularly in modeling the suspension system.

3.4.2. Linear Models

The linear models (3.46) and (3.48) are simulated in the evaluation scenario. Once again, the CarSim's D-class sedan is moving at $20(m/s)$ when it starts to steer at $-30°$ steering wheel angle. The simulation results including lateral velocity, yaw rate, and roll angle are plotted in Figure 3.21 along with the CarSim and Vehicle System Simulator results.

For the vehicle parameters given in (3.63), the "non-dimensional" state matrix $\mathbf{A}$ and the "non-dimensional" control matrix $\mathbf{B}$ of the linear two and three degree-of-freedom models (3.48) become

$$\mathbf{A}_{2-DOF} = \begin{bmatrix} 0 & 1 & 1 & 0 \\ 0 & -1.150 & 0 & -0.884 \\ 0 & 0 & 0 & 1 \\ 0 & 0.3097 & 0 & -0.8 \end{bmatrix} \quad , \quad \mathbf{B}_{2-DOF} = \begin{bmatrix} 0 \\ 0.0333 \\ 0 \\ 0.0356 \end{bmatrix} \tag{3.64}$$

$$\mathbf{A}_{3-DOF} = \begin{bmatrix} -1.880 & -0.811 & 1.0858 & 0.1621 \\ 0.3097 & -0.8 & 0 & 0 \\ 0 & 0 & 0 & 1 \\ 3.9782 & -0.401 & -5.916 & -0.883 \end{bmatrix} \quad , \quad \mathbf{B}_{3-DOF} = \begin{bmatrix} 0.0333 \\ 0.0356 \\ 0 \\ 0 \end{bmatrix} \tag{3.65}$$

Figure 3.25 shows that the vehicle lateral velocity, yaw rate, and roll angle throughout the simulation. It is concluded that in spite of simplification that were made to obtain these models, their estimation of yaw rate and roll angle are acceptable compared to the CarSim and the developed nonlinear model of VSS. It is possible to improve the results by tuning the vehicle parameter in the linear models.

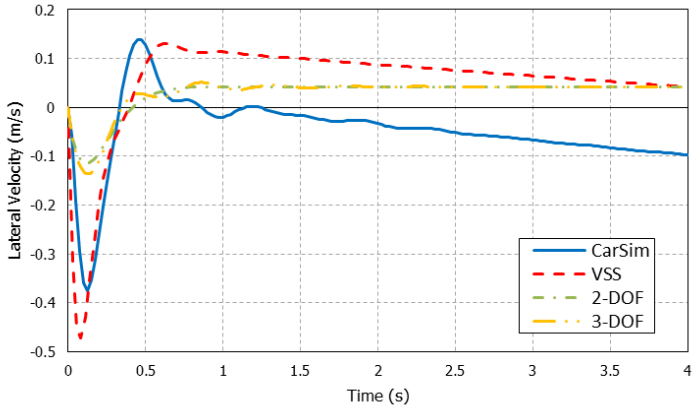

(a)

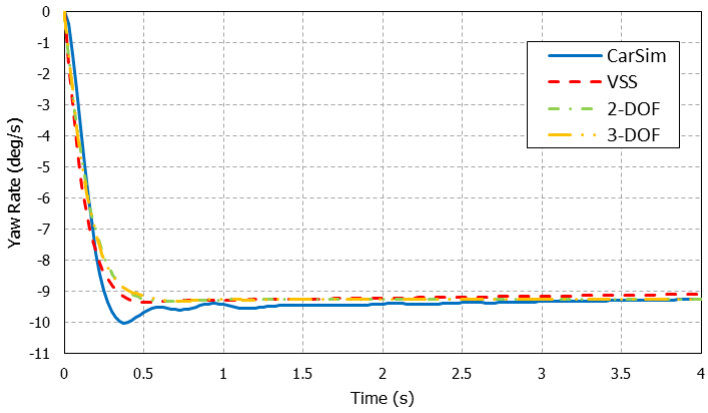

(b)

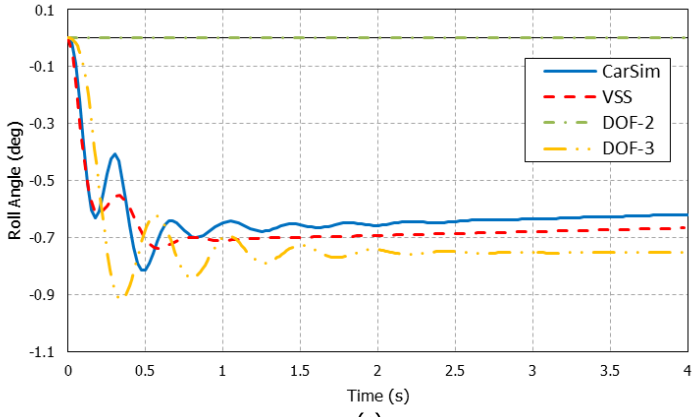

(c)

Figure 3.25 Evaluation results; vehicle states: (a) lateral velocity, (b) yaw rate, (c) roll angle

3.4.3. Non-dimensional Analysis

The effect of steering angle on vehicle dynamics in non-dimensional space is studied. The primary dimensions are vehicle speed, total mass, and front to rear axle length, and other vehicle parameters are non-dimensionalized accordingly. Regardless of vehicle speed, mass, and front to rear axle length, Figure 3.26 depicts the effect of wheel steering angle on vehicle states throughout the simulation. The results are in non-dimensional forms and can be scale up or down to any vehicle of the same proportions as the test vehicle (3.53).

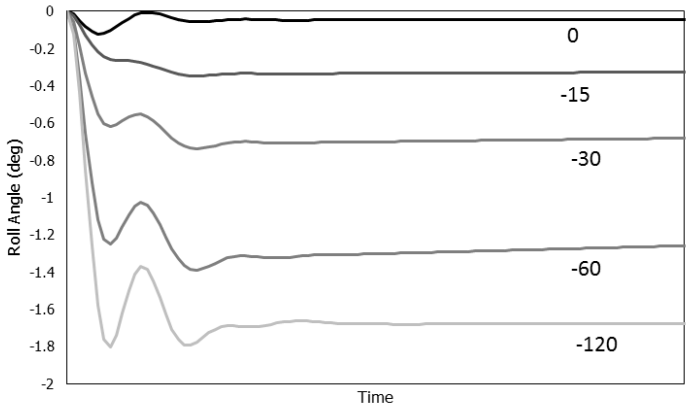

(a)

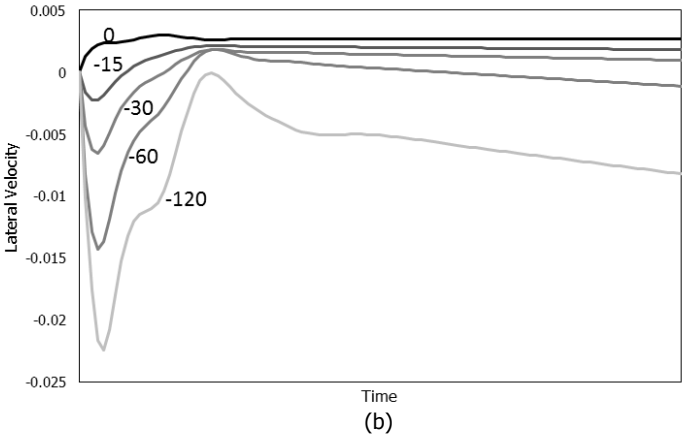

(b)

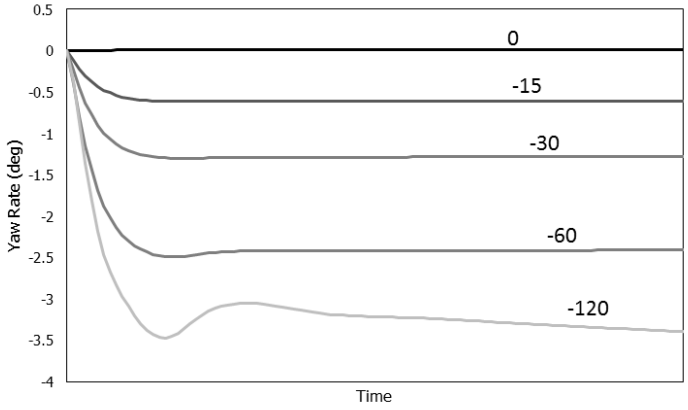

(c)

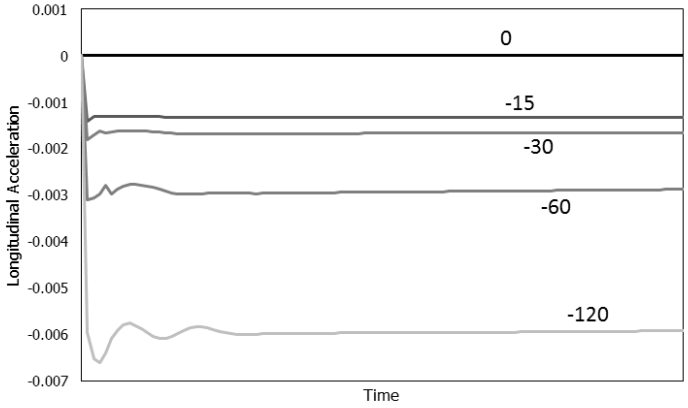

(d)

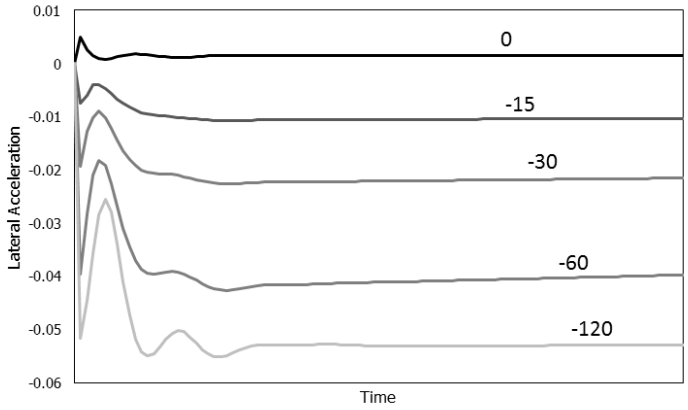

(e)

Figure 3.26 Effect of wheel steering angle (in degrees) on vehicle states: (a) roll angle, (b) lateral velocity, (c) yaw rate, (d) longitudinal acceleration, (e) lateral acceleration

Chapter 4
Vehicle Control Design Based On Game Theory

Stability in a vehicle system is determined by the total performance of all dynamics subsystems. Among different subsystems, vehicle driver and vehicle stability control systems share the most significant responsibility in providing stability in severe handling maneuvers. A rational driver tends to keep the vehicle stable throughout the maneuver; however, due to unexpected or uncontrolled events, vehicle stability is jeopardized and the driver is unable to control the vehicle. It is in these scenarios that vehicle stability control (VSC) system plays a crucial role in stabilizing the vehicle.

Vehicle active safety systems are designed to improve driving safety while the driver is still in control of the vehicle. The advancement of smart systems in vehicles that can augment the driver input, in order to improve the vehicle handling and dynamics, necessitates a better understanding of how the vehicle and driver inputs can co-exist in a manner that are complementary, not contradictory. The literature concerned with the interaction modeling of the vehicle driver and control system are classified in two categories.

In the first and the most popular category, the vehicle driver and the vehicle stability controller are two independent subsystems of the vehicle in which the performance and strategy of each system does not significantly affect the performance and strategy of the other system. For example, most existing driver models ignore the fact that human drivers respond differently as the vehicle control system is changed [Chen, 2000; Sharp, 2001; Cole, 2006], or most vehicle control literature has reported control designs that assume a predetermined steering input, and thus, ignoring the driver's transient response to the current event [Anwar, 2005; Esmailzadeh, 2003; Ghoneim, 2000; Tamaddoni, 2008; Zheng, 2006].

The second category includes researches that consider vehicle stability as collaboration between driver and the vehicle stability control system. Wenzel showed that considering a joint combination of a driver model and active front steering control may result in improved vehicle stability and performance [Wenzel, 2005]. Regardless of the complexity, cooperative control of the driver's input and vehicle control system control actions trivially results in globally optimal solution to vehicle stability problems.

In this research, the interaction modeling of driver steering control and vehicle yaw control is studied in a manner that both the driver and the vehicle stability controller determine their control action based on the current vehicle states, maneuver constraints, and the other system's performance by observing the history of past control performance. This observation requires that all subsystems are aware of or able to estimate the decision-making structure of each other.

Human learning takes place in the central nervous system in a wide variety of mental and physical tasks, one of which is to "learn" how his/her own vehicle with its factory built-in vehicle stability control system performs in various day-to-day maneuvers. "Learning" means that the driver is able to create a model of the dominating vehicle dynamics and the significant decision-making structure of the vehicle controller in his/her own unconscious mind.

For vehicle directional control, the steering wheel is the primary means for control actuation. Many driver models try to approximate the real driver's road tracking performance, assuming certain driver inputs and outputs. If the controller is aware of the driver's intentions, the driver mathematical model can be traced back iteratively to determine its significant factors. Accordingly, establishing a technique for detecting the driver's intentions or for recognizing driver model has been a challenging problem for vehicle system researchers. Kuge [2000] developed a driver behavior recognition method based on hidden Markov models to characterize and detect driving maneuvers and place it in the framework of a cognitive model of human behavior. In another research by McCall and his colleagues [McCall, 2007], driver's behavior and the lane change intent is analyzed using robust sparse Bayesian learning methodology and it is shown that by incorporating a state-of-the-art Sparse Bayesian Learning classifier with well-motivated

evaluation metrics, the likelihood of driver intent inference system algorithmic failure reduces.

In this research, a novel optimal driver-controller interaction strategy is developed based on linear quadratic Game Theory. The model includes the driver's directional control through introducing steering wheel angle and the vehicle direct yaw control (DYC) system through imposing a corrective yaw moment using differential braking of the four wheels. As a result, it is shown that globally optimal performance is obtained in the case that the effects of driver's decision making on the controller and vice versa are taken into account and the interactions are correctly modeled.

Throughout this research, it is assumed that the driver steering control can be modeled as a linear feedback control of the vehicle states, and the vehicle stability controller is formed by a direct yaw control system that provides handling stability and comfort as described in Section 2.4. For evaluation purposes, the D-class sedan vehicle described in Section 3.4 is used within the interaction models introduced later in this chapter. The test maneuver is a single-lane change of four meters, i.e. $y_{desired} = 4m$. The driver and controller feedback gains on significant states and control actions are listed in Table 4.1. The listed gains, later, form the control priorities $\mathbf{Q}, \mathbf{R}$ in this chapter.

Table 4.1 Feedback gains on significant vehicle states and control actions

	Lateral position error	Lateral velocity error	Yaw angle error	Yaw rate error	Steering angle	Corrective yaw moment
Driver	10	0.01	0.1	0.01	1	0
DYC	0	0.1	0	1	10	1e-7

In Section 4.1, the driver-controller interactions are modeled in continuous time using differential linear quadratic Game Theory. The preview-time characteristic of human driver is later taken into account in the discrete-time preview model in Section 4.2. Parameter sensitivity analysis and robust interaction modeling is discussed in details in Sections 4.3 and 4.4.

4.1. Continuous-Time Interaction Model

This section deals with continuous time interaction modeling of the driver steering and the vehicle direct yaw control as a dynamic game between the driver and the controller. In this game, the driver (player/agent 1) and the vehicle controller (player/agent 2) play cooperatively through their control actions, namely, the steering wheel angle δ_{sw} and the corrective yaw moment M_{zc}. To model such interactions, the linear bicycle model (3.44) is extended to introduce the corrective yaw moment as

$$\dot{x}(t) = \mathbf{A}_c x(t) + \mathbf{B}_{c1} \underbrace{\delta_{sw}(t)}_{u_1} + \mathbf{B}_{c2} \underbrace{M_{zc}(t)}_{u_2} \tag{4.1}$$

where $x_c(t)$ represents the time-continuous state, and

$$\mathbf{A}_c = \begin{bmatrix} 0 & 1 & V_x & 0 \\ 0 & -\dfrac{C_{\alpha F} + C_{\alpha B}}{MV_x} & 0 & -V_x - \dfrac{L_F C_{\alpha F} - L_B C_{\alpha B}}{MV_x} \\ 0 & 0 & 0 & 1 \\ 0 & \dfrac{L_F C_{\alpha F} - L_B C_{\alpha B}}{I_z V_x} & 0 & -\dfrac{L_F^2 C_{\alpha F} + L_R^2 C_{\alpha B}}{I_z V_x} \end{bmatrix}, \mathbf{B}_{c1} = \begin{bmatrix} 0 \\ \dfrac{C_{\alpha F}}{r_{st} M} \\ 0 \\ \dfrac{L_F C_{\alpha F}}{r_{st} I_z} \end{bmatrix}, \mathbf{B}_{c2} = \begin{bmatrix} 0 \\ 0 \\ 0 \\ \dfrac{1}{I_z} \end{bmatrix}$$

The tire cornering stiffness for front and rear axles are given by $C_{\alpha F}$ and $C_{\alpha B}$, respectively, and steering gear ratio r_{st} is defined by the ratio between the steering wheel angle and the steering angle at the front wheels as $r_{st} = \delta_{sw} / \delta_F$.

The cooperative actions of the two players, namely, human driver and vehicle stability controller, are assumed to have the tendency to minimize the corresponding sum of squares of attitude angle differences and to minimize the higher-order dynamics, typical terms that can be found analytically. Hence, it is assumed that the control priorities of the driver and the vehicle direct yaw controller are characterized in a form of quadratic cost functions given as

$$J_i(u_1, u_2) = \int_0^t \left(x^T \mathbf{Q}_i x + u_1^T \mathbf{R}_{i1} u_1 + u_2^T \mathbf{R}_{i2} u_2 \right) dt \tag{4.2}$$

where all weighting matrices are constant and symmetric with $\mathbf{Q}_i \geq 0$, $\mathbf{R}_{ij} = \mathbf{D}_{ij}^T \mathbf{D}_{ij} \geq 0$ and $\mathbf{R}_{ii} = \mathbf{D}_i^T \mathbf{D}_i > 0$, and $i = 1, 2$ is the player number.

In Nash (1951), the Nash equilibrium concept was introduced and in Başar and Olsder (1995) and Starr (1969) it was defined as the pair $\left(u_1^*, u_2^*\right)$ which corresponds to a Nash equilibrium if the following relations are satisfied for each admissible strategy $\left(u_1, u_2\right)$:

$$\begin{cases} J_1(u_1, u_2^*) \geq J_1(u_1^*, u_2^*), \\ J_2(u_1^*, u_2) \geq J_2(u_1^*, u_2^*). \end{cases} \tag{4.3}$$

The Nash equilibrium is defined such that it has the property that there is no incentive for any unilateral deviation by any one of the players. In the other words, at Nash equilibrium with $\left(u_1^*, u_2^*\right)$, the player who chooses to change his/her strategy cannot improve his/her payoff.

4.1.1. Control Design

The problem of continuous time vehicle-driver interaction model is now reduced to finding the Nash equilibrium for the continuous-time model of (4.1). The following theorem was modified from Ho et al. [1965] according to the game model (4.1):

Theorem 4.1 *Consider the game system (4.1) with the cost functions defined in (4.2). Let the strategies* $u_1^* = \delta_{sw}^*, u_2^* = \tau_{zc}^*$ *be such that there exist solutions* $\left(\mathbf{P}_1, \mathbf{P}_2\right)$ *to the differential equations*

$$\frac{d}{dt}\mathbf{P}_i = -\frac{\partial}{\partial x}\mathbf{H}_i\left(x^*, u_1^*, u_2^*, \mathbf{P}_i\right) - \frac{\partial}{\partial u_i}\mathbf{H}_i\left(x^*, u_1^*, u_2^*, \mathbf{P}_i\right).\frac{\partial u_j^*}{\partial x} \quad , \quad \left(i = 1,2\right) \tag{4.4}$$

where

$$\mathbf{H}_i\left(x, u_1, u_2, \mathbf{P}_i\right) = x^T\mathbf{Q}_i x + u_1^T\mathbf{R}_{i1}u_1 + u_2^T\mathbf{R}_{i2}u_2 + \mathbf{P}_i^T\left(\mathbf{A}_c x + \mathbf{B}_{c1}u_1 + \mathbf{B}_{c2}u_2\right) \tag{4.5}$$

such that for $i = 1,2$ *:*

$$\frac{\partial}{\partial u_i}\mathbf{H}_i\left(x^*, u_1^*, u_2^*, \mathbf{P}_i\right) = 0 \tag{4.6}$$

and x^* *satisfies*

$$\dot{x}^*(t) = \mathbf{A}_c x^*(t) + \mathbf{B}_{c1}u_1^* + \mathbf{B}_{c2}u_2^* \tag{4.7}$$

Then (u_1^*, u_2^*) *is Nash equilibrium with respect to the memoryless perfect state information structure, and the following equalities hold:*

$$u_i^* = -\mathbf{R}_{ii}^{-1}\mathbf{B}_{ci}^T\mathbf{P}_i(t) \tag{4.8}$$

Since the driver steering control and the vehicle yaw controller are restricted to the class of linear time-invariant feedback strategies, the admissible strategies are defined as

$$\Gamma_i^{fd} = \left\{u_i \in \Gamma_i \middle| \, u_i(x;t) = \mathbf{G}_i x(t)\right\}, \tag{4.9}$$

There exists a generically unique linear feedback Nash equilibrium [Ho, 1965; Başar, 1974] where the functions of Theorem 1 are given by $\mathbf{P}_i(t) = \mathbf{K}_i x(t)$.

Theorem 4.2 *Suppose* $\mathbf{K}_i$ *satisfy the coupled Riccati equations given by*

$$\mathbf{A}_c^T\mathbf{K}_i + \mathbf{K}_i\mathbf{A}_c + \mathbf{Q}_i - \mathbf{K}_i\mathbf{S}_i\mathbf{K}_i - \mathbf{K}_i\mathbf{S}_{\hat{i}}\mathbf{K}_{\hat{i}} - \mathbf{K}_{\hat{i}}\mathbf{S}_{\hat{i}}\mathbf{K}_i + \mathbf{K}_{\hat{i}}\mathbf{S}_{i\hat{i}}\mathbf{K}_{\hat{i}} = \mathbf{0}_n \tag{4.10}$$

where $i = (1,2)$ *and* $\hat{i}$ *is the counter-coalition, i.e. the player counter-acting to the player with index* i*, and*

$$\mathbf{S}_i = \mathbf{B}_{ci}\mathbf{R}_{ii}^{-1}\mathbf{B}_{ci}^T \quad , \quad \mathbf{S}_{i\hat{i}} = \mathbf{B}_{c\hat{i}}\mathbf{R}_{\hat{i}\hat{i}}^{-1}\mathbf{R}_{i\hat{i}}\mathbf{R}_{\hat{i}\hat{i}}^{-1}\mathbf{B}_{c\hat{i}}^T \tag{4.11}$$

Then the following strategy

$$u_i^*(t) = -\mathbf{R}_{ii}^{-1}\mathbf{B}_{ci}^T\mathbf{K}_i x(t) \tag{4.12}$$

is linear feedback Nash equilibrium for the game system (4.1) with the cost functions defined in (4.2).

The coupled Riccati equation (4.10) is hard to solve due to the presence of quadratic coupling terms between $\mathbf{K}_1$ and $\mathbf{K}_2$. To the best of our knowledge there are no explicit conditions guaranteeing the existence of solutions to equation (4.10). Implicit conditions and special cases are provided in Weeren et al. (1999) and Jungers et al. (2008). Only numerical algorithms without proof of convergence are available to solve these equations (Freiling et al., 1996; Jungers et al., 2008). If there exists a solution to the coupled Riccati

equation (4.10), it can be best found by iterative search of the following modified equation (4.13) until it converges to a stationary state:

$$\frac{d}{dt}\mathbf{K}_i = -\mathbf{A}_c^T\mathbf{K}_i - \mathbf{K}_i\mathbf{A}_c - \mathbf{Q}_i + \mathbf{K}_i\mathbf{S}_i\mathbf{K}_i + \mathbf{K}_i\mathbf{S}_{\hat{i}}\mathbf{K}_{\hat{i}} + \mathbf{K}_{\hat{i}}\mathbf{S}_{\hat{i}}\mathbf{K}_i - \mathbf{K}_{\hat{i}}\mathbf{S}_{i\hat{i}}\mathbf{K}_{\hat{i}} \tag{4.13}$$

where $i = (1,2)$ and $\hat{i}$ is the counter-coalition, i.e. the player counter-acting to the player with index i, and $\mathbf{S}_i, \mathbf{S}_{i\hat{i}}$ are defined the same as in equation (4.10).

Considering the cooperative control actions $u_1 = \delta_{sw}$ and $u_2 = M_{zc}$ representing the driver's steering control and the vehicle controller's corrective yaw moment, the globally optimal set of actions by Game Theory are defined as

$$\delta_{sw}^* = -\mathbf{R}_{11}^{-1}\mathbf{B}_{c1}^T\mathbf{K}_1\left(x - x_{des}\right) = \mathbf{G}_1\left(x - x_{des}\right) \tag{4.14}$$

$$\tau_{zc}^* = -\mathbf{R}_{22}^{-1}\mathbf{B}_{c2}^T\mathbf{K}_2\left(x - x_{des}\right) = \mathbf{G}_2\left(x - x_{des}\right) \tag{4.15}$$

where $\mathbf{K}_1, \mathbf{K}_2$ are the solutions of the coupled Riccati equation (4.10).

4.1.2. Simulation and Results

Computer simulations are carried out to verify the effectiveness of the proposed continuous time interaction model. The presented driver and controller models are, hence, evaluated using the nonlinear model that was introduced in Section 3.2 with the objective to stably steer the vehicle through a single lane change of four meters. The following defines the desired states in non-dimensional form for the evaluation maneuver:

$$x_{des} = \begin{pmatrix} 5 & 0 & 0 & \dot{\theta}_{z,des} \end{pmatrix}^T, \tag{4.16}$$

The desired value of yaw rate in order to provide handling comfort is obtained from

$$\dot{\theta}_{z,des} = \frac{V_x}{r_{st}\left(L_F + L_B\right)\left(1 + K_{us}V_x^2\right)}\delta_{sw} \tag{4.17}$$

where the understeering coefficient k_{us} is defined in Section 2.4.

To better assess the performance of the proposed driver-controller interaction framework based on Game Theory, an independent model of vehicle driver and direct yaw control (DYC) system are also simulated in the same scenario. These independent models are assumed in the form of linear feedback controllers and their corresponding feedback

gains are obtained by the linear quadratic regulation (LQR) strategy. In both cases, i.e. Game Theory (GT) and linear quadratic regulation (LQR), the control priorities for the driver and the controller are defined based on Table 4.1, and are rewritten as

$$Driver: \ \mathbf{Q}_1 = \begin{bmatrix} 10 & 0 & 0 & 0 \\ 0 & 0.01 & 0 & 0 \\ 0 & 0 & 0.1 & 0 \\ 0 & 0 & 0 & 0.01 \end{bmatrix}, \ \mathbf{R}_{11} = 1 \ , \ \mathbf{R}_{12} = 0 \tag{4.18}$$

$$DYC: \ \mathbf{Q}_2 = \begin{bmatrix} 0 & 0 & 0 & 0 \\ 0 & 0.1 & 0 & 0 \\ 0 & 0 & 0 & 0 \\ 0 & 0 & 0 & 1 \end{bmatrix}, \ \mathbf{R}_{21} = 10 \ , \ \mathbf{R}_{22} = 10^{-7} \tag{4.19}$$

Using the same $\mathbf{Q}$ and $\mathbf{R}$ matrices, the final state feedback gains for both strategies are calculated from Theorem 4.2 and listed as follows;

• Game Theory:

$$\begin{cases} \mathbf{G}_{1(GT)} = \begin{bmatrix} -0.809 & -0.146 & -8.624 & -0.713 \end{bmatrix} \\ \mathbf{G}_{2(GT)} = \begin{bmatrix} 0 & 504.08 & 0 & -10696 \end{bmatrix} \end{cases} \tag{4.20}$$

• LQR:

$$\begin{cases} \mathbf{G}_{1(LQR)} = \begin{bmatrix} -1.0 & -0.215 & -13.63 & -1.286 \end{bmatrix} \\ \mathbf{G}_{2(LQR)} = \begin{bmatrix} 0 & 129.93 & 0 & -599 \end{bmatrix} \end{cases} \tag{4.21}$$

where $\mathbf{G}_1$, $\mathbf{G}_2$ are the driver and the vehicle controller feedback gains, respectively.

The simulation is done using the built-in vehicle mathematics model in Vehicle System Simulator for three different scenarios:

- *Scenario "A":* the driver is supposed to act as an ideal linear quadratic regulator with the feedback gain $\mathbf{G}_{1(LQR)}$ defined in (4.20), and the vehicle controller is turned off.
- *Scenario "B":* the driver and the vehicle controller are both supposed to act as ideal linear quadratic regulators with the feedback gain $\mathbf{G}_{1(LQR)}$ and $\mathbf{G}_{2(LQR)}$, respectively.

- *Scenario "C":* the driver and the vehicle controller are both supposed to act as ideal feedback controller with the feedback gain $\mathbf{G}_{1(GT)}$ and $\mathbf{G}_{2(GT)}$ obtained from the Game Theory based framework as defined in (4.13) and (4.14), respectively.

Figure 4.1-3 shows the simulation results.

Figure 4.1(a) shows that the vehicle successfully performs a single lane change maneuver of four meters in all three cases; however, the vehicle in case C, i.e. the Game Theory framework, exhibits slower response with an overshoot of about 10%. Case A has the fastest response among all cases which implies that the vehicle DYC system slows down the vehicle response and in the other words, increases the settling time.

In spite of slower response, Figure 4.1(b,e) shows that the lateral and roll motions of the vehicle is more stable in case C with the Game Theory -based driver and controller models compared to case A and B, and they are more stable in case B compared to case A. This implies the performance of the vehicle stability control in limiting the lateral velocity and roll angle to prevent the undesired rollover.

Figure 4.1(c) shows the vehicle yaw angle throughout the lane change. Again, it reflects the slower response time and the overshoot characteristics in case C.

Figure 4.1(d) indicates that the vehicle controller in both cases B and C tends to provide the desired handling performance; however, the Game Theory framework keeps the vehicle yaw rate closer to its corresponding value of the desired yaw rate compared to the independently control models in case B.

Figure 4.1(f) shows that in all cases the vehicle speed was almost kept at $20(m/s)$ to insure the validity of the system linearization.

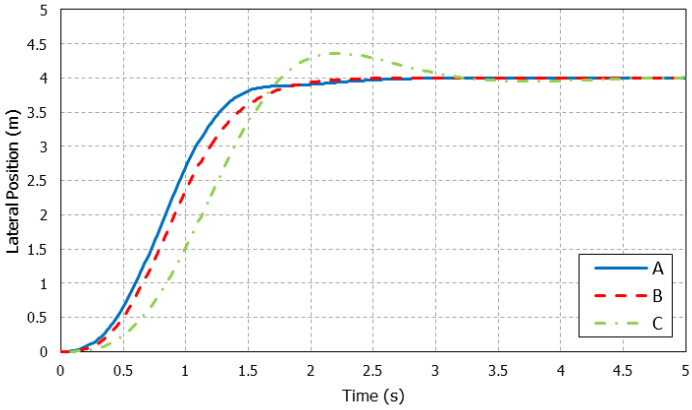
Lateral Position (m)
Time (s)
A
B
C

(a)

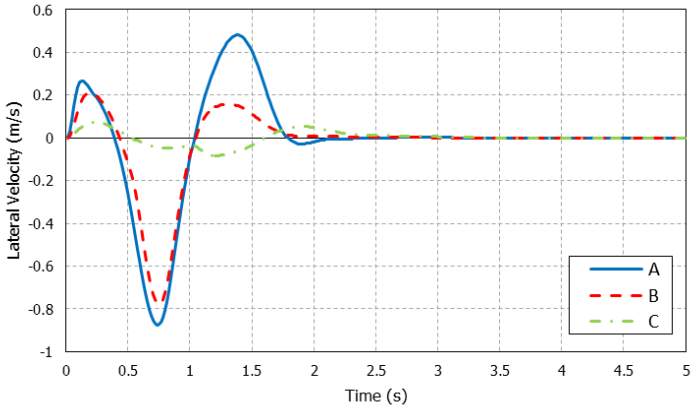
Lateral Velocity (m/s)
Time (s)
A
B
C

(b)

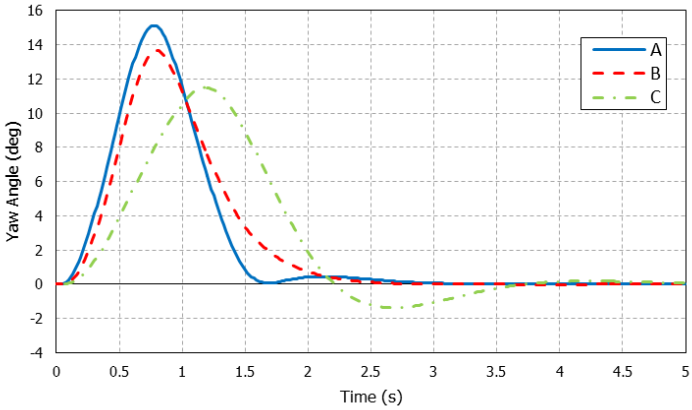
Yaw Angle (deg)
Time (s)
A
B
C

(c)

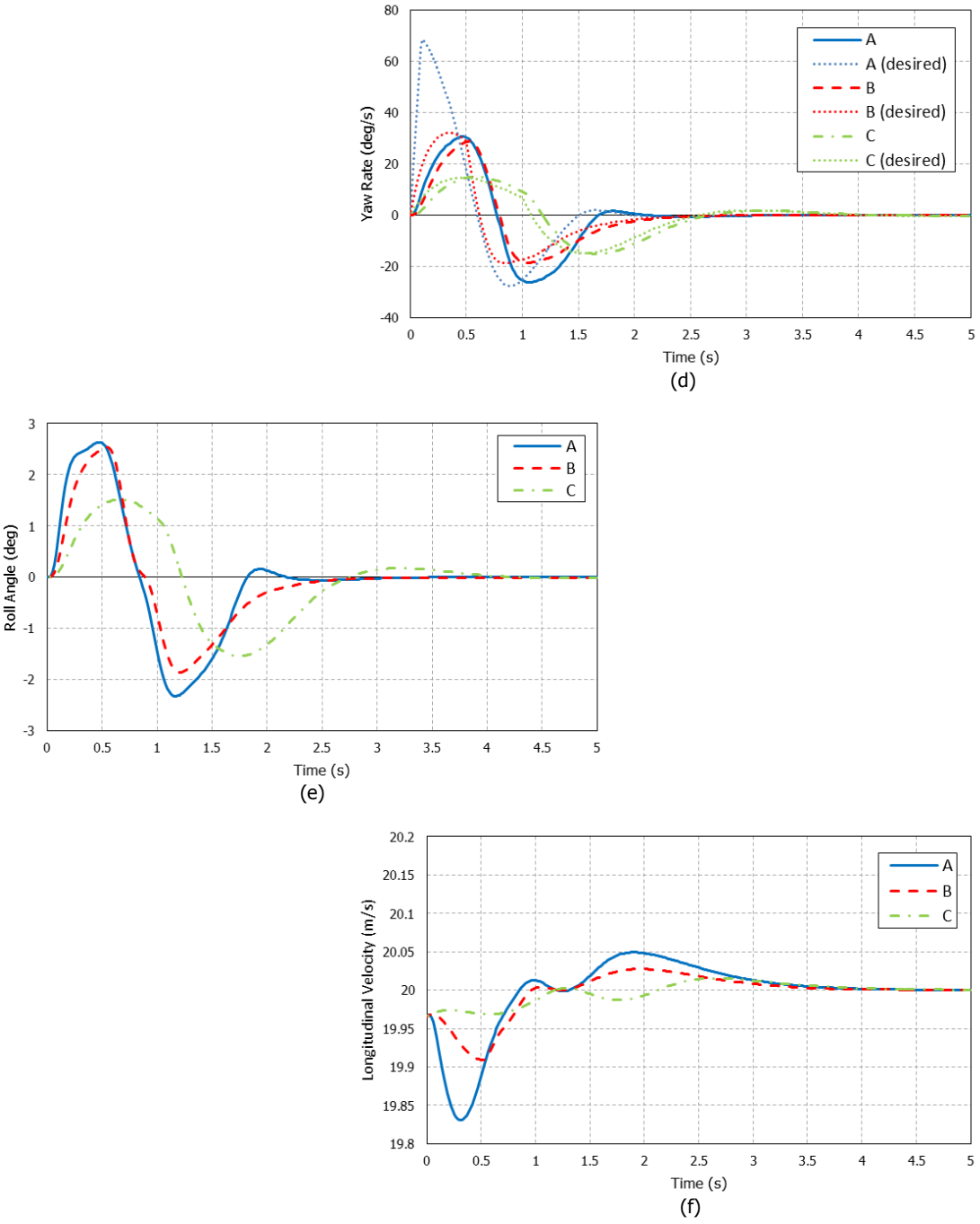

Figure 4.1 Continuous time interaction model; vehicle states: (a) lateral position, (b) lateral velocity, (c) yaw angle, (d) yaw rate, (e) roll angle, (f) longitudinal velocity

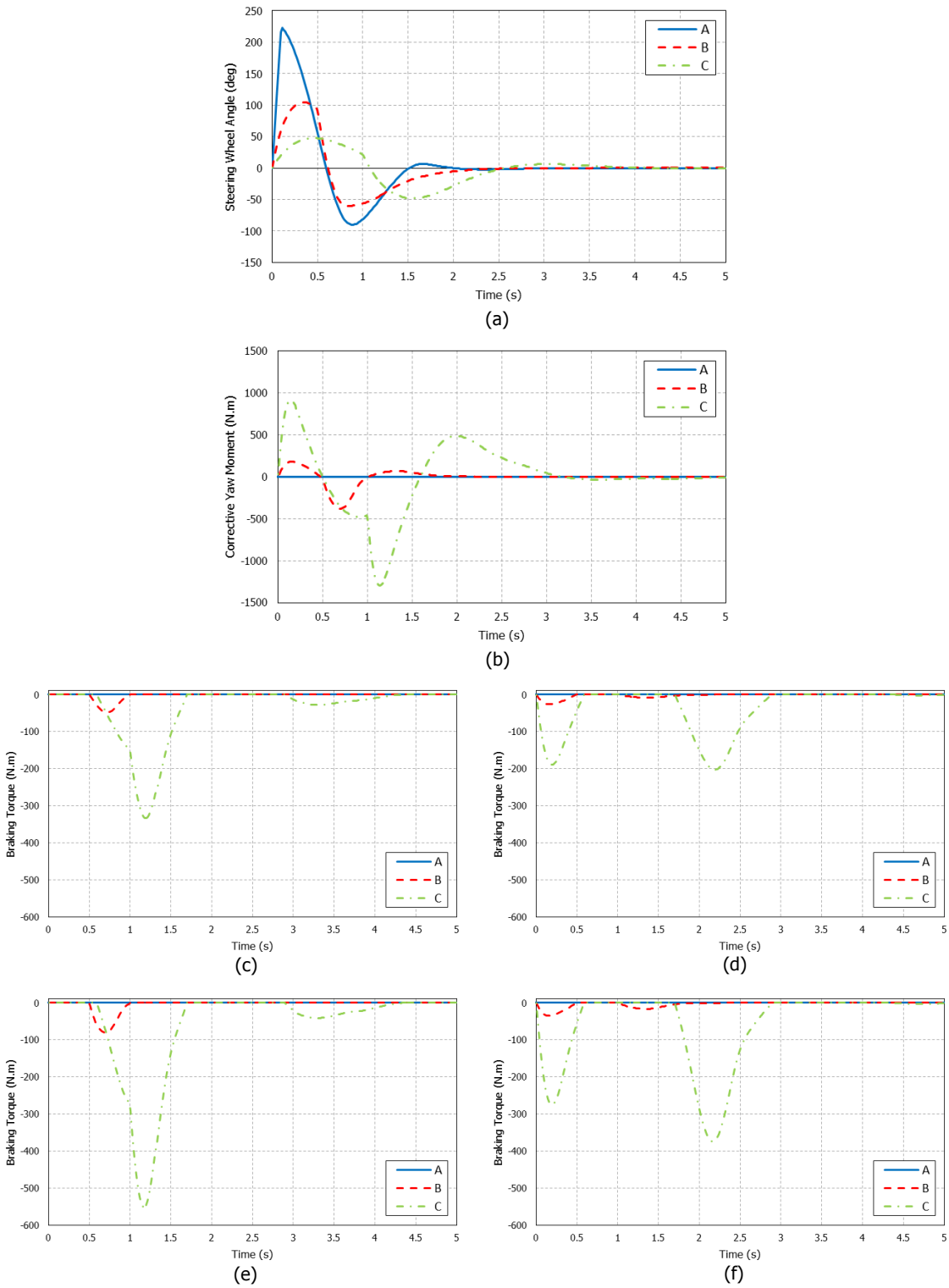

Figure 4.2 Continuous time interaction model; control inputs: (a) steering wheel angle, (b) corrective yaw moment

Figure 4.2 shows the driver's steering wheel angle and the corrective yaw moment required to maneuver the vehicle in a single lane change. It is concluded that as the vehicle controller is more engaged, the steering effort is more smoothed and the driver seems to be more relaxed, i.e. the peak values of the steering angle reduces. Figure 4.2(c-f) shows the wheel braking torques that are calculated using Differential Braking system described in Section 3.3.2.

4.2. Discrete-Time Interaction Model

Unlike Section 4.1, this section deals with discrete time modeling of driver-controller interactions in a form of discrete difference game. In this game, the driver (player/agent 1) and the vehicle controller (player/agent 2) play cooperatively through their control actions, namely, the steering wheel angle δ_{sw} and the corrective yaw moment M_{zc}. Through discretization, it is now possible to add preview-time characteristics of human driver in directional control. Hence, the discrete time model (3.59) is extended to introduce the corrective yaw moment as

$$\underbrace{\begin{bmatrix} x_d^+ \\ y_r^+ \end{bmatrix}}_{z^+} = \underbrace{\begin{bmatrix} \mathbf{A}_d & 0 \\ 0 & \mathbf{A}_r \end{bmatrix}}_{\mathbf{A}} \underbrace{\begin{bmatrix} x_d \\ y_r \end{bmatrix}}_{z} + \underbrace{\begin{bmatrix} \mathbf{B}_{d1} \\ 0 \end{bmatrix}}_{\mathbf{B}_1} \delta_{sw} + \underbrace{\begin{bmatrix} \mathbf{B}_{d2} \\ 0 \end{bmatrix}}_{\mathbf{B}_2} M_{zc} + \underbrace{\begin{bmatrix} 0 \\ \mathbf{B}_r \end{bmatrix}}_{\mathbf{E}} y_{r(N+1)} \tag{4.22}$$

where x_d, x_d^+ represent the discrete state (3.43) for current and next time step, respectively, and $\mathbf{A}_d, \mathbf{B}_{d1}, \mathbf{B}_{d2}$ are obtained from the discrete bilinear transformation of the corresponding continuous-time matrices $\mathbf{A}_c, \mathbf{B}_{c1}, \mathbf{B}_{c2}$ in (4.1), $\mathbf{A}_r, \mathbf{B}_r$ are defined in (3.58), and $y_{r(N+1)}$ is the road reference at N time step ahead.

Similar to (4.2), the control priorities for the driver, i.e. player 1, and the vehicle direct yaw controller, i.e. player 2, are defined in linear quadratic cost form as defined by

$$J_i = \frac{1}{2}\sum_{k=0}^{\infty}\left(z^T \mathbf{Q}_i z + \sum_{j=1}^{2} u_j^T \mathbf{R}_{ij} u_j \right) \tag{4.23}$$

where all weighting matrices are constant with $\mathbf{R}_{ii} > 0$. $\mathbf{Q}_i$ is symmetric and reflected in a quadratic cost function as

$$\mathbf{Q}_i = \mathbf{N}_i^T \mathbf{Q}_{di} \mathbf{N}_i \tag{4.24}$$

where the state error weighting matrices $\mathbf{Q}_{di}$ are 4×4 diagonal matrices and $\mathbf{N}_i$ for driver with road preview $(i = 1)$ and vehicle controller with no road information $(i = 2)$ are defined as

$$\mathbf{N}_1 = \left[\begin{array}{cccc|cccccc} 1 & 0 & 0 & 0 & 0 & -1 & 0 & 0 & \dots & 0 \\ 0 & 1 & 0 & 0 & 0 & 1/T_s & -1/T_s & 0 & \dots & 0 \\ 0 & 0 & 1 & 0 & 0 & 1/(V_x T_s) & -1/(V_x T_s) & 0 & \dots & 0 \\ \underbrace{0 \;\; 0 \;\; 0 \;\; 1}_{state\ gains} & & & & \underbrace{-1/(V_x T_s^2) \;\; 2/(V_x T_s^2) \;\; -1/(V_x T_s^2) \;\; 0 \;\; \dots \;\; 0}_{road\ preview\ gain} & & & & & \end{array}\right]_{4\times(4+N)} \tag{4.25}$$

$$\mathbf{N}_2 = \left[\begin{array}{cccc|ccc} 1 & 0 & 0 & 0 & 0 & \dots & 0 \\ 0 & 1 & 0 & 0 & 0 & \dots & 0 \\ 0 & 0 & 1 & 0 & 0 & \dots & 0 \\ \underbrace{0 \;\; 0 \;\; 0 \;\; 1}_{state\ gains} & & & & \underbrace{0 \;\; \dots \;\; 0}_{road\ preview\ gain} & & \end{array}\right]_{4\times(4+N)} \tag{4.26}$$

where T_s is the sampling time, and the road preview gains are introduced to define the state error with respect to the road reference information as

$$\begin{aligned} Y_{ref} &= Y_{r1} \\ V_{y,ref} &\simeq \frac{\Delta Y}{T_s} = \frac{Y_{r2} - Y_{r1}}{T_s} \\ \theta_{z,ref} &\simeq \frac{\Delta Y}{\Delta X} \simeq \frac{Y_{r2} - Y_{r1}}{V_x T_s} \\ \dot{\theta}_{z,ref} &\simeq \frac{\Delta \theta_{z,ref}}{T_s} \simeq \frac{\theta_{z,ref}^{+} - \theta_{z,ref}^{-}}{T_s} = \frac{Y_{r2} - 2Y_{r1} + Y_{r0}}{V_x T_s^2} \end{aligned} \tag{4.27}$$

The relative importance attached to path errors, attitude errors and steer angle are set by choosing the diagonal values of $\mathbf{Q}_{di}$ appropriately as described in [Sharp, 2001].

4.2.1. Control Design

The problem of preview time vehicle-driver interaction model is now reduced to finding the Nash equilibrium for the discrete-time model of (4.15). The linear Nash equilibrium

associated with a two-player linear quadratic difference game is defined by the following theorem:

Theorem 4.3 *Consider the difference game model (4.22) subject to the cost function (4.23). Suppose* $\mathbf{P}_i$ *satisfy the coupled Riccati equations for discrete linear quadratic games given by*

$$\mathbf{P}_i = \mathbf{Q}_i - \mathbf{G}_1^T \mathbf{R}_{i1} \mathbf{G}_1 - \mathbf{G}_2^T \mathbf{R}_{i2} \mathbf{G}_2 + \left(\mathbf{A} + \mathbf{B}_1 \mathbf{G}_1 + \mathbf{B}_2 \mathbf{G}_2\right)^T \mathbf{P}_i^+ \left(\mathbf{A} + \mathbf{B}_1 \mathbf{G}_1 + \mathbf{B}_2 \mathbf{G}_2\right) \tag{4.28}$$

where $i = (1,2)$ *, and* $\hat{i}$ *is the counter-coalition, i.e. the player counter-acting to the player with index* i *, and*

$$\mathbf{G}_i = -\left(\mathbf{R}_{ii} + \mathbf{B}_i^T \mathbf{P}_i^+ \mathbf{B}_i\right)^{-1} \mathbf{B}_i^T \mathbf{P}_i^+ \left(\mathbf{A} + \mathbf{B}_{\hat{i}} \mathbf{G}_{\hat{i}}\right) \tag{4.29}$$

Then the following strategy

$$u_i^* = -\mathbf{R}_{ii}^{-1} \mathbf{B}_i^T \mathbf{P}_i^+ z^+ \qquad (i = 1,2) \tag{4.30}$$

is linear feedback Nash equilibrium.

The solution to the Riccati equations (4.28) is found by reversing the direction of time, i.e.

$$\mathbf{P}_i^+ = \mathbf{Q}_i - \mathbf{G}_1^{+T} \mathbf{R}_{i1} \mathbf{G}_1^+ - \mathbf{G}_2^{+T} \mathbf{R}_{i2} \mathbf{G}_2^+ + \left(\mathbf{A} + \mathbf{B}_1 \mathbf{G}_1^+ + \mathbf{B}_2 \mathbf{G}_2^+\right)^T \mathbf{P}_i \left(\mathbf{A} + \mathbf{B}_1 \mathbf{G}_1^+ + \mathbf{B}_2 \mathbf{G}_2^+\right) \tag{4.31}$$

where

$$\mathbf{G}_1^+ = -\left(\mathbf{R}_{ii} + \mathbf{B}_i^T \mathbf{P}_i \mathbf{B}_i\right)^{-1} \mathbf{B}_i^T \mathbf{P}_i \left(\mathbf{A} + \mathbf{B}_i \mathbf{G}_{\hat{i}}^+\right) \tag{4.32}$$

Solving the equations (4.32) for $\mathbf{G}_1^+, \mathbf{G}_2^+$ yields

$$\begin{bmatrix} \mathbf{G}_1^+ \\ \mathbf{G}_2^+ \end{bmatrix} = -\begin{bmatrix} \mathbf{R}_{11} + \mathbf{B}_1^T \mathbf{P}_1 \mathbf{B}_1 & \mathbf{B}_1^T \mathbf{P}_1 \mathbf{B}_2 \\ \mathbf{B}_2^T \mathbf{P}_2 \mathbf{B}_1 & \mathbf{R}_{22} + \mathbf{B}_2^T \mathbf{P}_2 \mathbf{B}_2 \end{bmatrix}^{-1} \begin{bmatrix} \mathbf{B}_1^T \mathbf{P}_1 \\ \mathbf{B}_2^T \mathbf{P}_2 \end{bmatrix} \mathbf{A} \tag{4.33}$$

where can then be substituted in the Riccati equation (4.31) to obtain the Nash optimal controllers as defined in equation (4.30).

The matrices $\mathbf{P}_i, \mathbf{Q}_i$ can also be rewritten as

$$\mathbf{Q}_i = \begin{bmatrix} \mathbf{Q}_{di} & \mathbf{Q}_{mi} \\ \mathbf{Q}_{mi}^T & \mathbf{Q}_{ri} \end{bmatrix},\ \mathbf{P}_i = \begin{bmatrix} \mathbf{P}_{di} & \mathbf{P}_{mi} \\ \mathbf{P}_{mi}^T & \mathbf{P}_{ri} \end{bmatrix} \quad (i = 1,2) \tag{4.34}$$

to simplify the Riccati equations.

Hence, the optimal preview linear feedback control (4.30) becomes

$$u_i^* = -\mathbf{R}_{ii}^{-1}\mathbf{B}_{di}^T \begin{bmatrix} \mathbf{P}_{di}^+ & \mathbf{P}_{mi}^+ \end{bmatrix} z^+ \quad (i = 1,2) \tag{4.35}$$

Substituting $\mathbf{A}, \mathbf{B}_i, \mathbf{P}_i, \mathbf{Q}_i$ from equations (4.22) and (4.34) into (4.35) yields

$$\begin{bmatrix} \mathbf{G}_1^+ \\ \mathbf{G}_2^+ \end{bmatrix} = -\begin{bmatrix} \mathbf{R}_{11} + \mathbf{B}_{d1}^T\mathbf{P}_{d1}\mathbf{B}_{d1} & \mathbf{B}_{d1}^T\mathbf{P}_{d1}\mathbf{B}_{d2} \\ \mathbf{B}_{d2}^T\mathbf{P}_{d2}\mathbf{B}_{d1} & \mathbf{R}_{22} + \mathbf{B}_{d2}^T\mathbf{P}_{d2}\mathbf{B}_{d2} \end{bmatrix}^{-1} \begin{bmatrix} \mathbf{B}_{d1}^T\mathbf{P}_{d1} & \mathbf{B}_{d1}^T\mathbf{P}_{m1} \\ \mathbf{B}_{d2}^T\mathbf{P}_{d2} & \mathbf{B}_{d2}^T\mathbf{P}_{m2} \end{bmatrix} \mathbf{A} \tag{4.36}$$

or

$$\begin{bmatrix} \mathbf{G}_1^+ \\ \mathbf{G}_2^+ \end{bmatrix} = -\begin{bmatrix} \mathbf{R}_{11} + \mathbf{B}_{d1}^T\mathbf{P}_{d1}\mathbf{B}_{d1} & \mathbf{B}_{d1}^T\mathbf{P}_{d1}\mathbf{B}_{d2} \\ \mathbf{B}_{d2}^T\mathbf{P}_{d2}\mathbf{B}_{d1} & \mathbf{R}_{22} + \mathbf{B}_{d2}^T\mathbf{P}_{d2}\mathbf{B}_{d2} \end{bmatrix}^{-1} \begin{bmatrix} \mathbf{B}_{1d}^T\mathbf{P}_{1d}\mathbf{A}_d & \mathbf{B}_{1d}^T\mathbf{P}_{1m}\mathbf{A}_r \\ \mathbf{B}_{2d}^T\mathbf{P}_{2d}\mathbf{A}_d & \mathbf{B}_{2d}^T\mathbf{P}_{2m}\mathbf{A}_r \end{bmatrix} \tag{4.37}$$

For the sake of simplicity the inverse matrix is abbreviated as

$$\begin{bmatrix} \mathbf{\Delta}_1 & \mathbf{\Delta}_2 \\ \mathbf{\Delta}_3 & \mathbf{\Delta}_4 \end{bmatrix} \triangleq \begin{bmatrix} \mathbf{R}_{11} + \mathbf{B}_{d1}^T\mathbf{P}_{d1}\mathbf{B}_{d1} & \mathbf{B}_{d1}^T\mathbf{P}_{d1}\mathbf{B}_{d2} \\ \mathbf{B}_{d2}^T\mathbf{P}_{d2}\mathbf{B}_{d1} & \mathbf{R}_{22} + \mathbf{B}_{d2}^T\mathbf{P}_{d2}\mathbf{B}_{d2} \end{bmatrix}^{-1} \tag{4.38}$$

Substituting $\mathbf{G}_1^+, \mathbf{G}_2^+$ from Eq. (4.37) into (4.31) yields

$$\begin{aligned} \mathbf{P}_{di}^+ = \mathbf{Q}_{di} &- \mathbf{A}_d^T\left(\mathbf{\Delta}_1\mathbf{B}_{d1}^T\mathbf{P}_{d1} + \mathbf{\Delta}_2\mathbf{B}_{d2}^T\mathbf{P}_{d2}\right)^T \mathbf{R}_{i1}\left(\mathbf{\Delta}_1\mathbf{B}_{d1}^T\mathbf{P}_{d1} + \mathbf{\Delta}_2\mathbf{B}_{d2}^T\mathbf{P}_{d2}\right)\mathbf{A}_d \\ &- \mathbf{A}_d^T\left(\mathbf{\Delta}_3\mathbf{B}_{d1}^T\mathbf{P}_{d1} + \mathbf{\Delta}_4\mathbf{B}_{d2}^T\mathbf{P}_{d2}\right)^T \mathbf{R}_{i2}\left(\mathbf{\Delta}_3\mathbf{B}_{d1}^T\mathbf{P}_{d1} + \mathbf{\Delta}_4\mathbf{B}_{d2}^T\mathbf{P}_{d2}\right)\mathbf{A}_d \\ &+ \mathbf{A}_d^T\left(\mathbf{I} + \left(\mathbf{B}_{d1}\mathbf{\Delta}_1 + \mathbf{B}_{d2}\mathbf{\Delta}_3\right)\mathbf{B}_{d1}^T\mathbf{P}_{d1} + \left(\mathbf{B}_{d1}\mathbf{\Delta}_2 + \mathbf{B}_{d2}\mathbf{\Delta}_4\right)\mathbf{B}_{d2}^T\mathbf{P}_{d2}\right)^T \mathbf{P}_{di} \\ &\quad \left(\mathbf{I} + \left(\mathbf{B}_{d1}\mathbf{\Delta}_1 + \mathbf{B}_{d2}\mathbf{\Delta}_3\right)\mathbf{B}_{d1}^T\mathbf{P}_{d1} + \left(\mathbf{B}_{d1}\mathbf{\Delta}_2 + \mathbf{B}_{d2}\mathbf{\Delta}_4\right)\mathbf{B}_{d2}^T\mathbf{P}_{d2}\right)\mathbf{A}_d \end{aligned} \tag{4.39}$$

and

$$\begin{aligned} \mathbf{P}_{mi}^+ = \mathbf{Q}_{mi} &- \mathbf{A}_d^T\left(\mathbf{\Delta}_1\mathbf{B}_{d1}^T\mathbf{P}_{d1} + \mathbf{\Delta}_2\mathbf{B}_{d2}^T\mathbf{P}_{d2}\right)^T \mathbf{R}_{i1}\left(\mathbf{\Delta}_1\mathbf{B}_{d1}^T\mathbf{P}_{m1} + \mathbf{\Delta}_2\mathbf{B}_{d2}^T\mathbf{P}_{m2}\right)\mathbf{A}_r \\ &- \mathbf{A}_d^T\left(\mathbf{\Delta}_3\mathbf{B}_{d1}^T\mathbf{P}_{d1} + \mathbf{\Delta}_4\mathbf{B}_{d2}^T\mathbf{P}_{d2}\right)^T \mathbf{R}_{i2}\left(\mathbf{\Delta}_3\mathbf{B}_{d1}^T\mathbf{P}_{m1} + \mathbf{\Delta}_4\mathbf{B}_{d2}^T\mathbf{P}_{m2}\right)\mathbf{A}_r \\ &- \mathbf{A}_d^T\left(\mathbf{I} + \left(\mathbf{B}_{d1}\mathbf{\Delta}_1 + \mathbf{B}_{d2}\mathbf{\Delta}_3\right)\mathbf{B}_{d1}^T\mathbf{P}_{d1} + \left(\mathbf{B}_{d1}\mathbf{\Delta}_2 + \mathbf{B}_{d2}\mathbf{\Delta}_4\right)\mathbf{B}_{d2}^T\mathbf{P}_{d2}\right)^T \mathbf{P}_{di} \\ &\quad \left(\left(\mathbf{B}_{d1}\mathbf{\Delta}_1 + \mathbf{B}_{d2}\mathbf{\Delta}_3\right)\mathbf{B}_{d1}^T\mathbf{P}_{m1} + \left(\mathbf{B}_{d1}\mathbf{\Delta}_2 + \mathbf{B}_{d2}\mathbf{\Delta}_4\right)\mathbf{B}_{d2}^T\mathbf{P}_{m2}\right)\mathbf{A}_r \end{aligned} \tag{4.40}$$

The optimal controller is obtained by first solving equations (4.39), and then feeding the resulting time-independent $\mathbf{P}_{di}$ matrices into equations (4.40) to find the matrices $\mathbf{P}_{mi}$. The stationary solutions $\mathbf{P}_{di}^{+} = \mathbf{P}_{di}$ and $\mathbf{P}_{mi}^{+} = \mathbf{P}_{mi}$ of equations (4.39) and (4.40) can be found in an iterative process. Substituting the stationary $\mathbf{P}_{di}, \mathbf{P}_{mi}$ into Eq. (4.30) yields the optimal preview feedback control u_i^* that guarantees the Nash equilibrium.

4.2.2. Simulation and Results

Computer simulations are carried out to verify the effectiveness of the proposed discrete time preview interaction model. The derived models of the vehicle driver and controller are, hence, evaluated using the nonlinear model that was introduced in Section 3.2. The primary objective of the evaluation scenario is defined in Section 4.1.2 in order to stably steer the vehicle through a single lane change of four meters.

The continuous-time system matrices of model (4.1) are discretized using the MATLAB function '*c2d*' (continuous to discrete) [MathWorks, 2010]. Assuming a sampling frequency of $100\,Hz$, i.e. sampling time $T_s = 0.01\,\mathrm{s}$, the discrete-time system matrices read as

$$\mathbf{A}_d = \begin{bmatrix} 1 & 0.0099 & 0.01 & 0 \\ 0 & 0.9885 & 0 & -0.0088 \\ 0 & 0 & 1 & 0.01 \\ 0 & 0.0031 & 0 & 0.992 \end{bmatrix}, \mathbf{B}_{d1} = 10^{-3} \times \begin{bmatrix} 0.002 \\ 0.330 \\ 0.002 \\ 0.355 \end{bmatrix}, \mathbf{B}_{d2} = \begin{bmatrix} 0 \\ -0.0001 \\ 0.0001 \\ 0.0266 \end{bmatrix} \tag{4.41}$$

To reserve solution accuracy, the integration time step frequency was set to $10^4\,Hz$, while using a "Down Sample" block in Simulink to reduce it to the sampling frequency as shown in Figure 4.3.

To better assess the effects of the preview time in the presented optimal preview control framework, three drivers are selected with the same control priorities as defined in (4.23), but with different preview time ability: no preview time $(T_p = 0\,s)$, short preview time $(T_p = 0.1\,s)$, and large preview time $(T_p = 1\,s)$. For all driving scenarios, the DYC system

is turn on and act as an ideal Nash player as defined by the optimal feedback controller in (4.30).

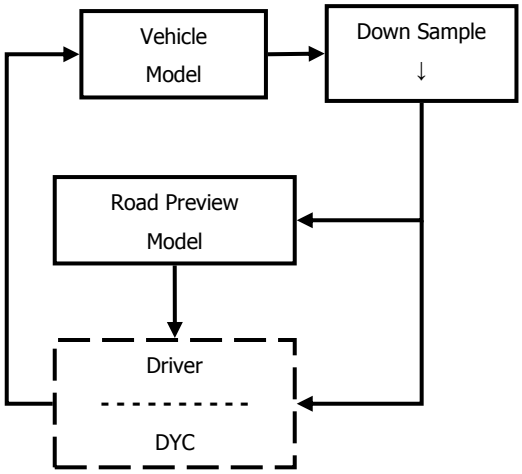

Figure 4.3 Down-sampling of frequency in simulation model

Figure 4.4-5 show the simulation results.

Figure 4.4(a) shows that all three drivers successfully steers the vehicle through a single lane change maneuver of four meters; however, the vehicle with the driver of larger preview time ability kicks off the lane changing sooner. As the preview time decreases, the vehicle exhibits slower response and more overshoot.

Figure 4.4(b,e) show that the vehicle lateral and roll motions is more stable as the preview time increases. In the other words, the preview time gives the vehicle more time to cope with the dynamics of the previewed maneuver.

Figure 4.4(d) indicates that the vehicle yaw rate is more close to its corresponding desired yaw rate as the preview time increases; thus, it is concluded that the handling performance is best guaranteed for the driver with higher preview time ability.

Figure 4.4(f) shows that in all cases the vehicle speed was almost kept at $20(m/s)$ which insures the validity of the system linearization.

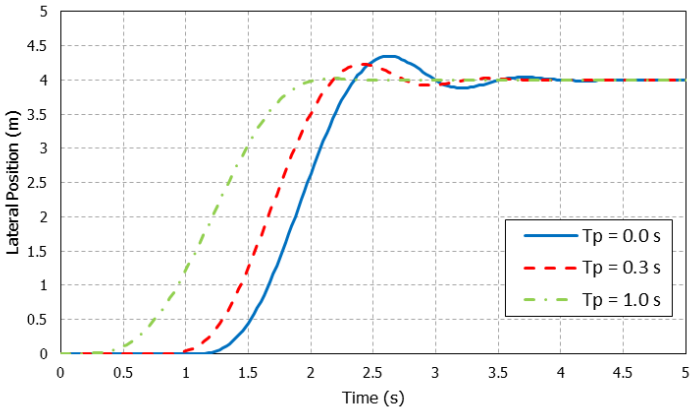
Lateral Position (m)
Time (s)
Tp = 0.0 s
Tp = 0.3 s
Tp = 1.0 s

(a)

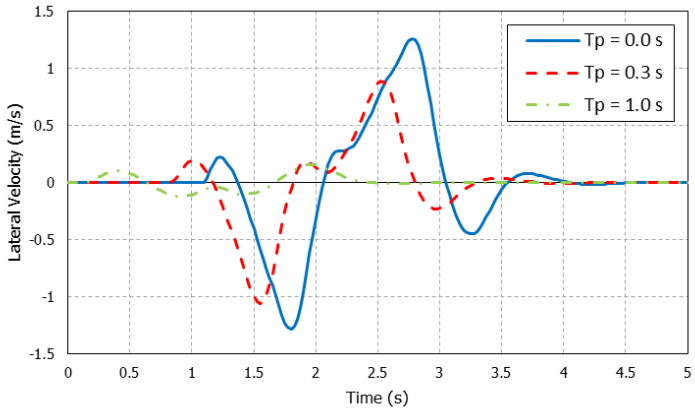
Lateral Velocity (m/s)
Time (s)
Tp = 0.0 s
Tp = 0.3 s
Tp = 1.0 s

(b)

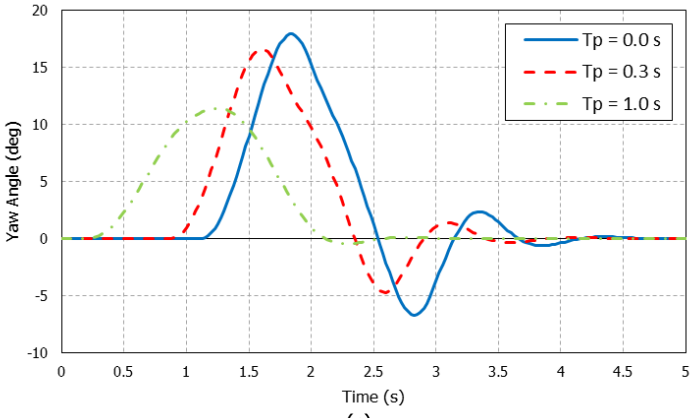
Yaw Angle (deg)
Time (s)
Tp = 0.0 s
Tp = 0.3 s
Tp = 1.0 s

(c)

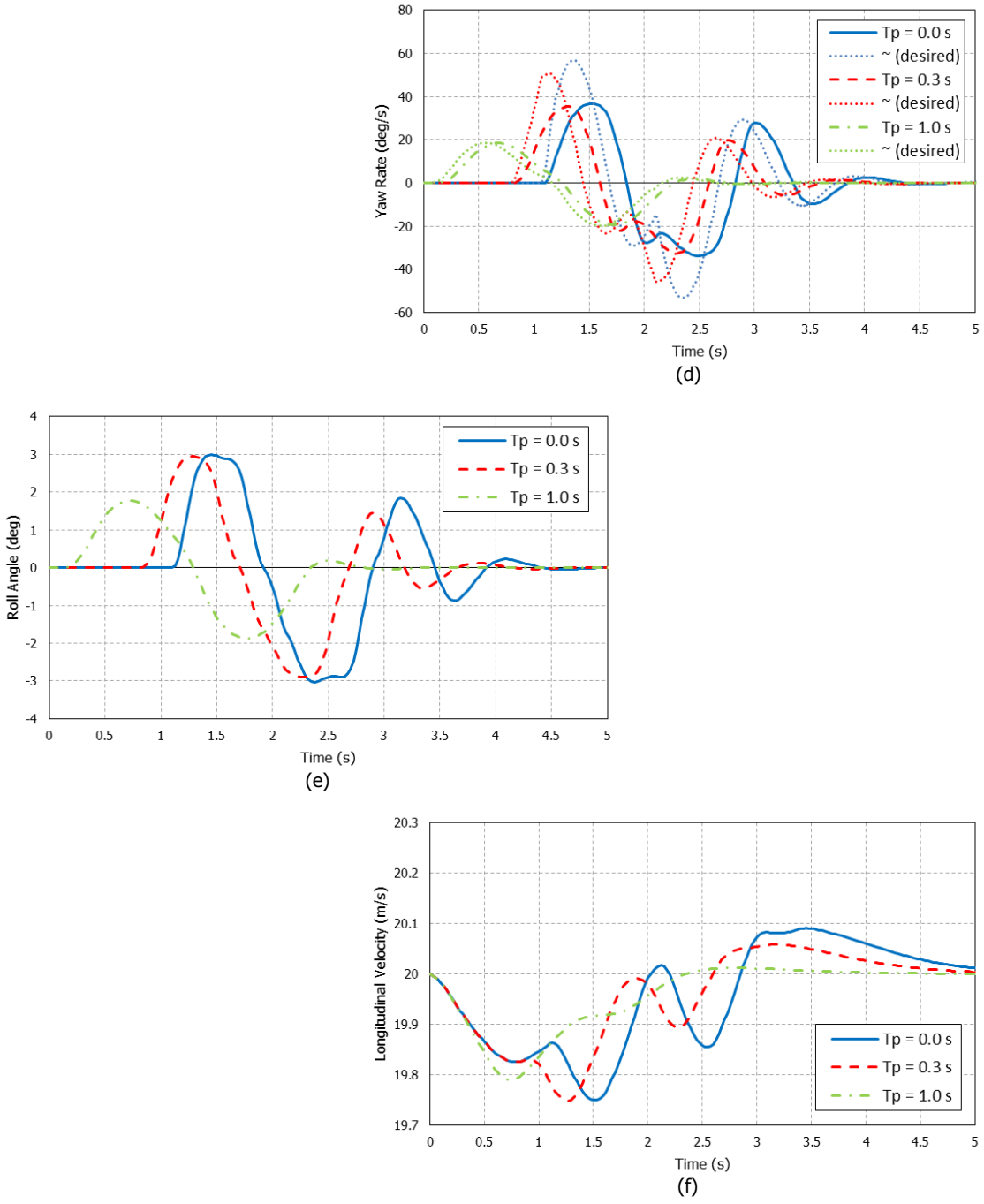

Figure 4.4 Discrete time interaction model; vehicle states: (a) lateral position, (b) lateral velocity, (c) yaw angle, (d) yaw rate, (e) roll angle, (f) longitudinal velocity

Figure 4.5 shows the driver's steering angle and the corrective yaw moment. It is concluded that as the preview time increases the driver and the controller get involved sooner to follow the direction change. Based on Figure 4.5(a), as the preview time increases, the steering action is extended in time, but the peak value drops. Similar trend can be seen for the controller's effort, i.e. corrective yaw moment, in Figure 4.5(b).

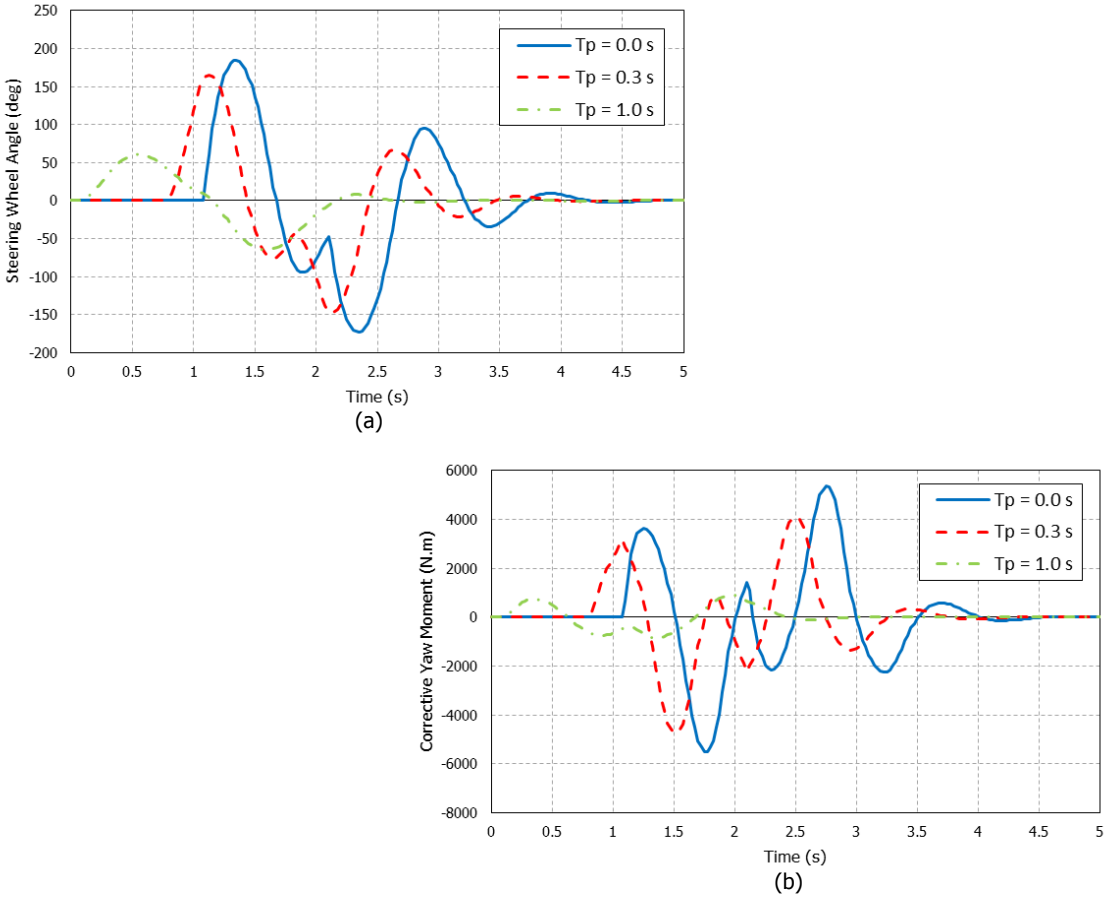

Figure 4.5 Discrete time interaction model; control inputs: (a) steering wheel angle, (b) corrective yaw moment

4.3. Sensitivity Analysis

The proposed vehicle driver-controller interaction relies on the use of a mathematical model and the quality of this model depends on how closely its response matches that of the physical plant, specifically the human driver. Since it is very difficult to obtain a mathematical model that is identical to the physical plant, design techniques must be

designed in a robust manner in the face of uncertainty and unknown disturbances and it requires a sensitivity analysis of the uncertain parameters. The sources of this uncertainty in the mathematical model description may be unknown, in which case some general uncertainty is imposed on the linear feedback gains of the driver steering control model.

4.3.1. μ-Sensitivity

The basis of robust stability criteria for both unstructured and structured perturbations is the well-known "small gain theorem" introduced by Zames (1966):

Theorem 4.4 (Small Gain Theorem) *Consider the feedback interconnection depicted in Figure 4.1. Suppose* $\mathbf{P}$ *is the plant and let* $\gamma > 0$. *Then this feedback interconnection is internally stable for all unstructured uncertainty* $\mathbf{\Delta}$ *with* $\|\mathbf{\Delta}\|_\infty \le 1/\gamma$ *if and only if* $\|\mathbf{P}\|_\infty < \gamma$.

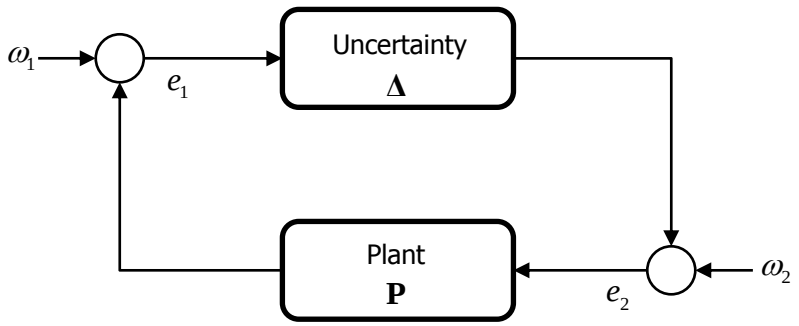

Figure 4.6 Standard feedback configuration

For the standard feedback configuration shown in Figure 4.6, the structured singular value of $\mathbf{P}$ with respect to uncertainty structure $\mathbf{\Delta}$ is defined by

$$\mu_{\mathbf{\Delta}}(\mathbf{P}) = \frac{1}{\min\left(\bar{\sigma}(\mathbf{\Delta}) : |\mathbf{I} - \mathbf{P}\mathbf{\Delta}| = 0\right)} \tag{4.42}$$

unless no $\mathbf{\Delta}$ makes $\mathbf{I} - \mathbf{P}\mathbf{\Delta}$ singular, in which case $\mu_{\mathbf{\Delta}}(\mathbf{P}) = 0$. Here, $\bar{\sigma}(\mathbf{\Delta})$ represents the maximum singular value of matrix $\mathbf{\Delta}$.

The following theorem [Packard, 1993] is a natural extension of the small gain theorem to the structured uncertainty case:

Theorem 4.5 *Consider the feedback interconnection depicted in Figure 4.1. Assuming that* $\gamma > 0$, *this feedback interconnection is internally stable for all structured* $\boldsymbol{\Delta}$ *with* $\|\boldsymbol{\Delta}\|_\infty \le 1/\gamma$ *if and only if* $\sup_{\delta \in \boldsymbol{\Delta}} \mu_{\boldsymbol{\Delta}}(\mathbf{P}) < \gamma$.

Hence, the peak value of the μ-plot of $\mathbf{P}$ determines the size of the perturbations that the loop is robustly stable against.

For the continuous time system (4.1) with the linear feedback controls (4.14) and (4.15), the sensitivity of the system regarding the driver mode is investigated. The uncertain plant model is represented by

$$\mathbf{P} = \begin{bmatrix} \mathbf{A}_c + \mathbf{B}_{c1}\mathbf{G}_1(\mathbf{I} + \mathbf{W}) & \mathbf{B}_{c2}\mathbf{G}_2 \\ 0 & \mathbf{A}_c + \mathbf{B}_{c2}\mathbf{G}_2 \end{bmatrix} \tag{4.43}$$

where the uncertainty matrix $\mathbf{W}$ is a diagonal matrix, and $\mathbf{I}$ is the identity matrix.

4.3.2. Simulation and Results

Computer simulations are carried out to investigate the sensitivity of the proposed continuous time interaction model to the structured uncertainties in the driver's steering control performance which is best reflected in the driver's feedback gain $\mathbf{G}_1$.

The Bode diagram of the vehicle-driver system for a vehicle speed of $20(m/s)$ and a variation of $\pm 40\%$ for driver control gain $\mathbf{G}_1$ with respect to the nominal optimal gains are shown for the transfer functions between the lateral position y (and yaw angle θ_z) and the vehicle control input, i.e. corrective yaw moment τ_{zc}.

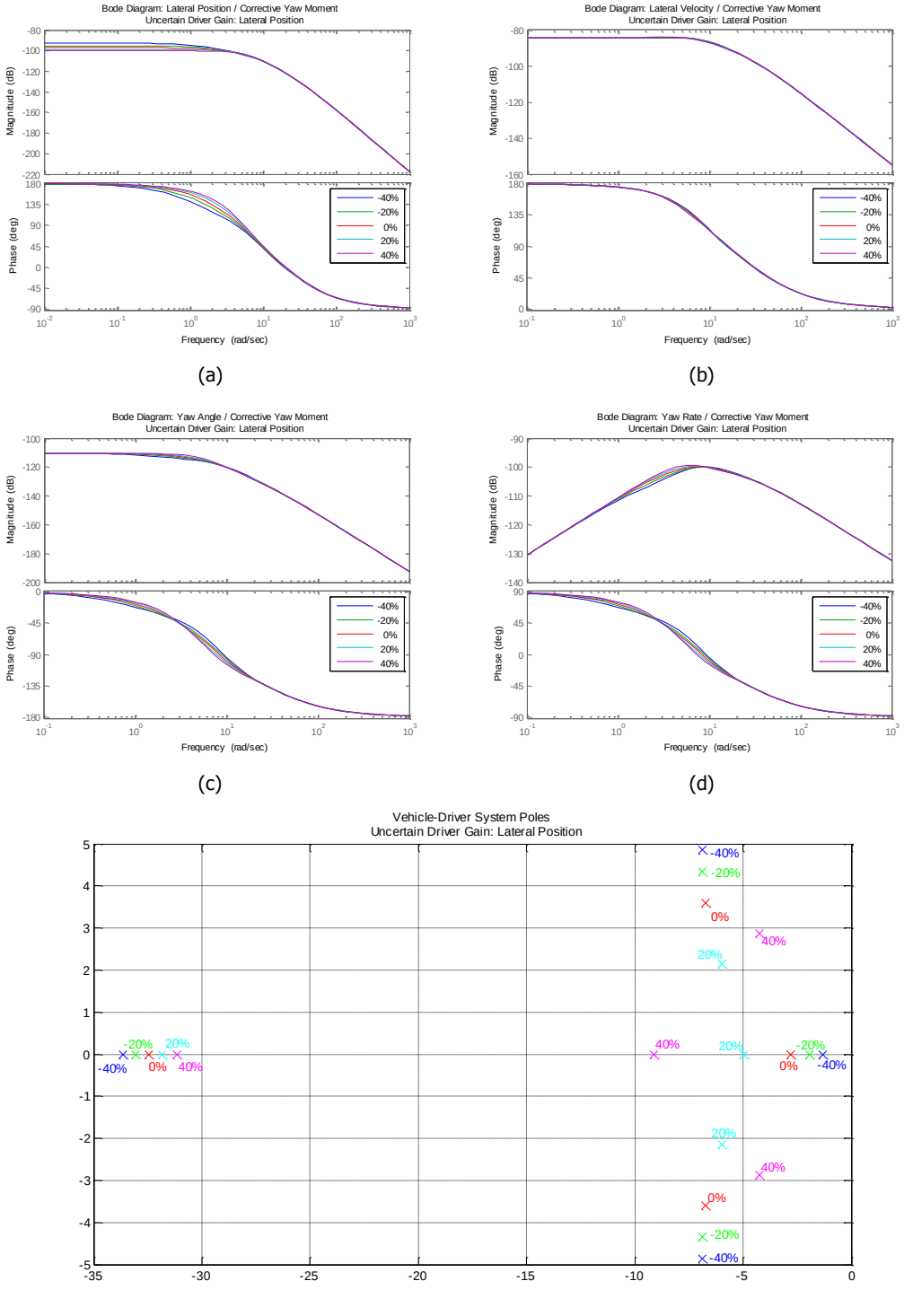

Figure 4.7 Effect of uncertainty in driver feedback gain of lateral position on vehicle-driver system

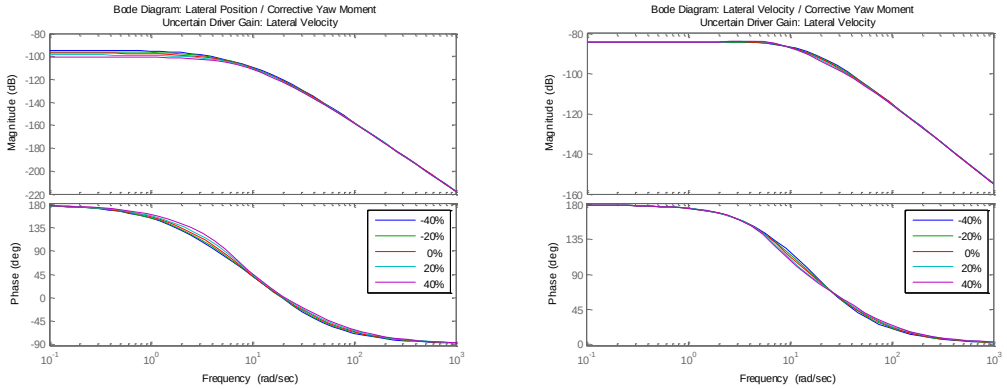

(a)

(b)

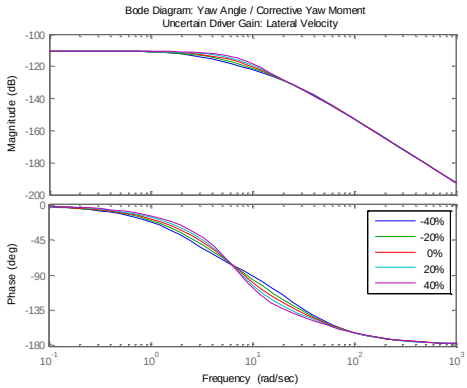

(c)

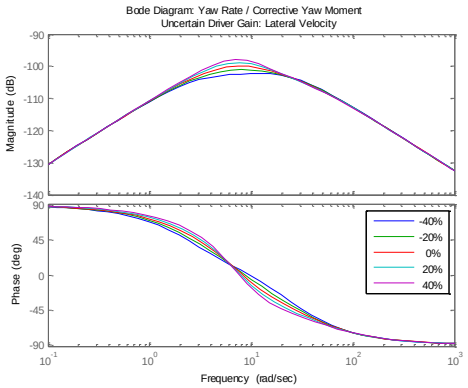

(d)

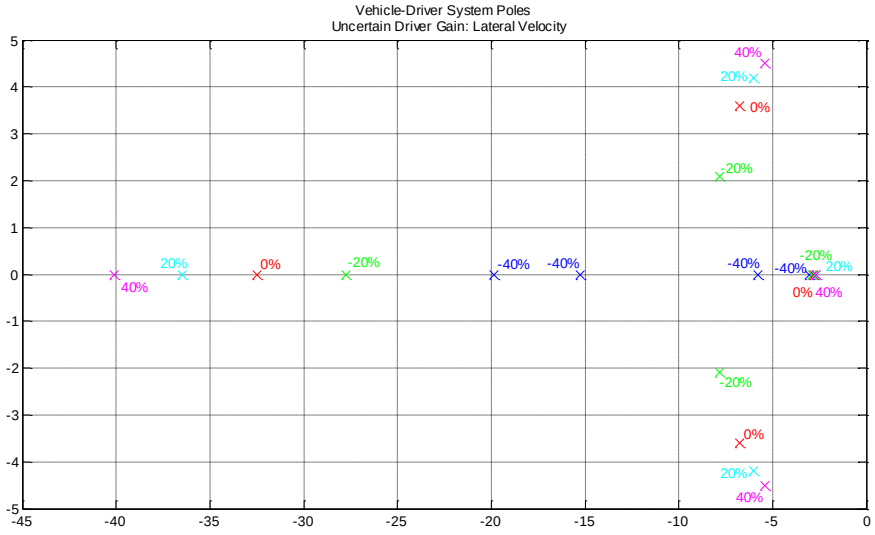

(e)

Figure 4.8 Effect of uncertainty in driver feedback gain of lateral velocity on vehicle-driver system

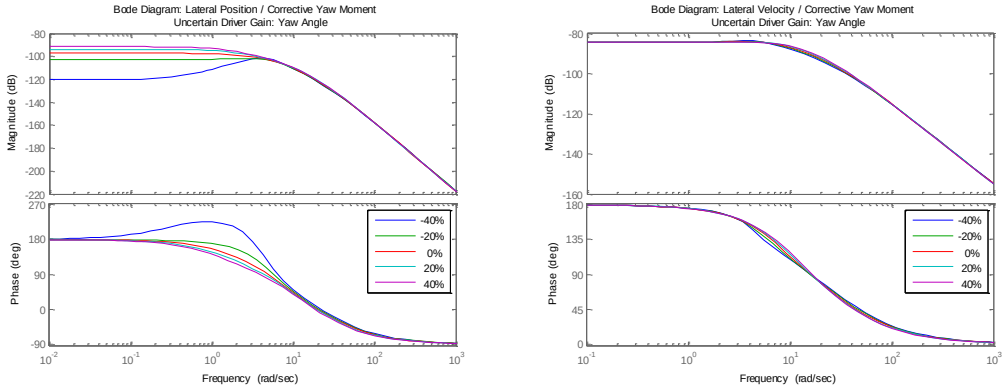

(a)

(b)

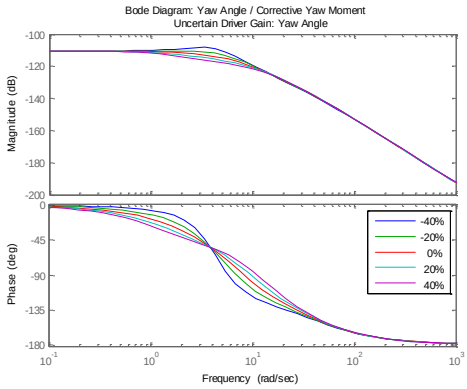

(c)

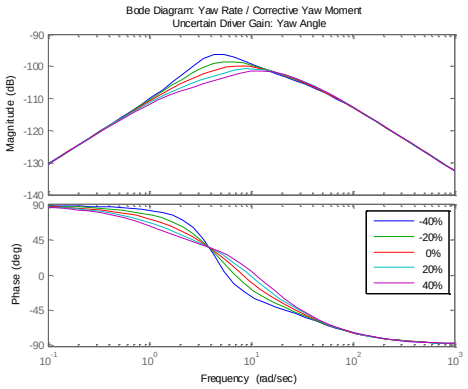

(d)

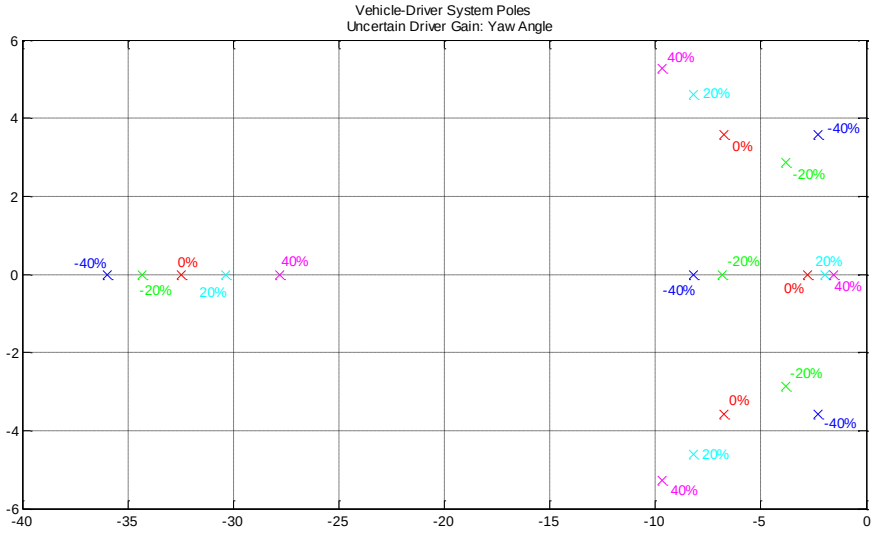

(e)

Figure 4.9 Effect of uncertainty in driver feedback gain of yaw angle on vehicle-driver system

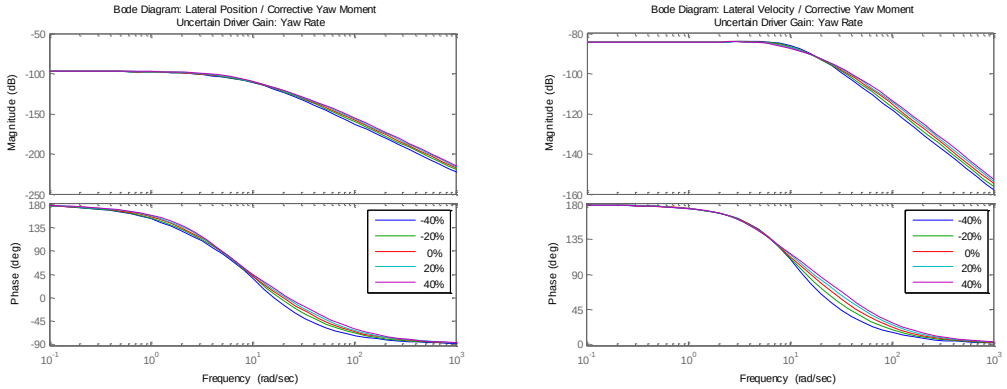

(a)

(b)

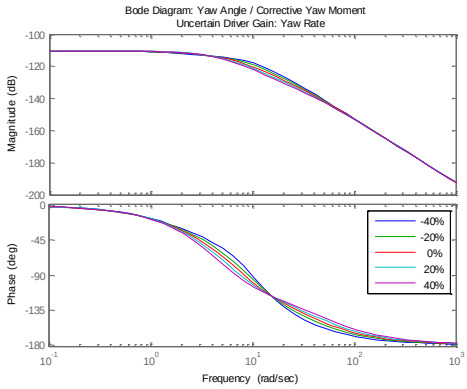

(c)

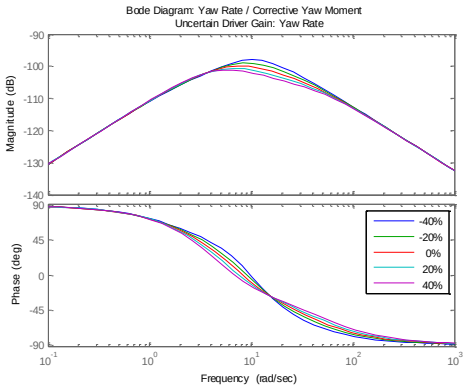

(d)

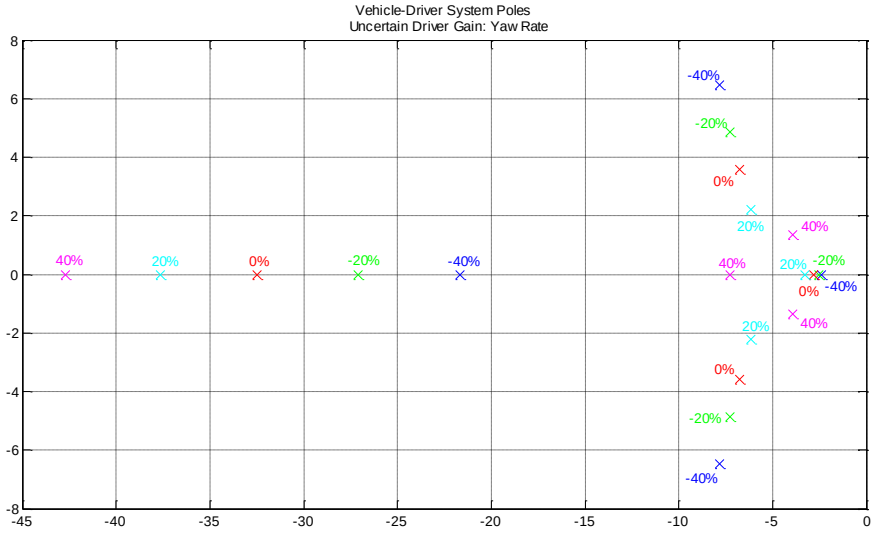

(e)

Figure 4.10 Effect of uncertainty in driver feedback gain of yaw rate on vehicle-driver system

Figure 4.7-10 show that the vehicle-driver system is stable with respect to changes in driver feedback gains; however, as the lower bound of uncertainty in the driver's gain corresponding to the yaw angle expands the vehicle lateral position moves toward instability as it is shown in Figure 4.9(a,e). Hence, it is concluded that the driver's gain for the yaw angle is the most sensitive parameter of the open-loop vehicle-driver system.

For closed-loop analysis, μ-sensitivity of the vehicle-driver system is investigated. Three cases are studied: (a) cooperative control framework through the Game Theory interaction model (4.20), (b) independent control strategies through the LQR interaction model (4.21), (c) the driver performs independently based on the LQR gains but the vehicle controller acts as the optimal Nash player.

The μ-plot of the plant (4.43) is shown in Figure 4.11. The blue bars indicate the sensitivity of the driver-controller interaction model to the uncertainty in the driver's feedback gain corresponding to the lateral position error, while the cyan, yellow, and the red bars indicate the uncertainties in the gains corresponding to the lateral velocity error, yaw angle error, and yaw rate error, respectively.

Figure 4.11(a) implies that the proposed continuous time driver-controller interaction model based on Game Theory is sensitive to the uncertainties in the driver's feedback gain corresponding to the lateral position error, yaw angle error, and yaw rate error, while the system is robust with respect to the uncertainty in the feedback gain corresponding to the lateral velocity error. The conclusions seems sound since this interaction model gives the globally optimal based on its current knowledge of the driver's steering control model and if the driver feedback gains contain uncertainty, the global optimum cannot be attained.

The independent actions of the driver and the controller in the driver-controller interaction model based on the linear quadratic regulation strategy is mostly relied on the driver's actions as the Figure 4.11(b) indicates that the system is only sensitive to the uncertainties in the driver's feedback gain corresponding to the lateral position and yaw angle errors and the uncertainty in the feedback gain corresponding to the yaw rate error does not affect the system performance.

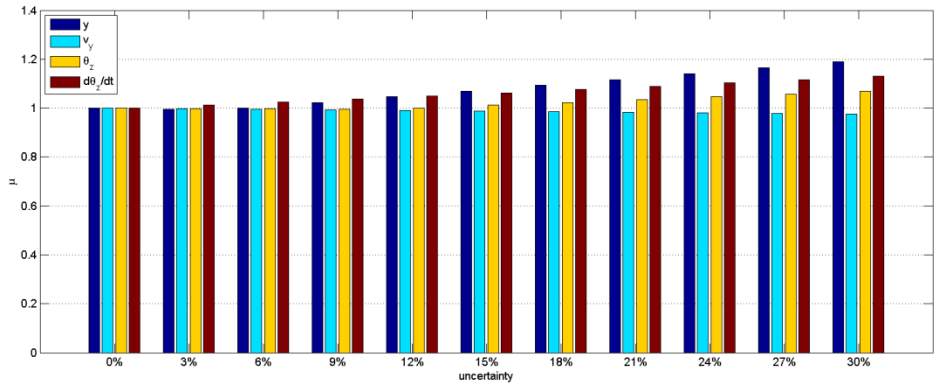

(a)

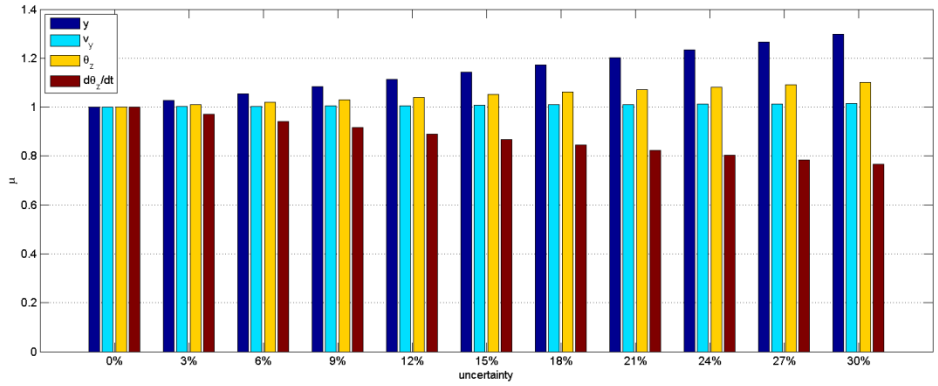

(b)

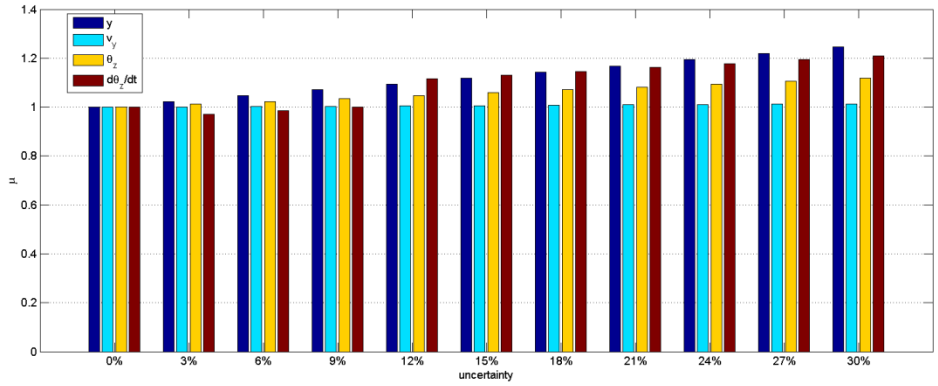

(c)

Figure 4.11 μ-plot of the continuous-time driver-controller interaction model: (a) Game Theory, (b) LQR, (c) mixed

Figure 4.11(c) shows that the mixed interaction model, i.e. when the driver performs independently based on the LQR gains and the vehicle controller acts as the optimal Nash player, shows almost the same sensitivity behavior as in the Game Theory framework shown in Figure 4.11(a); however, for the uncertainties less than 9% in the driver's feedback gain corresponding to the yaw rate error, the system is robust and the mixed interaction model is only sensitive to those uncertainties of more than 9%.

4.4. Robust Interaction Model

For the purpose of control design, a low-order feedback steering control for the driver model was developed. Therefore, it is reasonable to expect that the driver model uncertainties exist. It is necessary to obtain a reasonable picture of the driver model uncertainty that represents the difference between a real driver and the driver model at any instant in time, or to represent the change in driving behavior with time. Section 4.3 investigated the sensitivity of each driver's control gain on the system total performance. This section studies the robust control design methodology for the vehicle direct yaw control system.

In this research, the driver model uncertainty is assumed to lie within the cost priority matrices $\mathbf{Q}_1$ and $\mathbf{R}_{11}, \mathbf{R}_{12}$. Assuming that driver's steering input varies in a bounded tube of its estimation as shown in Figure 4.12, a modified version of Game Theory is derived to cope with uncertainties emerged from the driver model inaccuracy and other sources. The Integral Sliding Mode (ISM) control yields to a game that the min-max robust Nash strategies can be applied.

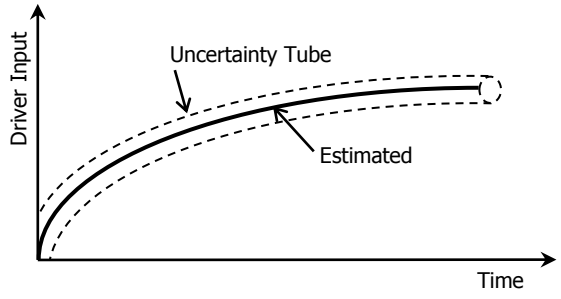

Figure 4.12 Uncertainty tube of driver input around estimate value

Again consider the continuous time game system (4.1) with the same quadratic cost function given in (4.2), but in the presence of the steering angle uncertainties imposed by the driver:

$$\dot{x}(t) = \mathbf{A}_c x(t) + \mathbf{B}_{c1}\left(\underbrace{\delta_{sw}(t)}_{u_1} + \bar{\delta}(t) \right) + \mathbf{B}_{c2} \underbrace{M_{zc}(t)}_{u_2} \tag{4.44}$$

where $\mathbf{A}_c, \mathbf{B}_{c1}, \mathbf{B}_{c2}$ are the known system matrices representing their best approximation of the real world, and $\bar{\delta}(t)$ is the unknown exciting signal representing the uncertainty in the driver model with respect to its corresponding optimum based on Game Theory interaction framework and satisfies the following assumption:

Assumption 4.1. *The unknown signal* $\bar{\delta}(t)$ *is smooth disturbances and bounded:*

$$\forall t \geq 0, \quad \bar{\delta}(t) \leq \mathbf{F} x(t) + \bar{\delta}_0 \tag{4.45}$$

where $\mathbf{F} \in \Re^{1\times 4}$ *and* $\bar{\delta}_0 > 0$.

4.4.1. Robust Control Design

The vehicle controller is supposed to reject the uncertainty in the driver model and make the interaction model robust. Hence, the methodology of Integral Sliding Mode (ISM) is applied and the robust Nash strategies are designed as

$$\begin{cases} u_1 = u_{o1} \\ u_2 = u_{o2} + u_\delta \end{cases} \tag{4.46}$$

where u_{o1}, u_{o2} are assumed to be the optimal control strategies as defined in (4.12) for the certain system defined in (4.1), and u_δ is designed to be discontinuous for rejecting the perturbation term $\bar{\delta}(t)$.

Substituting the control (4.46) in the uncertain game model (4.44) leads to:

$$\dot{x}(t) = \mathbf{A}_c x(t) + \mathbf{B}_{c1}\left(u_{o1}(t) + \bar{\delta}(t) \right) + \mathbf{B}_{c2}\left(u_{o2}(t) + u_\delta(t) \right) \tag{4.47}$$

Following the Integral Sliding Mode methodology, the sliding mode surface for the vehicle controller is defined as

$$s(x,t) = s_o(x,t) + s_\delta(x,t) \tag{4.48}$$

This switching function (4.48) consists of two parts that will be defined later; the first part s_o may be designed as the linear combination of the system states; and the second part s_δ includes the integral term.

Time derivative of the sliding surface (4.48) is:

$$\begin{aligned}\dot{s}(x,t) &= \dot{s}_o(x,t) + \dot{s}_\delta(x,t) \\ &= \frac{\partial s_o(x,t)}{\partial x}\dot{x} + \frac{\partial s_o(x,t)}{\partial t} + \dot{s}_\delta(x,t) \\ &= \frac{\partial s_o(x,t)}{\partial x}\left(\mathbf{A}_c x(t) + \mathbf{B}_{c1}\left(u_{o1}(t) + \bar{\delta}(t)\right) + \mathbf{B}_{c2}\left(u_{o2}(t) + u_\delta(t)\right)\right) \\ &\quad + \frac{\partial s_o(x,t)}{\partial t} + \dot{s}_\delta(x,t)\end{aligned} \tag{4.49}$$

The auxiliary variables s_o and s_δ are selected as

$$s_o(x;t) = \mathbf{G}^T x(t) \tag{4.50}$$

$$\begin{aligned}\dot{s}_\delta(x,t) &= -\frac{\partial s_o(x,t)}{\partial t} - \frac{\partial s_o(x,t)}{\partial x}\left(\mathbf{A}_c x(t) + \sum_{i=1}^{2}\mathbf{B}_{ci}u_{oi}(t)\right) \\ &= -\mathbf{G}^T\left(\mathbf{A}_c x(t) + \sum_{i=1}^{2}\mathbf{B}_{ci}u_{oi}(t)\right)\end{aligned} \tag{4.51}$$

$$s_\delta(x_0,t_0) = -s_o(x_0,t_0)$$

to simplify the switching function (4.48) into

$$\dot{s}(x,t) = \mathbf{G}^T\left(\mathbf{B}_{c1}\bar{\delta}(t) + \mathbf{B}_{c2}u_\delta(t)\right) \tag{4.52}$$

For stability analysis and robust control design, the following Lyapunov candidate is introduced:

$$V(x,t) = \frac{1}{2}s^2(x,t) \geq 0 \quad , \quad \forall t \tag{4.53}$$

The time derivate of $V(x,t)$ is

$$\dot{V}(x,t) = s(x,t)\dot{s}(x,t) = s(x,t)\left(\mathbf{G}^T\left(\mathbf{B}_{c1}\bar{\delta}(t) + \mathbf{B}_{c2}u_\delta(t)\right)\right) \tag{4.54}$$

The stability is insured by choosing the disturbance rejection control u_δ as

$$u_\delta = -\mathbf{B}_{c2}^T \left(\mathbf{B}_{c2}\mathbf{B}_{c2}^T\right)^{-1} \mathbf{B}_{c1} \left(\mathbf{F}x(t) + \bar{\delta}_0\right) \mathrm{sgn}\left(s(x,t)\right) \tag{4.55}$$

where sgn() is the sign function.

Substituting the control (4.55) into (4.54) yields

$$\begin{aligned} \dot{V}_i &= s(x,t)\mathbf{G}^T\mathbf{B}_{c1}\left(\bar{\delta}(t) - \left(\mathbf{F}x(t) + \bar{\delta}_0\right)\mathrm{sgn}(s(x,t))\right) \\ &\le s(x,t)\mathbf{G}^T\mathbf{B}_{c1}\left(\bar{\delta}(t) - \mathbf{F}x(t) - \bar{\delta}_0\right)\mathrm{sgn}\left(s(x,t)\right) \le 0 \quad , \quad \forall t \end{aligned} \tag{4.56}$$

Since the time derivative of the Lyapunov candidate (4.53) is negative, the system stability (4.48) is guaranteed based on the Lyapunov direct theorem by the proposed control (4.55).

The uncertain system (4.44) can be, hence, rewritten as

$$\begin{aligned} \dot{x}(t) = &\underbrace{\left(\mathbf{A}_c - \mathbf{B}_{c1}\mathbf{F}\,\mathrm{sgn}\left(s(x,t)\right)\right)}_{\mathbf{A}_{eq}} x(t) \\ &+\mathbf{B}_{c1}u_{o1}(t) + \mathbf{B}_{c2}u_{o2}(t) \underbrace{-\mathbf{B}_{c1}\bar{\delta}_0\,\mathrm{sgn}\left(s(x,t)\right)}_{\omega(t)} + \mathbf{B}_{c1}\bar{\delta}(t) \end{aligned} \tag{4.57}$$

Where the sliding surface is obtained from

$$s(x,t) = \mathbf{G}^T x(t) - \mathbf{G}^T \int_0^t \left(\mathbf{A}_c x(\varepsilon) + \sum_{i=1}^{2} \mathbf{B}_{ci} u_{oi}(\varepsilon) \right) d\varepsilon \tag{4.58}$$

Depending on the sliding surface (4.58), the system (4.57) takes one of the following forms:

$$\begin{cases} \dot{x}(t) = \mathbf{A}_c x(t) + \mathbf{B}_{c1}u_{o1}(t) + \mathbf{B}_{c2}u_{o2}(t) + \mathbf{B}_1\bar{\delta}(t) & , s(x,t) = 0 \\ \dot{x}(t) = \left(\mathbf{A}_c - \mathbf{B}_{c1}\mathbf{F}\right)x(t) + \mathbf{B}_{c1}u_{o1}(t) + \mathbf{B}_{c2}u_{o2}(t) - \mathbf{B}_{c1}\bar{\delta}_0 + \mathbf{B}_{c1}\bar{\delta}(t) & , s(x,t) > 0 \\ \dot{x}(t) = \left(\mathbf{A}_c + \mathbf{B}_{c1}\mathbf{F}\right)x(t) + \mathbf{B}_{c1}u_{o1}(t) + \mathbf{B}_{c2}u_{o2}(t) + \mathbf{B}_{c1}\bar{\delta}_0 + \mathbf{B}_{c1}\bar{\delta}(t) & , s(x,t) < 0 \end{cases} \tag{4.59}$$

Assuming that the disturbance $\bar{\delta}(t)$ is white noise and $\omega(t)$ is known, the optimal solution for the set of linear two-player differential games of equation (4.59) is defined by the following theorem:

Theorem 4.6 *Suppose* $\mathbf{K}_i$ *satisfy the coupled Riccati equations given by*

$$\mathbf{A}_{eq}^{T}\mathbf{K}_i + \mathbf{K}_i\mathbf{A}_{eq} + \mathbf{Q}_i - \mathbf{K}_i\mathbf{S}_i\mathbf{K}_i - \mathbf{K}_i\mathbf{S}_{\hat{i}}\mathbf{K}_{\hat{i}} - \mathbf{K}_{\hat{i}}\mathbf{S}_{\hat{i}}\mathbf{K}_i + \mathbf{K}_{\hat{i}}\mathbf{S}_{i\hat{i}}\mathbf{K}_{\hat{i}} = \mathbf{0} \tag{4.60}$$

and the shifting vector k_i resolving uniquely the set of coupled parameterized linear differential equations:

$$\mathbf{A}_{eq}^{T}k_i + \mathbf{K}_i w - \mathbf{K}_i\mathbf{S}_i k_i - \mathbf{K}_i\mathbf{S}_{\hat{i}}k_{\hat{i}} - \mathbf{K}_{\hat{i}}\mathbf{S}_{\hat{i}}k_i + \mathbf{K}_{\hat{i}}\mathbf{S}_{i\hat{i}}k_{\hat{i}} = \mathbf{0} \tag{4.61}$$

where $i = (1,2)$ and $\hat{i}$ is the counter-coalition, i.e. the player counter-acting to the player with index i, and

$$\mathbf{S}_i = \mathbf{B}_{ci}\mathbf{R}_{ii}^{-1}\mathbf{B}_{ci}^{T} \quad , \quad \mathbf{S}_{i\hat{i}} = \mathbf{B}_{c\hat{i}}\mathbf{R}_{\hat{i}\hat{i}}^{-1}\mathbf{R}_{i\hat{i}}\mathbf{R}_{\hat{i}\hat{i}}^{-1}\mathbf{B}_{c\hat{i}}^{T}$$

Then the following strategy

$$u_{oi}^{*}(t) = -\mathbf{R}_{ii}^{-1}\mathbf{B}_{ci}^{T}\left(\mathbf{K}_i x(t) + k_i\right) \tag{4.62}$$

is a linear feedback Nash equilibrium.

Theorem 4.6 gives three sets of Nash equilibrium for the uncertain game model (4.59). Hence, the optimal robust control (4.62) for each set can be rewritten as

$$\begin{aligned} \delta_{sw}^{*}(t) &= -\mathbf{R}_{11}^{-1}\mathbf{B}_{c1}^{T}\left(\mathbf{K}_1 x(t) + k_1\right) = \mathbf{G}_1 x(t) + g_1 \\ M_{zc}^{*}(t) &= -\mathbf{R}_{22}^{-1}\mathbf{B}_{c2}^{T}\left(\mathbf{K}_2 x(t) + k_2\right) = \mathbf{G}_2 x(t) + g_2 \end{aligned} \tag{4.63}$$

where $\mathbf{K}_i$ and k_i are given by (4.60) and (4.61).

4.4.2. Simulation and Results

Computer simulations are carried out to verify the effectiveness of the proposed robust interaction model. The presented driver and controller models are, hence, evaluated using the nonlinear model that was introduced in Section 3.2 with the same primary objective as defined in Section 4.1.2, i.e. to stably steer the vehicle through a single lane change of four meters.

The driver is considered to deviate from the optimal Nash equilibrium (4.15) by disturbance parameter $\bar{\delta}(t)$ which is bounded as defined in (4.45) with

$$\mathbf{F} = (20\%)\mathbf{B}_1 \quad , \quad \bar{\delta}_0 = 10° \tag{4.64}$$

The system matrix $\mathbf{A}_{eq}$ and the known disturbance parameter ω are, hence, found by

$$\begin{cases} \mathbf{A}_{eq}=\begin{bmatrix}0 & 1 & 20 & 0\\ 0 & -8.28 & 0 & -17.68\\ 0 & 0 & 0 & 1\\ 0 & 0.801 & 0 & -5.755\end{bmatrix}, \quad \omega(t)=\begin{bmatrix}0\\0\\0\\0\end{bmatrix} & , s=0 \\ \mathbf{A}_{eq}=\begin{bmatrix}0 & 1 & 20 & 0\\ 0 & -10.58 & 0 & -18.57\\ 0 & 0 & 0 & 1\\ 0 & 0.082 & 0 & -6.095\end{bmatrix}, \quad \omega(t)=\begin{bmatrix}0\\-0.837\\0\\-0.321\end{bmatrix} & , s>0 \\ \mathbf{A}_{eq}=\begin{bmatrix}0 & 1 & 20 & 0\\ 0 & -5.97 & 0 & -16.80\\ 0 & 0 & 0 & 1\\ 0 & 1.685 & 0 & -5.416\end{bmatrix}, \quad \omega(t)=\begin{bmatrix}0\\0.837\\0\\0.321\end{bmatrix} & , s<0 \end{cases} \tag{4.65}$$

Using the same $\mathbf{Q}$ and $\mathbf{R}$ matrices, the final state feedback gains for all three conditions are calculated and listed as follows;

$$\begin{cases} \left.\begin{aligned}\mathbf{G}_1&=\begin{bmatrix}-0.806 & -0.146 & -8.624 & -0.713\end{bmatrix}, & g_1&=0\\ \mathbf{G}_2&=\begin{bmatrix}0 & -677.9 & 0 & -6216.2\end{bmatrix}, & g_2&=0\end{aligned}\right\} & , s=0 \\ \left.\begin{aligned}\mathbf{G}_1&=\begin{bmatrix}-0.750 & -0.067 & -7.819 & -0.726\end{bmatrix}, & g_1&=-0.063\\ \mathbf{G}_2&=\begin{bmatrix}0 & -132.4 & 0 & -7783.1\end{bmatrix}, & g_2&=-893.7\end{aligned}\right\} & , s>0 \\ \left.\begin{aligned}\mathbf{G}_1&=\begin{bmatrix}-0.867 & -0.261 & -9.582 & -0.659\end{bmatrix}, & g_1&=0.106\\ \mathbf{G}_2&=\begin{bmatrix}0 & -1107.3 & 0 & -4450.1\end{bmatrix}, & g_2&=826.38\end{aligned}\right\} & , s<0 \end{cases} \tag{4.66}$$

where $\mathbf{G}_1$, $\mathbf{G}_2$ are the feedback gains and g_1, g_2 are shift vector of the driver and the vehicle controller, respectively.

Figure 4.13-15 show the simulation results.

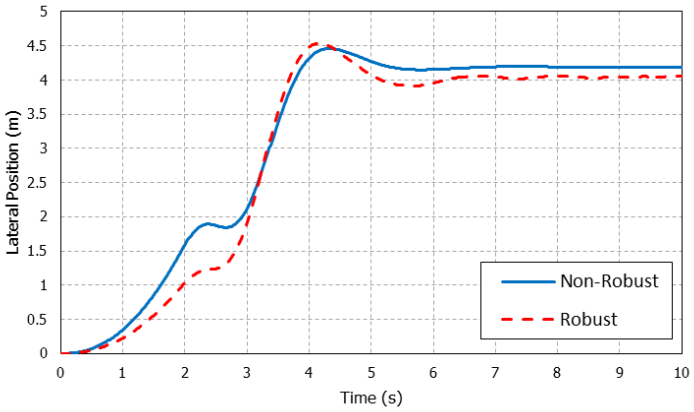
Lateral Position (m)
Time (s)
Non-Robust
Robust

(a)

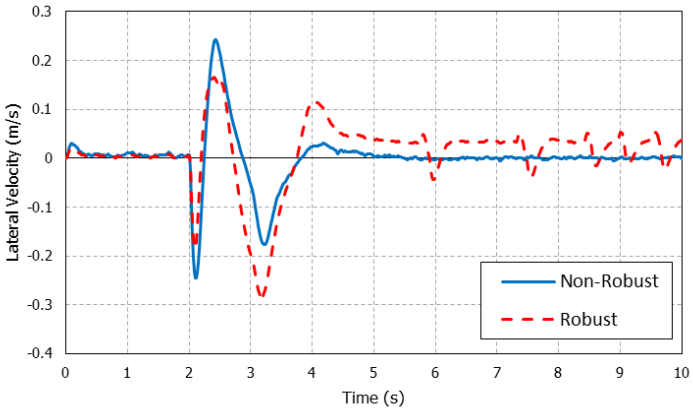
Lateral Velocity (m/s)
Time (s)
Non-Robust
Robust

(b)

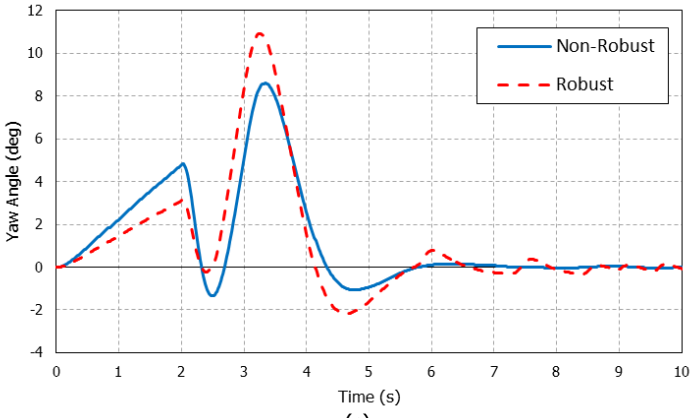
Yaw Angle (deg)
Time (s)
Non-Robust
Robust

(c)

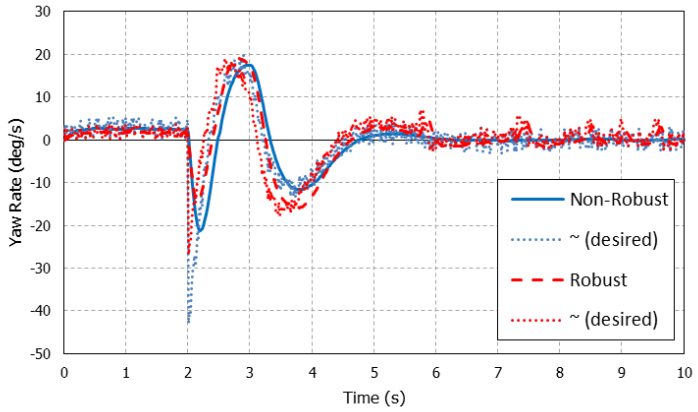

(d)

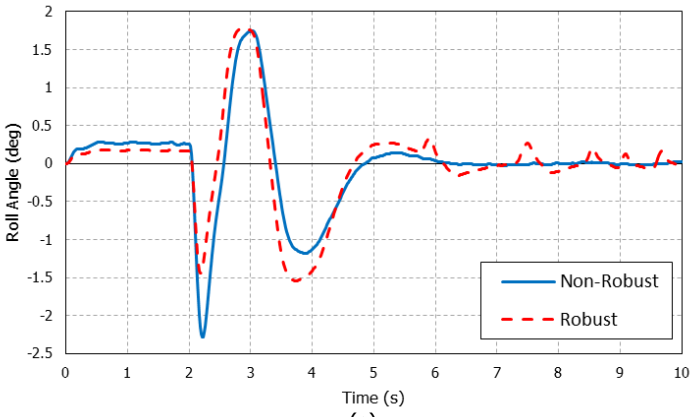

(e)

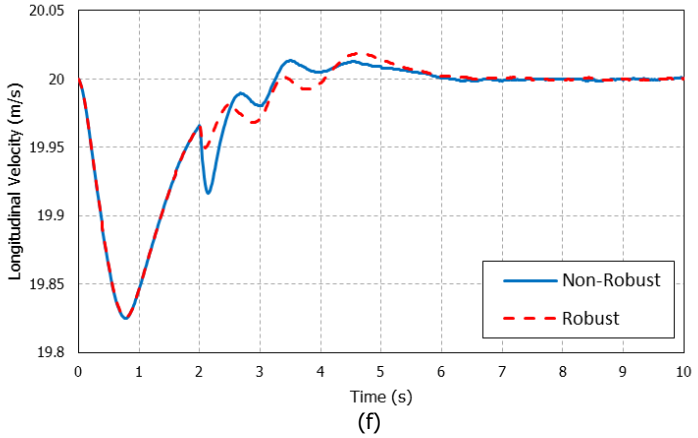

(f)

Figure 4.13 Robust interaction model; vehicle states: (a) lateral position, (b) lateral velocity, (c) yaw angle, (d) yaw rate, (e) roll angle, (f) longitudinal velocity

Figure 4.13 shows that the vehicle performs a single lane change with robust and non-robust vehicle controllers. It is concluded that the robust controller provides more handling comfort as the vehicle yaw rate error with respect to its corresponding desired yaw rate is lower compared to the vehicle with non-robust control system. Figure 4.13(f) shows that in all cases the vehicle speed was almost kept at $20(m/s)$ which insures the validity of the system linearization.

Figure 4.14 shows the time history of the switching functions including the sliding surface $s(x,t)$ and the disturbance rejection part of the sliding surface $s(x,t)$ represented by $s_\delta(x,t)$. It is shown that as the system is stabilized the sliding surface $s(x,t)$ moves toward the equilibrium point, i.e. goes to zero.

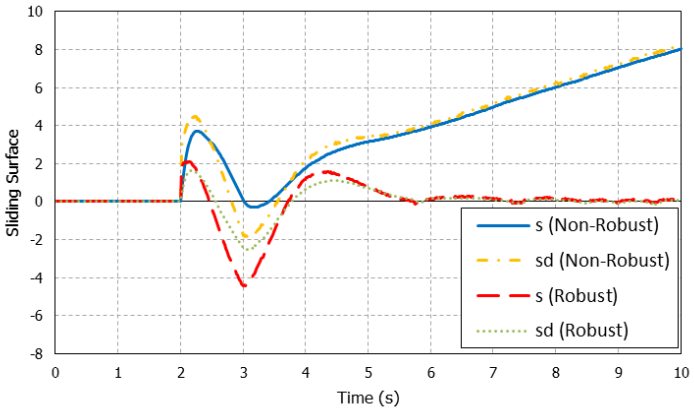

Figure 4.14 Robust interaction model: sliding surface

Figure 4.15 shows the driver's steering angle and the controller's corrective yaw moment. The peak value of the steering angle in the robust controller is less than the peak value of the steering angle in the vehicle with the non-robust controller. Figure 4.15(b) indicates spike behavior in the controller's corrective yaw moment for the robust system due to the chattering effect imposed by the sliding mode control method.

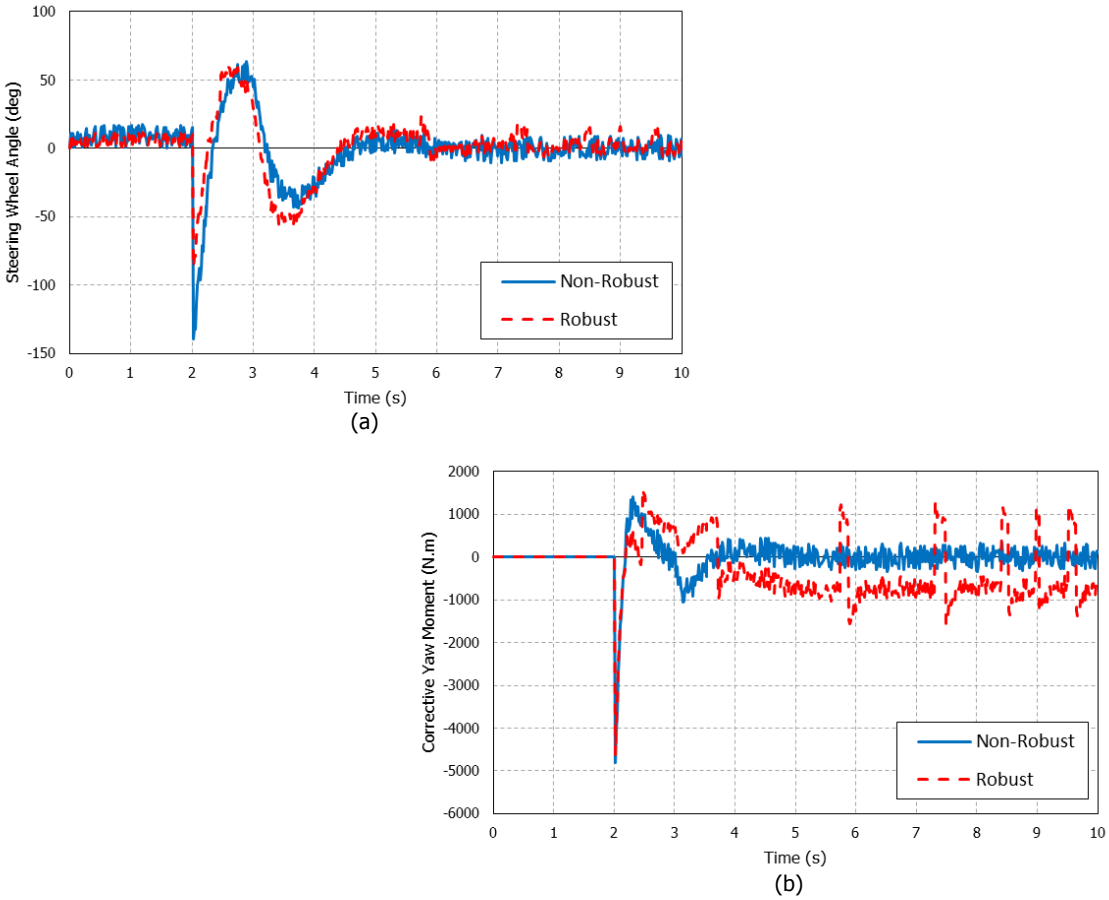

Figure 4.15 Robust interaction model; control inputs: (a) steering wheel angle, (b) corrective yaw moment

Chapter 5
Discussion and Future Work

5.1. Discussion

First, several linear and nonlinear vehicle models were developed and validated with CarSim which is a known vehicle dynamics simulation software. The linear forms of these models were used to develop control strategies while the nonlinear models provided the evaluation platform for controller strategies. The validation results show that the developed vehicle dynamics model is suitable for handling scenarios in this research.

As the main contribution of this research, a new structure for optimal linear car steering and yaw control has been devised based on the game theory concept. Using the definition of a linear quadratic difference game, the driver's steering input and the controller's corrective yaw moment are defined as two dynamic players of the game "vehicle stability", and their corresponding control efforts are optimized through Nash equilibrium.

An advantage of the proposed controller not to be overlooked is the stability aspect. Results show that the final control system successfully performs the desired maneuvers. It is also concluded that in case of driver with preview time, the look-ahead preview information brings more time to the driver to cope with the desired path, and reduces the instability in lateral, yaw, and roll motions due the sudden direction change. Compared to the previewed control cases, a vehicle with no preview experiences larger steering angle peaks, and consequently, more severe roll and yaw dynamics. Similarly, the wheel braking torque action is extended in time and its peak value is lowered as the preview time increases. Finally, the DYC system effect on the vehicle is studied for the system with three seconds of preview time. The results show that the uncontrolled system

requires less steering effort, but results in more lateral velocity and yaw rate. The vehicle stability control system successfully reduces the lateral velocity and yaw rate to ensure vehicle stability in lateral and yaw motions. The proposed control strategy based on linear quadratic difference game theory seems promising to bring higher limit performance of vehicle handling and stability. Further studies are required to explore and expand the future application of Game Theory in the vehicle control and driver modeling fields.

Finally, the Nash optimal strategy was modified using Integral Sliding Mode control to find an optimal vehicle stability controller to the case where bounded uncertainties in driver control were present. It was shown that although the system was disturbed by bounded uncertainties, the robust controller performs better than the regular controller in stabilizing the lateral and yaw motions of the vehicle.

Although not demonstrated in this work, more extensive vehicle testing is likely to show that a closed-loop yaw control system based on Nash strategy not only improves vehicle performance, but also increases driver confidence in an emergency maneuver, because the controller takes more responsibility when Nash strategy is applied. However, based on the existing subtleties in workload distribution between the driver and the controller, the proposed controller needs to be carefully studied in the future.

5.2. Future Work

The proposed future work includes:

i. developing a multifaceted chassis control that integrates four wheel steering, active suspension, antilock braking, and traction control strategies in order to implement the proposed direct yaw control;

ii. identifying the parameter involved in driver control priorities and developing a real-time adaptive control law that adapts to changes in the driver model;

iii. evaluating the proposed interaction model on an actual vehicle systems with human driver.

References

Abou-Kandil, H., Bertrand, P. (1986) “Analytic solution for a class of linear quadratic open-loop Nash games”, International Journal of Control, v43, pp. 997-1002.

Anwar, S. (2005), “Yaw stability control of an automotive vehicle via generalized predictive algorithm”, IEEE Proc. of American Control Conference, pp 435-440.

Başar, T. (1974) “A counterexample in linear-quadratic games: Existence of nonlinear Nash solutions”, Optimization Theory and Applications, v14, n4, pp 425-430.

Başar, T., Olsder, G.J. (1995) “Dynamic noncooperative game theory”, 2nd edition, Academic Press, London.

Becker, G., Fromm, H., Maruhn, H. (1931) “Schwingungen in Automobillenkungen” (“Vibrations of the Steering Systems of Automobiles”), Krayn, Berlin.

Bernard, J.E. (1973) “Some time-saving methods for the digital simulation of highway vehicles”, Simulation, v21, n6, pp 161-165.

Bryan, G.H. (1911) “Stability in Aviation”, Macmillan & Co., London.

Broulheit, G. (1925). “La Suspension de la Direction de la Voiture Automobile: Shimmy et Danadinement’ (“The Suspension of the Automobile Steering Mechanism: Shimmy and Tramp”), Société des Ingénieurs Civils de France, bulletin 78.

Buckingham, E. (1914) “On physically similar systems; illustrations of the use of dimensional equations”, Physics Review Letters, v4, pp. 345-376.

Bundorf, R.T. (1967) “The influence of vehicle design parameters on characteristic speed and understeer”, Transactions of the Society of Automotive Engineers, SAE #670078.

Burton, D., Delaney, A., Newstead, S., Logan, D., Fildes, B. (2004) “Evaluation of Anti-lock Braking Systems Effectiveness”, Research Report 04/01, Royal Automobile Club of Victoria, Melbourne, Australia.

Canudas de Wit, C., Olsson, H., Åström, K. J., Lischinsky, P. (1995) “A new model for control of systems with friction”, IEEE American Control Conference, v40, n3, pp. 419-425.

Cerone, V., Milanese, M., Regruto, D. (2008) “Combined Automatic Lane-Keeping and Driver's Steering Through a 2-DOF Control Strategy”, IEEE Trans. on Control Systems and Technology, v17, n1, pp. 135-142.

Chen, L.K., Ulsoy, G. (2000) “Identification of a Nonlinear Driver Model via NARMAX Modeling”, IEEE Proc. of American Control Conference, Chicago, USA, pp. 2533-2537.

Cole, D.J., Pick, A.J., Odhams, A.M.C. (2006) “Predictive and linear quadratic methods for potential application to modelling driver steering control”, Vehicle System Dynamics, v44, n3, pp. 259-284.

Cournot, A.A. (1838) “Recherches sur les Principles Mathematiques de la Theorie des Richesses”, Hachette, Paris.

Donges, E. (1978) “A Two-Level Model of Driver Steering Behavior”, Human Factors, v20, n6, pp. 691-707.

Douglas, J.W., Schafer, T.C. (1971) “The Chrysler ‘Sure-Brake’ – The First Production Four-Wheel Anti-Skid System”, SAE Technical Paper Series 710248, Society of Automotive Engineers, Warrendale, PA.

Edgeworth, F.Y. (1881) “Mathematical Psychics: An Essay on the Application of Mathematics to the Moral Sciences”, C. Kegan Paul and Co., London.

Ellam, C. (1958) “Some engineering aspects of high-performance aircraft”, Proc. of the Institution of Mechanical Engineers, v172, pp. 1105-1112.

Engwerda, J.C. (1998) “On the open-loop Nash equilibrium in LQ-games”, Economic Dynamics and Control, v22, pp. 729-762.

Engwerda, J.C. (2005) “LQ Dynamic Optimization and Differential Games”, New York: John Wiley and Sons.

Esmailzadeh, E., Goodarzi, A. Vossoughi, G.R. (2003) “Optimal yaw moment control law for improved vehicle handling”, Mechatronics, v13, pp. 659-675.

Evans, R.D. (1935) “Properties of tires affecting riding, steering, and handling”, Journal of the Society of Automotive Engineers, v36, n2, p. 41.

Ferguson, S.A. (2007) “The effectiveness of electronic stability control in reducing real-world crashes: a literature review”, Traffic Injury Prevention, v8, n4, pp. 329–338.

Ghoneim, Y.A., Lin, W.C., Sidlosky, D.M., Chen, H.H., Chin, Y-K., Tedrake, M.J. (2000) “Integrated chassis control system to enhance vehicle stability”, Vehicle Design, v23, n1/2, pp 124-144.

Givens, L. (1975) “A primer on cruise controls”, Automotive Engineering, pp. 26-32.

Goland, M., Jindra, F. (1961) “Car Handling Characteristics”, Automobile Engineer, v51, n8, pp. 296-302.

Harsanyi, J.C. (1956) “Approaches to the bargaining problem before and after the theory of games: a critical discussion of Zeuthen’s, Hick’s, and Nash’s theories”, Econometrica, v24, pp. 114-157.

Ho, Y., Bryson, A., Baron, S. (1965) “Differential games and optimal pursuit-evasion strategies”, IEEE Trans. on Automatic Control, v10, n4, pp 385-389.

Jindra, F. (1976) “Mathematical Model of Four-Wheeled Vehicle for Hybrid Computer Vehicle Handling Program”, Department of Transportation - National Highway Traffic Safety Administration, DOT HS-801-800.

Kanai, K., Uchikado, S., Fujishiro, T., Ito, K., and Kawabe, T. (1989) "Design of Adaptive Yawrate Control System of a Car", Transaction of SICE (in Japanese), v23, n8.

Klinkner, W. (1995) “Electronic Stability Program: The new Active Safety System of Mercedes-Benz”, EuroMotor: Vehicle-Vehicle and Vehicle-Roadside Interaction, Institut für Kraftfahrwesen Aachen (IKA), Aachen.

Kuge N., Yamamura, T., Shimoyama, O. (2000) “A Driver Behavior Recongnition Method Based on a Driver Model Framework”, SAE Paper #2000-01-0349.

Leffler, H. (1994) “Consideration of Lateral and Longitudinal Vehicle Stability by Function Enhanced Brake and Stability Control System”, SAE Paper #940832.

Lukes, D.L., Russell, D.L. (1971) “Linear-quadratic games”, Mathematical Analysis and Applications, v33, pp. 96-123.

MathWorks (2010) “MATLAB R2010a”, The MathWorks Inc., v7.10, available at: http://www.mathworks.com/products/matlab/

Matsuno, Y. (1984) “Bilinear Transformation Method”, Orlando: Academic Press.

Matsushita, Y., Yuhara, N., and Arato, Y. (1986) "Modeling of Vehicle Improvement of Handling Quality by Adaptive Four-Wheel Steering Control System", Transaction of JSAE (in Japanese), n36.

MacAdam, C.C. (1988) “Development of Driver/Vehicle Steering Interaction Models for Dynamic Analysis”, Final Technical Report, UMTRI-88-53, TACOM Contract DAAE07-85-C-R069.

McCall, J.C., Wipf, D.P., Trivedi, M.M., Rao, B.D. (2007) “Lane Change Intent Analysis Using Robust Operators and Sparse Bayesian Learning”, IEEE Trans. on Intelligent Transportation Systems, v8, n3, pp. 431-440.

McRuer, D.T., Allen, R.W., Weir, D.H., Klein, R.H. (1977) “New Results in Driver Steering Control Models”, Human Factors, v19, n4, pp. 381-397.

Mechanical Simulation (2009) “CarSim 8”, Mechanical Simulation Corporation, available at: http://www.carsim.com/

Milliken, W.F., Whitcomb, D.W. (1956) “General introduction to a programme of dynamic research”, Proceedings of the Automobile Division; The Institution of Mechanical Engineers , v7, pp 287-309.

Morman, K.N. (1977) “Non-Linear Model Formulation for the Static and Dynamic Analyses of Front Suspensions”, SAE Technical Paper Series , Paper #770052.

Nalecz, A.G. (1987) “Investigation into the Effects of Suspension Design on Stability of Light Vehicles”, SAE Technical Paper Series, Paper #870497.

Nalecz, A.G. (1992) “Development and Validation of Light Vehicle Dynamics Simulation (LVDS)”, SAE Technical Paper Series, Paper #920056.

Nash, J. (1950) “The Bargaining Problem”, Econometrica, v18, pp 155-162.

Nash, J. (1951) “Non-Cooperative Games”, Annals of Mathematica, v54, pp 286-295.

Nash, J. (1953) “Two-Person Cooperative Game”, Econometrica, v21, n1, pp 128-140.

Nissan Motor Co. (1971) “Electro Antilock System (installed in Nissan President)", 240 Landmarks of Japanese Automotive Technology, Society of Automotive Engineers in Japan.

Oakley, W.J., Roller, A.E., Cattin, W.J. (1973) “Development of the Brake System for the General Motors Experimental Safety Vehicle”, SAE Technical Paper Series 730081, Society of Automotive Engineers, Warrendale, PA.

Olley, M. (1934) “Stable and Unstable Steering”, Unpublished Report, General Motors.

Olley, M. (1937) “Suspension and Handling”, Engineering Report, General Motors.

Ornstein, G. (1963) “The automatic analog determination of human transfer function coefficients”, Medical and Biological Engineering and Computing, v1, n3, pp. 377–387.

Pacejka, H.B. (2006) “Tire and Vehicle Dynamics”, 2nd Edition, London.

Packard, A., Doyle, J. (1993) “The Complex Structured Singular Value”, Automatica, v29, n1, pp. 71-109.

Papavassilopoulos, G.P., Medanic, J., Cruz, J. (1979) “On the existence of Nash strategies for a class of analytic differential games”, Optimization Theory and Applications, v27, pp. 309-314.

Pareto, V. (1896) “Cours d’economie politique”, F. Rouge, Lausanne.

Petersen, M.R., Starkey, J.M. (1996) “Nonlinear Vehicle Performance Simulation with Test Correlation and Sensitivity Analysis”, SAE Technical Paper Series, Paper #960521.

Plöchl, M., Edelmann, J. (2007) “Driver Models in Automobile Dynamics Application”, Vehicle System Dynamics, v45, n7, pp. 699-741.

Rashevsky, N. (1959) “Mathematical biophysics of automobile driving”, Bulletin of Mathematical Biology, v21, n4, pp. 375–385.

SAE (1992) “Antilock Brake Review,” Society of Automotive Engineers, Warrendale, PA, Technical Report J2246.

Segel, L. (1956a) “Research in the Fundamentals of Automobile Control and Stability”, SAE National Summer Meeting, Atlantic City.

Segel, L. (1956b) “Theoretical prediction and experimental substantiation of the response of the automobile to steering control”, Proceedings of the Automobile Division; The Institution of Mechanical Engineers , v7, pp 310-330.

Sharp, R.S., Casanova, D., Symonds, P. (2000) “A Mathematical Model for Driver Steering Control, with Design, Tuning and Performance Results”, Vehicle System Dynamics, v33, n5, pp. 289-326.

Sharp, R.S., Valtetsiotis, V. (2001) “Optimal Preview Car Steering Control”, Vehicle System Dynamics, v35, pp. 101-117.

Speckhart, F.H. (1973) “A Computer Simulation for Three-Dimensional Vehicle Dynamics”, SAE Technical Paper Series, Paper #730526.

Takiguchi, T., Yasuda, N., Furutani, S., Kanazawa, H., and Inoue, H., (1986) "Improvement of Vehicle Dynamics by Vehicle-Speed-Sensing Four-Wheel Steering System", SAE Technical Paper Series, Paper #860624.

Tamaddoni, S.H., Taheri, S., Ahmadian, M. (2011) “Linear Quadratic Game Theory Approach to Optimal Preview Control of Vehicle Lateral Motion”, 2011 SAE World Congress, April 12-14, Detroit, USA (accepted)

Tamaddoni, S.H., Taheri, S., Ahmadian, M. (2011) “Optimal Preview Game Theory Approach to Vehicle Stability Controller Design”, Vehicle System Dynamics (accepted)

Tamaddoni, S.H., Taheri, S., Ahmadian, M. (2011) “Optimal Vehicle Stability Control Design Based on Preview Game Theory Concept”, IEEE American Control Conference, June 30-July 2, San Francisco, USA

Tamaddoni, S.H., Taheri, S., Ahmadian, M. (2010) “Optimal Vehicle Stability Controller Based on Nash Strategy for Differential LQ Games”, International Journal of Vehicle Autonomous Systems, v8, n2/3/4, 2010, pp. 171-189

Tamaddoni, S.H., Taheri, S., Ahmadian, M. (2010) "Development of Nash Optimal Driver Based Vehicle Stability Control Algorithm", Proceedings of Transport Research Arena (TRA), June 8-10, Brussels, Belgium

Tamaddoni, S.H., Taheri, S., Ahmadian, M. (2010) "Cooperative DYC System Design For Optimal Vehicle Handling Enhancement", IEEE American Control Conference, Baltimore, USA, June 30-July 2, 2010, pp. 1495-1500

Tamaddoni, S.H., Taheri, S., Ahmadian, M. (2009) "Optimal VSC Design Based on Nash Strategy for Differential 2-Player Games", IEEE International Conference on Systems, Man, and Cybernetics, October11-14, San Antonio, USA, pp. 2415-2420

Tamaddoni, S.H., Taheri, S. (2008) "Yaw Stability Control of Tractor Semi-trailers", SAE Commercial Vehicle Engineering Congress and Exhibition, October 7-9, Chicago, USA, Paper #2008-01-2595.

Tanaka, T., Isoda, K., Ohsaki, M., Shigehara, T. (1991) "Traction Control System for Improved Driving Safety", SAE 912583

Tanelli, M., Osorio, G., di Bernardo, M., Savaresi, S.M., Astolfi, A. (2007) "Limit Cycles Analysis in Hybrid Anti-lock Braking Systems", IEEE Conf. on Decision and Control, New Orleans, USA, Dec 12-14, pp. 3865-3870.

Walker, G.E.L. (1950) "Directional stability, a study of factors involved in private car design", Automobile Engineer, v40, n530-533, pp 281-370.

Weir, D.H., McRuer, D.T. (1970) "Dynamics of driver vehicle steering control", Automatica, v6, n1, pp. 87-98.

Wenzel, T.A., Burnham, K.J., Williams, R.A., Blundell, M.V. (2005) "Closed-loop driver/vehicle model for automotive control", 18th International Conference on Systems Engineering, pp. 46-51.

Whitcomb, D.W., Milliken, W.F. (1956) “Design implications of a general theory of automobile stability and control”, Proceeding of the Automobile Division; The Institution of Mechanical Engineers, v7, pp. 367-391.

Wong, J.Y. (2001) “Theory of Ground Vehicles”, 3rd edition, John-Wiley & Sons, USA.

Young, H.C., Kim, J. (1996) “Stability analysis of the human controlled vehicle moving along a curved path”, Vehicle System Dynamics, v25, pp. 51–69.

Zeuthen, F. (1930) “Problems of Monopoly and Economic Warfare”, George Routledeg and Sons, London.

Zermelo, E. (1913) “Uber eine Anwendung der Mengenlehre auf die Theorie des Schachspiels”, Proc. of the Fifth International Congress of Mathematicians, v2, Cambridge University Press, Cambridge, pp. 501-504.

Zheng, S., Tang, H., Han, Z., Zhang, Y. (2006) “Controller design for vehicle stability enhancement”, Control Engineering Practice, v14, pp. 1413-1421.

Appendix A
Nomenclature

Dimensional Parameter	Non-Dimensional Parameter	Description
α	α	Tire side slip angle
δ_{sw}	δ_{sw}	Steering wheel angle
δ_F	δ_F	Front wheel steering angle
κ	κ	Longitudinal slip
σ	σ/L	Lateral tire relaxation length
θ_w	θ_w	Wheel rotational angle
θ_x	θ_x	Vehicle Roll angle
θ_y	θ_y	Vehicle Pitch angle
θ_z	θ_z	Vehicle yaw angle
τ_{accel}	$\tau_{accel}/\left(MU^2\right)$	Vehicle total driving torque
τ_{decel}	$\tau_{decel}/\left(MU^2\right)$	Vehicle total braking torque
τ_{wBr}	$\tau_{wBr}/\left(MU^2\right)$	Wheel braking torque
τ_{wDr}	$\tau_{wDr}/\left(MU^2\right)$	Wheel driving torque
τ_{zc}	$\tau_{zc}/\left(MU^2\right)$	Corrective yaw moment (non-dimensional)
A_x	A_xL/U^2	Vehicle longitudinal acceleration
Dimensional	Non-Dimensional	Description

Parameter	Parameter	
A_y	$A_y L/U^2$	Vehicle lateral acceleration
C_x	$C_x/(MUL)$	Total roll stiffness
C_κ	$C_\kappa L/(MU^2)$	Tire longitudinal slip stiffness
C_α	$C_\alpha L/(MU^2)$	Tire cornering stiffness
F_x	$F_x L/(MU^2)$	Longitudinal tire force
F_y	$F_y L/(MU^2)$	Lateral tire force
F_z	$F_z L/(MU^2)$	Vertical force on tire
G	GL/U^2	Gravity
H	H/L	Roll center height w.r.t. ground
H_s	H_s/L	Roll centre height w.r.t. chassis
I_w	$I_w/(ML^2)$	Wheel total mass moment of inertia about the rotation axis
I_x	$I_x/(ML^2)$	Roll moment of inertia (about vehicle x-axis)
I_{xz}	$I_{xz}/(ML^2)$	Roll-yaw product of inertia
I_y	$I_y/(ML^2)$	Pitch moment of inertia (about vehicle y-axis)
I_z	$I_z/(ML^2)$	Yaw moment of inertia (about vehicle z-axis)
J	–	Cost (objective) function
K_{us}	$K_{us}U^2$	Understeer coefficient
K_x	$K_x/(MU^2)$	Vehicle roll stiffness
K_y	$K_y/(MU^2)$	Vehicle pitch stiffness
K_{dcc}	$K_{dcc}/(ML)$	Cruise control differential gain

Dimensional Parameter	Non-Dimensional Parameter	Description
K_{icc}	$K_{icc}L/\left(MU^2\right)$	Cruise control integral gain
K_{pcc}	$K_{pcc}/\left(MU\right)$	Cruise control proportional gain
L	1	Vehicle wheelbase
L_B	L_B/L	Horizontal distance between vehicle CG and rear axle
L_F	L_F/L	Horizontal distance between vehicle CG and front axle
M	1	Total vehicle mass
M_s	M_s/M	Non-rolling part of total vehicle mass
M_{zc}	$M_{zc}/\left(MU^2\right)$	Corrective yaw moment (see τ_{zc})
r_{st}	r_{st}	Steering ratio
R_w	R_w/L	Tire effective rolling radius
T_p	T_pU/L	Driver preview time
T_s	T_sU/L	Discretization sampling time
u	–	Control input
U	1	Vehicle speed
V_x	V_x/U	Vehicle longitudinal velocity
V_y	V_y/U	Vehicle lateral velocity
W	W/L	Vehicle track width
X	X/L	Vehicle longitudinal position
x_c	–	Continuous-time state
x_d	–	Discrete-time state

Dimensional Parameter	Non-Dimensional Parameter	Description
Y	Y/L	Vehicle lateral position
z	–	Vehicle discrete-time preview state

APPENDIX B
Vehicle Body Dynamics

The vehicle body dynamics equations of motion are included in this appendix.

- Longitudinal dynamics:

$$m\dot{v}_x - mv_y\dot{\theta}_z - m_s h_s\ddot{\theta}_z \sin\theta_x - m_s h_s\ddot{\theta}_y \cos\theta_x \cos\theta_y + m_s h_s\dot{\theta}_z^2 \cos\theta_x \sin\theta_y + \ldots$$
$$m_s h_s\dot{\theta}_y^2 \cos\theta_x \sin\theta_y + m_s h_s\dot{\theta}_x\dot{\theta}_y \sin\theta_x - 2m_s h_s\dot{\theta}_x\dot{\theta}_z \cos\theta_x \cos\theta_y = \ldots$$
$$f_{xFR}\cos\delta_F + f_{xFL}\cos\delta_F + f_{xBR} + f_{xBL} - f_{yFR}\sin\delta_F - f_{yFL}\sin\delta_F$$

- Lateral dynamics:

$$m\dot{v}_y + mv_x\dot{\theta}_z - m_s h_s\dot{\theta}_x^2 \sin\theta_x - m_s h_s\dot{\theta}_z^2 \sin\theta_x + m_s h_s\ddot{\theta}_x \cos\theta_x \cos\theta_y - m_s h_s\ddot{\theta}_z \cos\theta_x \sin\theta_y + \ldots$$
$$m_s h_s\dot{\theta}_x^2 \cos\theta_x \sin\theta_y - 2m_s h_s\dot{\theta}_y\dot{\theta}_z \cos\theta_x \cos\theta_y = \ldots$$
$$f_{xFR}\sin\delta_F + f_{xFL}\sin\delta_F + f_{yFR}\cos\delta_F + f_{yFL}\cos\delta_F + f_{yBR} + f_{yBL}$$

- Roll dynamics:

$$\left(i_{sy}(\cos^2\theta_x - 1) - i_{sz}\cos^2\theta_x\right)\left(\cos^2\theta_y - 1\right) + i_{sx}\cos^2\theta_y\left(\ddot{\theta}_x - \dot{\theta}_z\dot{\theta}_y\right) - \left(i_{sy} - i_{sz}\right)\dot{\theta}_z^2 \cos\theta_y \cos\theta_x \sin\theta_x + \ldots$$
$$\dot{\theta}_y\dot{\theta}_z\left(i_{sz}(\cos^2\theta_x - 1) - i_{sy}\cos^2\theta_x\right) - \left(i_{sy} - i_{sz}\right)\dot{\theta}_x\dot{\theta}_z \sin\theta_y \cos\theta_x \sin\theta_x + \ldots$$
$$-\ddot{\theta}_z\left(\cos\theta_y \sin\theta_y\left(i_{sx} + i_{sy}\left(\cos^2\theta_x - 1\right) - i_{sz}\cos^2\theta_x\right)\right) + \left(\ddot{\theta}_y + \dot{\theta}_x\dot{\theta}_z\right)\left(i_{sy} - i_{sz}\right)\cos\theta_x \sin\theta_x \sin\theta_y + \ldots$$
$$+m_s h_s^2\ddot{\theta}_x\left(\sin^2\theta_x + \cos^2\theta_x \cos^2\theta_y\right) + m_s h_s\dot{v}_y \cos\theta_x \cos\theta_y + m_s h_s^2\ddot{\theta}_y \cos\theta_x \sin\theta_x \sin\theta_y + \ldots$$
$$+m_s h_s v_x\dot{\theta}_z \cos\theta_x \cos\theta_y - 2m_s h_s^2\dot{\theta}_y\dot{\theta}_z \cos^2\theta_x \cos^2\theta_y + m_s h_s^2\left(\dot{\theta}_y^2 - \dot{\theta}_z^2\right)\cos\theta_x \cos\theta_y \sin\theta_x + \ldots$$
$$-m_s h_s^2\left(\ddot{\theta}_z + \dot{\theta}_x\dot{\theta}_y\right)\cos^2\theta_x \cos\theta_y \sin\theta_y = -k_x\theta_x - c_x\dot{\theta}_x + m_s h_s g \sin\theta_x$$

- Pitch dynamics:

$$
\begin{aligned}
&i_{sy}\ddot{\theta}_y \cos^2\theta_x + i_{sz}\ddot{\theta}_y \sin^2\theta_x - i_{sx}\dot{\theta}_z^2 \cos\theta_y \sin\theta_y + \left(i_{sy}\cos^2\theta_x + i_{sx}\cos^2\theta_y + i_{sz}\sin^2\theta_x\right)\dot{\theta}_x\dot{\theta}_z + \ldots \\
&-m_s h_s\left(\dot{v}_x + v_y\dot{\theta}_z\right)\cos\theta_x\cos\theta_y + \left(i_{sz}\dot{\theta}_z^2 + m_s h_s^2\left(\dot{\theta}_x^2 - \dot{\theta}_z^2\right)\right)\cos^2\theta_x\cos\theta_y\sin\theta_y + \ldots \\
&m_s h_s^2\left(\ddot{\theta}_y + 2\dot{\theta}_x\dot{\theta}_z\right)\cos^2\theta_x\cos^2\theta_y + i_{sy}\dot{\theta}_z^2\cos\theta_y\sin^2\theta_x\sin\theta_y - m_s h_s^2\ddot{\theta}_y\cos^2\theta_x\sin^2\theta_y + \ldots \\
&\left(\left(i_{sy} - i_{sz}\right)\ddot{\theta}_z - m_s h_s^2\dot{\theta}_x\dot{\theta}_y\right)\cos\theta_x\cos\theta_y\sin\theta_x + \left(i_{sy} - i_{sz}\right)\ddot{\theta}_x\cos\theta_x\sin\theta_x\sin\theta_y + \ldots \\
&\left(i_{sz} + i_{sy}\right)\dot{\theta}_x\dot{\theta}_z\cos^2\theta_x\sin^2\theta_y + m_s h_s^2\left(\ddot{\theta}_z\cos\theta_y + \ddot{\theta}_x\sin\theta_y\right)\sin\theta_x\cos\theta_x = \ldots \\
&-k_y\theta_y - c_y\dot{\theta}_y - m_s h_s g\cos\theta_x\sin\theta_y
\end{aligned}
$$

- Yaw dynamics:

$$
\begin{aligned}
&\left(i_{uz} + \left(i_{sz}\cos^2\theta_x + i_{sy}\sin^2\theta_x\right)\cos^2\theta_y + i_{sx}\sin^2\theta_y\right)\ddot{\theta}_z + \ldots \\
&\left(\ddot{\theta}_x - \dot{\theta}_y\dot{\theta}_z\right)\left(i_{sz}\cos^2\theta_x + i_{sy}\sin^2\theta_x - i_{sx}\right)\cos\theta_y\sin\theta_y + \left(\ddot{\theta}_y + \dot{\theta}_x\dot{\theta}_z\right)\left(i_{sy} - i_{sz}\right)\cos\theta_x\cos\theta_y\sin\theta_x + \ldots \\
&m_s h_s\sin\theta_x\left(v_y\dot{\theta}_z - h_s\dot{\theta}_y\left(\dot{\theta}_x\sin\theta_x + \dot{\theta}_y\cos\theta_x\sin\theta_y\right) - \dot{v}_x + h_s\dot{\theta}_z\left(\dot{\theta}_x\cos\theta_y - \dot{\theta}_z\sin\theta_y\right)\cos\theta_x + \ldots\right. \\
&h_s\ddot{\theta}_z\sin\theta_x + h_s\cos\theta_x\cos\theta_y\left(\ddot{\theta}_y + \dot{\theta}_x\dot{\theta}_z\right) - m_s h_s\cos\theta_x\sin\theta_y\left(\dot{v}_y - h_s\dot{\theta}_x^2\sin\theta_x - h_s\dot{\theta}_x\dot{\theta}_y\cos\theta_x\sin\theta_y\right) + \ldots \\
&v_x\dot{\theta}_z - h_s\dot{\theta}_z\left(\dot{\theta}_z\sin\theta_x + \dot{\theta}_y\cos\theta_x\cos\theta_y\right) + h_s\cos\theta_x\cos\theta_y\left(\ddot{\theta}_x - \dot{\theta}_y\dot{\theta}_z\right) - \ddot{\theta}_z h_s\cos\theta_x\sin\theta_y\Big) = \ldots \\
&\frac{w}{2}\left(f_{xFR}\cos\delta_F - f_{xFL}\cos\delta_F + f_{xBR} - f_{xBL} - f_{yFR}\sin\delta_F + f_{yFL}\sin\delta_F\right) + \ldots \\
&\left(l_F f_{xFR}\sin\delta_F + l_F f_{xFL}\sin\delta_F + l_F f_{yFR}\cos\delta_F + l_F f_{yFL}\cos\delta_F - l_B f_{yBR} - {}_B\ f_{yBL}\right)
\end{aligned}
$$

APPENDIX C

Evaluation Parse File

** Vehicle System Simulator 2010 parse file

DATABASE
Database name (dbname) = '-30 Steering at 72 km/h'
Vehicle Model (vehdir) = 'SedanD'
Simulink Model (simdir) = 'vss_model'
Plot Config (plotdir) = 'default'
Event Config (eventdir) = 'default'
Solver (solver) = 'ode3'
Sampling Frequency (freq) = 100 (Hz)
Start Time (tstart) = 0 (s)
Stop Time (tstop) = 4 (s)

VEHICLE
Vehicle Name (name) = 'D-Class Sedan'
Gravity (g) = 9.8066 (m/s^2)
Total Mass (m) = 1450 (kg)
Sprung Mass (ms) = 1370 (kg)
Roll Inertial (Ix) = 606.1 ($kg.m^2$)
Pitch Inertia (Iy) = 4192 ($kg.m^2$)
Yaw Inertial (Iz) = 4192 ($kg.m^2$)
Roll-Yaw Inertial (Ixz) = 0 ($kg.m^2$)
Roll Stiffness (Kp) = 30000 (N.m/rad)
Roll Damping (Cp) = 3000 (N.m.s/rad)
CG Height (h) = 0.54 (m)
CG-Axle Height (hs) = 0. 405 (m)
CG-Front Axle Distance (lf) = 1.11 (m)
CG-Rear Axle Distance (lr) = 1.67 (m)
Track Width (w) = 1.565 (m)

FRONT RIGHT TIRE
Tire Effective Radius (Rw) = 0.373 (m)
Wheel Inertia (Iw) = 1.2 ($kg.m^2$)
Fx Model = 'LuGre'
Fx Tire = 'LuGre 5'
Fy Model = 'Pacejka'
Fy Tire = 'Pacejka 5'
Combined Slip = 'On'

FRONT LEFT TIRE
Tire Effective Radius (Rw) = 0.373 (m)
Wheel Inertia (Iw) = 1.2 (kg.m^2)
Fx Model = 'LuGre'
Fx Tire = 'LuGre 5'
Fy Model = 'Pacejka'
Fy Tire = 'Pacejka 5'
Combined Slip = 'On'
REAR RIGHT TIRE
Tire Effective Radius (Rw) = 0.373 (m)
Wheel Inertia (Iw) = 1.2 (kg.m^2)
Fx Model = 'LuGre'
Fx Tire = 'LuGre 5'
Fy Model = 'Pacejka'
Fy Tire = 'Pacejka 5'
Combined Slip = 'On'

REAR LEFT TIRE
Tire Effective Radius (Rw) = 0.373 (m)
Wheel Inertia (Iw) = 1.2 (kg.m^2)
Fx Model = 'LuGre'
Fx Tire = 'LuGre 5'
Fy Model = 'Pacejka'
Fy Tire = 'Pacejka 5'

LUGRE 5
Model Name = 'LuGre 5'
Model Type = 'Fx'
(muc) = 0.927
(mus) =10
(alpha) = 0.2922
(sigma0) = 118.18
(sigma1) = 0.76
(sigma2) = 0
(kappa0) = 1
(vs) = 0.0216

PACEJKA 5
Model Name = 'Pacejka 5'
Model Type = 'Fy'
(PCY1) = 1.8300
(PDY1) = 1.1044
(PDY2) = -0.2659
(PEY1) = 0.0382
(PEY2) = -0.0483
(PEY3) = -8.0155
(PEY4) = 0
(PKY1) = -21.1460
(PKY2) = 1.4813
(PHY1) = 0.0039

(PHY2) = 2.7190e-004
(PVY1) = 0.0051
(PVY2) = -0.0252

EVENT
Event Name = 'Open-loop Speed'
Event #1 = ''
Initial Speed (u0) = 20 (m/s)

SIMULINK
Model Name = 'vss_model'
Model Location = '\Lib\model\vss_model.mdl'

PLOT
Plot Config Location = '\Lib\plot\default.mat'
Plot #1 = ''